

**SPECTROSCOPIC AND KINETIC STUDIES OF
THE DOPAMINE β -HYDROXYLASE-ANION
COMPLEXES**

Eileen Zhou

B.S. Tsinghua University, 1984

A thesis submitted to the faculty of the
Oregon Graduate Institute of Science & Technology
in partial fulfillment of the
requirements for the degree
Doctor of Philosophy
in
Biochemistry
July, 1993

The dissertation "Spectroscopic and Kinetic Studies of the Dopamine β -Hydroxylase-Anion Complexes" by Eileen Zhou has been examined and approved by the following Examination Committee:

Ninian J. Blackburn, Thesis Advisor
Professor

Joann Sanders-Loehr
Professor

James M. Cregg
Associate Professor

William Fish
Associate Professor

ACKNOWLEDGMENTS

I sincerely thanks the help and guidance given by my supervisor, Dr. Ninian Blackburn. It provides me tremendous experience and knowledge to work under Dr. Blackburn. This experience with make me become a better scientist in the future. I also want to express the gratitude to my committee members, Dr. Joann Loehr, Dr. James Cregg, and Dr. Bill Fish, who spent a lot of time to read my dissertation and provided a lot of opinion although they have very busy schedule on their research and teaching. Dr. Brian Reedy and Katlin Grammar are my coworker who are needed to be thanked for their cooperation and help, without them, it is impossible to finish my experiments which are required for my graduation. I also need to thank all the faculty members, staffs, and students in the department for their help and advice. OGI is a wonderful place for proceeding scientific research and graduate education; the environment is marvelous, and people are friendly. I certainly enjoy to get my education here.

TABLE OF CONTENTS

Acknowledgments	iii
List of Figures	viii
List of Tables	xii
Abstract	xiii
Abbreviation	xv
Chapter	
I. INTRODUCTION	1
1.1. Biological Functions of Dopamine β -hydroxylase	1
1.2. Copper Proteins	6
1.2.1. Type I Copper Proteins	7
1.2.2. Type II Copper Proteins	9
1.2.3. Type III Copper Proteins	12
1.3. Properties of DBH	17
1.3.1. Protein Structure	17
1.3.2. Copper Centers in DBH	18
1.3.3. Kinetic Studies	22
1.3.4. Mechanism based inhibitors	25
1.3.5. The Primary Structure of DBH	28
1.4. Anion Binding to Copper Proteins	31
II. DBH PREPARATION AND CHARACTERIZATION	40
2.1. Isolation and Preparation of DBH	40
2.2. Protein Concentration Measurement	42
2.3. Enzyme Activity Measurement	43

2. 4.	Copper Content Analysis	44
2. 5.	DBH Reconstitution with Copper	45
2. 6.	Preparation of Fully Oxidized DBH	45
III.	THE FULLY OXIDIZED DBH-AZIDE COMPLEX	46
3. 1.	Introduction	46
3. 2.	Experimental Methods	47
3.2.1.	UV / vis spectra of azide to DBH charge transfer transition	47
3.2.2.	CD spectra of DBH-azide and SOD-azide complexes	47
3.2.3.	Infrared spectra of DBH-azide and SOD-azide complexes	48
3. 3.	Results and Discussion	49
3.3.1.	The absorption spectrum of the azide-DBH complex	49
3.3.2.	CD spectra of DBH-azide and SOD-azide complexes	57
3.3.3.	IR spectra of DBH-azide and SOD-azide complexes	71
3. 4.	Conclusion	78
IV.	THE HALF-APO DBH-AZIDE COMPLEX	79
4. 1.	Introduction	79
4. 2.	Experimental Methods	83
4.2.1.	Preparation of half-apo DBH	83
4.2.2.	Spectroscopic studies of the half-apo DBH-azide complex	84
4. 3.	Results	85
4.3.1.	Properties of half-apo DBH	85
4.3.2.	Absorption spectra of the half-apo DBH-azide complex	88
4.3.3.	CD spectra of the half-apo DBH-azide complex	90
4.3.4.	EPR spectra of half-apo DBH	94
4.3.4.	IR spectra of the half-apo DBH-azide complex	94

4. 4.	Discussion	101
4.4.1.	Absorption spectra of azido-half-apo DBH	101
4.4.2	EPR spectra of half-apo DBH and fully reconstituted DBH	103
4.4.3.	CD spectra of azido-half-apo DBH	104
4.4.4.	IR spectra of azido-half-apo DBH	105
4. 5.	Conclusion	106
V.	DBH INHIBITION BY N_3^- and SCN^- — ENZYME KINETIC STUDIES	107
5. 1.	Introduction	107
5. 2.	Experimental Methods	110
5.2.1.	DBH inhibition by SCN^- with tyramine or ascorbate as the variable substrate	110
5.2.2.	DBH inhibition by N_3^- and SCN^- with oxygen as the variable substrate	110
5.2.3.	EPR spectra of DBH in the presence of varying concentrations of SCN^-	111
5. 3.	Results and Discussion	112
5.3.1.	DBH inhibition by SCN^- with tyramine or ascorbate as the variable substrate	112
5.3.2.	DBH inhibition by SCN^- with oxygen as the variable substrate	123
5.3.3.	DBH inhibition by azide with oxygen as the variable substrate	130
5.3.4.	DBH EPR spectra in the presence of different amount of SCN^-	137
5. 4.	Conclusion	142

VI. MECHANISM OF THE DBH CATALYZED REACTION	144
6. 1. Existing Mechanisms	144
6. 2. Whether Radical is Formed during the Reaction	148
6. 3. The Mechanism of DBH Catalyzed Reaction	154
6. 4. Future Work	160
References	161
Vita	170

LIST OF FIGURES

1. 1. Molecular mechanism of adrenergic synapses	4
1. 2. Convergence of excitatory and inhibitory neurotransmitters and neurohormones of Ca channels in cardiac muscle	4
1. 3. Molecular mechanism of dopaminergic synapses	5
1. 4. Comparison of the optical and EPR spectra of a blue copper site and a normal tetragonal copper center	8
1. 5. The copper site in azurin	8
1.6. Stereo drawing of the copper-binding site in plastocyanin	11
1.7. Stereo drawing of Cu / Zn SOD	11
1.8. The copper site of galactose oxidase	13
1.9. Stereo drawing of the active site in nitrite reductase	13
1.10. Schematic view of the arthropodan hemocyanin oxygen binding site	15
1.11. Stereo drawing of the trinuclear copper site plus ligands of the ascorbate oxidase atomic model	16
1.12. Postulated DBH mechanism involving distinct copper sites with separate functions	26
1.13. Primary amino acid sequence of bovine DBH aligned with the corresponding sequences derived from the human cDNA and the bovine cDNA	29
1. 14. An optimized alignment of the similarity region between human DBH and bovine PAM	32

1.15. Absorption energy level diagram of a mononuclear copper azide complex	32
1.16. EPR titration of the $^{63}\text{Cu-DBH-CN}^-$ complex with NaN_3	37
2. 1. The eluent from FPLC	42
3. 1. Absorption spectra of the azido-complex of fully oxidized DBH	50
3. 2. Absorption spectra of model azide-Cu complexes	51, 52
3. 3. Hill plot for titration of DBH with azide	58
3. 4. CD spectra of fully oxidized DBH and the DBH-azide complex	60
3. 5. CD spectra of SOD and the SOD-azide complex	61
3. 6. Optical and circular dichroism spectra of bovine SOD	62
3. 7. CD spectra of amine oxidase in the presence of azide at various concentrations	67
3.8. Absorption and circular dichroism spectra of Met apo-hemocyanin-azide, met azide-hemocyanin, met azide-tyrosinase complexes	68
3.9. Four isomers of a tris-(L- α -amino acid) complex	69
3.10. The CD and absorption spectra of four isomers of $[\text{Co (L-ala)}_3]$	70
3.11. Fourier transfer infrared spectra of the azide complexes of bovine SOD and DBH	73
3.12. Infrared spectra of azide-Cu model compounds prepared with $^{14}\text{N}^{14}\text{N}^{14}\text{N}$ and $^{14}\text{N}^{14}\text{N}^{15}\text{N}$	74
3.13. The resonance structures of the bound azide	75
4. 1. FTIR spectrum of the CO complex of reduced DBH in the 2200 - 2000 cm^{-1} range	81
4. 2. Hill plot for titration of half-apo DBH with azide	91
4. 3. CD spectra of half-apo DBH and the half-apo DBH-azide complex	92
4. 4. CD spectra of the half-apo DBH-azide and DBH-azide complexes	93

4. 5.	EPR spectra of half-apo DBH at -170 °C	95
4. 6.	EPR spectra of oxidized half-apo DBH at -170 °C	96
4. 7.	EPR spectra of fully reconstituted half-apo DBH at -170 °C	97
4. 8.	IR spectra of apo-DBH-azide and SOD-azide complexes at high azide concentration	99
4.9.	IR spectra of the DBH-azide complex at the low azide concentration and the half-apo DBH-azide complex	100
4.10.	The possible environment of the copper centers in each DBH subunit	106
5. 1.	Double reciprocal plots of DBH inhibition by SCN^- with oxygen and ascorbate saturating and tyramine as the variable substrate	113
5. 2.	Replots of DBH inhibition by SCN^- with oxygen and ascorbate saturating and tyramine as the variable substrate	114
5. 3.	Double reciprocal plots of DBH inhibition by SCN^- with oxygen and tyramine saturating and ascorbate as the variable substrate	116
5. 4.	Replots of DBH inhibition by SCN^- with oxygen and tyramine saturating and ascorbate as the variable substrate	117
5. 5.	Mechanism of uncompetitive inhibition	119
5. 6.	Inhibition of DBH by azide with ascorbic acid and oxygen saturating and tyramine as variable substrate	120
5. 7.	Inhibition of DBH by azide with tyramine and oxygen saturating and ascorbate ad variable substrate	122
5. 8.	Double reciprocal plots of DBH inhibition by SCN^- with tyramine and ascorbate saturating and oxygen as variable substrate	124
5. 9.	Replot of DBH inhibition by SCN^- with tyramine and ascorbate saturating and oxygen as variable substrate	125

5.10.	Structures of DBH inhibitors containing sulfur atom.	129
5.11.	Double reciprocal plots of DBH inhibition by azide with tyramine and ascorbate saturating and oxygen as variable substrate	131
5.12.	Replot of the slope versus azide concentration for DBH inhibition by azide with tyramine and ascorbate saturating and oxygen as variable substrate	134
5.13.	Replot of the intercept at the $1/V$ axis versus [azide] for DBH inhibition by azide with tyramine and ascorbate saturating and oxygen as variable substrate	134
5.14.	DBH EPR spectra in the presence of SCN^- at $-170\text{ }^\circ\text{C}$	139
5.15	Relation between Cu^{2+} concentration of fully reconstituted DBH and added SCN^- concentration	140
6. 1.	Two mechanisms for the DBH reaction proposed by Villafranca	145
6. 2.	A proposed chemical mechanism for the DBH reaction through a single active site copper atom	147
6. 3.	A proposed mechanism for the DBH reaction involving a tyramine radical and μ -peroxo species	147
6. 4.	EPR spectra of freeze-quenched DBH	150
6. 5.	EPR spectra of apo-DBH in the presence of $K_3Fe(CN)_6$ at $-167\text{ }^\circ\text{C}$	153
6. 6.	EPR spectra of apo-DBH in the presence of ascorbate at $-170\text{ }^\circ\text{C}$	156
6. 7.	The mechanism of the DBH reaction based on studies in this dissertation	157-159

LIST OF TABLES

1. 1.	Substrates of DBH	23
1. 2.	Spectroscopic properties of Cu-azido complexes	34 - 36
3. 1.	Comparison of optical properties between DBH-azide and beef plasma amine oxidase-azide complexes	71
3. 2.	Vibrational frequencies and calculated force constant of the asymmetric intraazide stretch of isotopically labeled copper azide model complexes	74
4. 1.	Effect of coordination number and basicity on ν (CO) of inorganic Cu (I) carbonyls	82
4. 2.	CO-stretching frequencies for carbonyl complexes of copper proteins	82
4. 3.	Stoichiometry of CO binding to DBH	87
4. 4.	The activity comparison of fully reconstituted and half-apo DBH right after preparations	87
4. 5.	The copper content after fully reconstituted DBH passing through columns	89
4. 6.	Comparison of azide binding properties in fully reconstituted and half-apo DBH	89
5. 1.	Predicted and observed kinetic patterns and apparent kinetic constants	129

LIST OF TABLES

1. 1.	Substrates of DBH	23
1. 2.	Spectroscopic properties of Cu-azido complexes	34 - 36
3. 1.	Comparison of optical properties between DBH-azide and beef plasma amine oxidase-azide complexes	71
3. 2.	Vibrational frequencies and calculated force constant of the asymmetric intraazide stretch of isotopically labeled copper azide model complexes	74
4. 1.	Effect of coordination number and basicity on ν (CO) of inorganic Cu (I) carbonyls	82
4. 2.	CO-stretching frequencies for carbonyl complexes of copper proteins	82
4. 3.	Stoichiometry of CO binding to DBH	87
4. 4.	The activity comparison of fully reconstituted and half-apo DBH right after preparations	87
4. 5.	The copper content after fully reconstituted DBH passing through columns	89
4. 6.	Comparison of azide binding properties in fully reconstituted and half-apo DBH	89
5. 1.	Predicted and observed kinetic patterns and apparent kinetic constants	129

ABSTRACT

Spectroscopic and Kinetic Studies of the Dopamine β -Hydroxylase-Anion Complexes

Eileen Zhou

Oregon Graduate Institute of Science and Technology, 1993

Supervising Professor: Dr. Ninian J. Blackburn

The successful preparation of half-apo dopamine β -hydroxylase made it possible to compare the properties of fully reconstituted dopamine β -hydroxylase with two coppers per subunit (Cu_a - the electron transfer site and Cu_b - the O_2 and CO binding site) and half-apo DBH containing only Cu_b . Half-apo DBH showed 1.0 CO / Cu ratio for CO binding, and 0.96 Hill constant upon the binding of azide, comparing with 0.5 CO / Cu ratio and 0.69 Hill constant for fully reconstituted DBH. The fully reconstituted DBH-azide and half-apo DBH-azide complexes had similar electronic spectra including absorption, CD, and EPR spectra, indicating that two Cu^{2+} centers in each subunit contained the same number of ligands with similar symmetry. However, the differences of FTIR spectra between the fully metallated and half-apo DBH- N_3^- complexes suggested that Cu_a and Cu_b possess different kinds of ligands — Cu_b may contain an O type ligand from an amino acid other than tyrosinate, Cu_a on the other hand may contain only His and H_2O ligands.

N_3^- and SCN^- displayed different types of inhibition toward DBH. SCN^- was an uncompetitive inhibitor with respect to the substrates, tyramine and ascorbate, but a competitive inhibitor for oxygen. N_3^- , however, was an uncompetitive inhibitor with tyramine as the variable substrate and a mixed-type inhibitor with ascorbate and oxygen as the variable substrates. Therefore, SCN^- coordinated only to Cu_b , and N_3^- to both Cu_a and Cu_b . DBH EPR spectra in the presence of SCN^- decreased their intensities, but decreased to only about half of the initial intensity, regardless how much SCN^- was titrated into the system. SCN^- thus reduced Cu_b^{2+} into Cu_b^+ only. The mechanism of the DBH reaction may go through a concerted electron transfer process and radical intermediates. The radicals generated during turnover were different between the ascorbate reduced DBH form and the $\text{K}_3\text{Fe}(\text{CN})_6$ oxidized DBH form. This study proved that two coppers in each subunit of DBH were distinct structurally and functionally.

Abbreviation

AA	atomic absorption spectrophotometer
CD	circular dichroism
Con A	Concanavalin A-sepharose 4B
CT	charge transfer
Da	dopamine
[Cu(dien)N ₃] ⁺	[Cu (diethylenetriamine)N ₃] ⁺
[Cu (terpy) N ₃] ⁺	[Cu (2, 2', 2'' - terpyridine)N ₃] ⁺
[Cu (Me ₅ dien) N ₃] ⁺	[Cu (1, 1, 4, 7, 7-pentamethyldiethylenetriamine)N ₃] ⁺
[Cu (Me ₆ tren) N ₃] ⁺	[Cu (2, 2', 2'' -tris (N, N-dimethylamino)triethylamine)N ₃] ⁺
[Cu (Et ₄ dien) N ₃] ⁺	[Cu (1, 1, 7, 7-tetraethyldiethylenetriamine)N ₃] ⁺
[Cu (py ₂) N ₃] ⁺	[Cu (bis[2-(2-pyridyl) ethyl]amine)N ₃] ⁺
[Cu (L'-O- N ₃)] ⁺	[Cu (2 - [N, N-bis(2-pyridylethyl)amino]methylphenol)] ⁺
[Cu ₂ (L-Et) N ₃] ²⁺	[Cu ₂ (N, N, N', N' -tetrakis[2-(1-ethylbenzimidazolyl)]2-hydroxy -1, 3- diaminopropane) N ₃] ²⁺
[Cu ₂ (bpeac) N ₃] ²⁺	[Cu ₂ (2, 6-bis-[bis[2-(1-pyrazolyl)ethyl]amino]- <i>p</i> -cresol)N ₃] ²⁺
[Cu ₂ (N ₆ O) N ₃] ²⁺	[Cu ₂ (2, 6 -bis[bis-[2-(1-pyrazolyl)ethyl]aminomethyl]- <i>p</i> -cresol)N ₃] ²⁺
[Cu ₂ (L-O-) N ₃] ²⁺	[Cu ₂ (2, 6-bis[N, N-bis(2-pyridylethyl)aminomethyl]phenol)N ₃] ²⁺

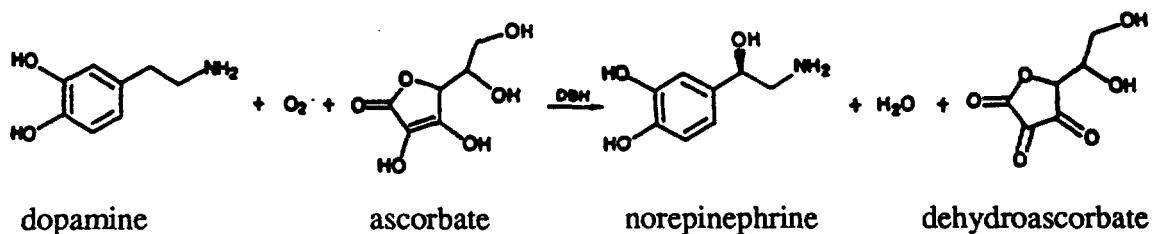
DBH	dopamine β -hydroxylase
E	epinephrine
ESEEM	electron spin-echo envelope modulation
EPR	electron paramagnetic resonance
EXAFS	extended X-ray absorption fine structure
fac	facial
FPLC	fast protein liquid chromatography
FTIR	Fourier transfer infrared spectra
G	Gauss
He	hemocyanin
IR	infrared spectra
K_a	ligand association constant
K_i	inhibitor dissociation constant
K_m	Michaelis constant
LMCT	ligand to metal charge transfer transition
LUMO	lowest unoccupied molecular orbital
mer	meridinal
N_3^-	azide ion
NE	norepinephrine
NIR	nitrite reductase
PAM	peptidylglycine α -amidating monooxygenase
PMSF	phenylmethylsulfonyl fluoride
SCN^-	thiocyanin ion
V_{max}	maximum velocity for an enzyme catalyzed reaction

CHAPTER I

INTRODUCTION

1. 1. Biological Function of Dopamine β -Hydroxylase

Dopamine β -hydroxylase (DBH) catalyzes the conversion of dopamine (a neurotransmitter) to an important main neurotransmitter, norepinephrine (NE), in the catecholamine secreting vesicles (chromaffin granules) of the adrenal medulla and in the sympathetic nervous system (see Scheme 1.1.). This conversion is a central step in the physiologically important catecholamine biosynthetic pathway.



Scheme 1. 1.

A chromaffin granule is composed of 42 % dry weight protein, 13.7 % adrenaline (epinephrine), 5.2 % noradrenaline (norepinephrine), 0.2 % dopamine, 16.8 % nucleotides, and 15.0 % phospholipids (Winkler & Carmichael, 1982). There are five major enzymatic components in chromaffin granules: dopamine β -hydroxylase, Mg²⁺ - activated ATPase, cytochrome b-561, NADH oxidoreductase, and phosphatidylinositol kinase. The ATPase, cytochrome b-561, NADH oxidoreductase, and phosphatidylinositol kinase are membrane bound. DBH exists in a soluble and a

membrane bound form (Winkler, 1976). According to immunological quantitation, from 4 % (Helle et al, 1978) to 6 % (Hortnagl et al, 1974) of the soluble proteins can be attributed to this enzyme, but DBH represents up to 25 % of the total membrane proteins (4.8 times more per mg protein than in the soluble lysate) (Hortnagl et al, 1972).

In the 1970s, it was realized that a transmitter did not only change the membrane conductance and was involved in activation of second messenger systems, such as metabolic processes, genes, as well as ion channels, but also had many effects on a neuron. Neurotransmitters that are defined as first messengers act at different receptors, activating the different second messenger systems. The catecholamines (dopamine, norepinephrine, and epinephrine), which contain a catechol nucleus and share a common synthetic pathway, can affect a variety of cells from platelets to neurons. Being the main neurotransmitter of ganglion cells in the sympathetic nervous system and of locus ceruleus cells that project widely throughout the vertebrate brain, norepinephrine (NE) is the most prevalent in the nervous system. As indicated in Fig. 1.1. A (from Shepherd, 1988), synthesis of catecholamines (1) begins with the amino acid tyrosine, which is taken up by nerve cells from the blood. NE synthesis takes place in the cell body or in the synaptic terminals; it is packaged into vesicles that enter a storage pool as shown in (2). With depolarization and Ca^{2+} influx, the NE is released by exocytosis (3), and acts on postsynaptic receptors (4), termed α_1 - adrenergic receptors. The primary effect of NE, mediated through second messengers, is on Ca^{2+} channels. In addition, the released NE acts on α_2 receptors, located primarily on the presynaptic terminal (5). Through second messengers and protein phosphorylation, α_2 receptors exert diverse controls on the state of the synapse, including changes in the gating of K^+ channels. This may take place by the direction of a G protein. Termination of NE action occurs by reuptake (6) into the

presynaptic terminal, where the level of NE is controlled through enzymatic degradation by monoamine oxidase (MAO) or inactivation by catechol-O-methyltransferase (COMT).

There is the second type of adrenergic receptor, the β receptor (Fig. 1.1. B). This differs from the α receptor mainly in being primarily postsynaptic, and linked to the cAMP second messenger system. One effect of this system is to decrease the membrane conductance of the postsynaptic cell and inhibit its firing. Ionophoresis of NE or cAMP produces a suppression of impulse firing similar to that produced by stimulation of the noradrenergic fibers of the locus ceruleus that innervate the cerebellum. These actions are blocked by ionophoresis of β -receptor blockers such as antipsychotic drugs and prostaglandins, or by drugs that block activation of adenylate cyclase.

Norepinephrine can also be converted to epinephrine (E, adrenaline), which has been traditionally regarded as a hormone and is crucial in preparing the body for action and stress. Both NE and E stimulate adenylate cyclase through a Gs protein, whereas acetylcholine (Ach) mediates parasympathetic suppression through a Gi protein (see Fig. 1.2.). The effects of cAMP are mediated by phosphorylation of the Ca channel or a closely associated protein (Tsien, 1987).

On the other hand, for neurons that utilize dopamine (DA) as the transmitter, the biogenic amine synthetic pathway stops at dopamine β -hydroxylase, the storage (2) and release (3) mechanisms appear to be similar to those for NE discussed above (see Fig. 1. 3.). DA also acts on two types of receptors (4), both of which are linked to adenylate cyclase - cAMP second messenger systems. Stimulation of D_1 - receptors causes an increase in cAMP levels, whereas stimulation of D_2 receptors cause a decrease in cAMP,

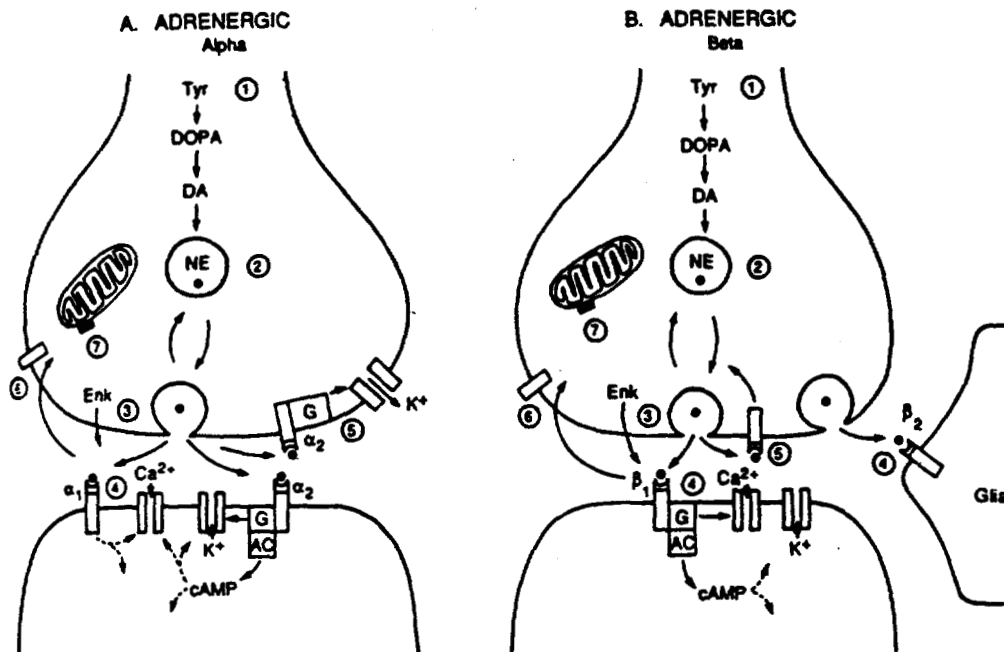


Fig. 1.1. Molecular mechanism of adrenergic synapses. **A. α -Adrenergic synapse:** ① synthetic pathway is through tyrosine (Tyr) to 3,4-dihydroxyphenylalanine (DOPA; catalyzed by tyrosine hydroxylase) to dopamine (DA; catalyzed by DOPA decarboxylase) to norepinephrine (NE; catalyzed by dopamine- β -hydroxylase); ② transport and storage (storage is blocked by reserpine); ③ release by exocytosis (increased by amphetamine); corelease with neuropeptides such as enkephalin, Enk; ④ binding of NE to postsynaptic receptors. Examples are shown of binding to α_1 receptor which leads to modulation of Ca^{2+} channels, and binding to α_2 receptors, which are linked to adenylate cyclase and modulate K^+ channels; there may also be direct actions of G proteins on K^+ channels; ⑤ binding of NE to presynaptic α_2 receptors; ⑥ reuptake, which terminates NE action (blocked by tricyclic antidepressant drugs); ⑦ degradation by monoamine oxidase (MAO) [there may also be inactivation by catechol-O-methyltransferase (COMT)]. **B. β -Adrenergic synapse:** ①–③ synthesis, transport, storage, and release as in A above; ④ binding of NE to β_1 receptor which leads to phosphorylation of ionic channels through cAMP; β_2 receptors are also found on glia; ⑤–⑦ presynaptic receptors, reuptake, degradation, and inactivation, as in A above.

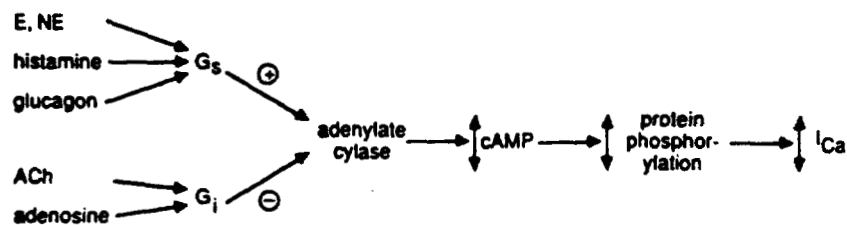


Fig. 1.2. Convergence of excitatory (+) and inhibitory (-) neurotransmitters and neurohormones on Ca channels in cardiac muscle. Abbreviations: E, epinephrine; NE, norepinephrine; ACh, acetylcholine; G_s and G_i , stimulatory and inhibitory G-binding proteins; I_{Ca} , calcium current. (From Tsien, 1987)

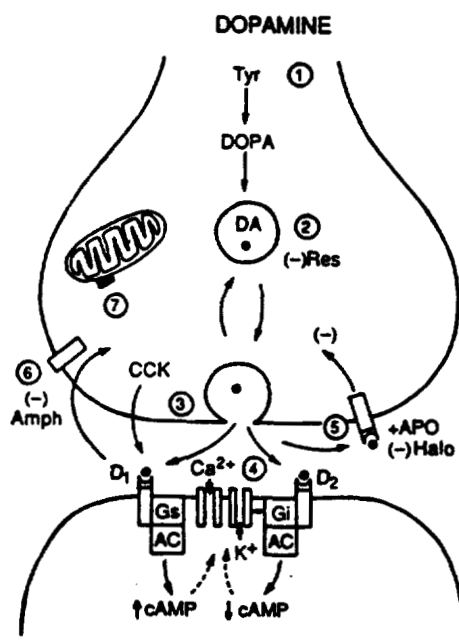


Fig. 1. 3. Molecular mechanism of dopaminergic synapses: ① synthesis by enzymatic pathway from Tyr to DOPA to DA (see legend, Fig. 8.6); ② transport and storage (storage inhibited by reserpine, Res); ③ release of DA by exocytosis; corelease of a neuropeptide such as cholecystikinin (CCK); ④ binding to D₁ receptor, acting through stimulatory G protein (G_s) to increase levels of cAMP, or to D₂ receptor, acting through inhibitory G protein to lower levels of cAMP (antipsychotic drugs such as butyrophenones block D₂ receptors); G protein can also have a direct action on K⁺ channels at some synapses; ⑤ binding of DA to presynaptic receptors [typically D₂; DA receptors are stimulated by psychoactive drugs such as apomorphine (APO), blocked by haloperidol (Halo)]; ⑥ reuptake terminates DA action; ⑦ degradation by MAO and inactivation by COMT.

in the postsynaptic neuron. There are also autoreceptors (5) on the presynaptic terminal, which are thought to exert an inhibitory feedback effect on the DA neuron. The action of DA is terminated largely by reuptake (6). Mechanisms for degradation by MAO and inactivation (7) by COMT are similar to those for NE. Dopamine is interesting because antipsychotic drugs that alleviate the symptoms of Schizophrenia may act by interfering with transmission at dopaminergic synapses in the brain. Schizophrenia may be caused by over-activity of DA neurons in the brain.

Thus, the activity of DBH determines the concentrations of both dopamine and norepinephrine in cells. If DBH appears in the very active state, then most of the dopamine would be converted to norepinephrine, otherwise DA should be the main transmitter in neurons. Therefore, the activity of DBH becomes very important for controlling all different kinds of secondary messengers.

1. 2. Copper Proteins

Dopamine β -hydroxylase is a copper protein. Copper-containing enzymes and proteins are widely distributed in both animals and plants. They appear to have two main functions: (1) electron transport, (2) dioxygen transport and metabolism. The diverse roles played by copper proteins provide an interesting parallel to the functions of iron-heme and flavin-containing proteins; only relatively low abundance prevents copper proteins from occupying the paramount position among redox-active metal proteins in biology. Copper proteins are usually classified into three main categories. The type I copper proteins, also called blue copper proteins, have an intense visible absorption band

which gives a characteristic deep blue color. This type of protein has unusual small copper hyperfine coupling constants in the electron paramagnetic resonance (EPR) spectra. The type II copper proteins, or non-blue copper proteins, are colorless, with normal copper EPR signals. The type III copper proteins have binuclear copper active sites, in which two coppers are magnetically coupled and lack a copper EPR signal.

1.2.1. The type I copper proteins

The blue copper proteins are important electron transfer agents in biological systems. These proteins may be divided into a group of electron carriers in which only the blue copper site is present and a second group in which both blue and other types of coppers are functional. The later group, the so-called blue oxidases, include the laccases, ceruloplasmin, and ascorbate oxidase. The former group include plastocyanins, azurin, and stellacyanin (Gray and Solomon, 1981). A blue copper center in a protein exhibits an intense absorption band ($\epsilon = 5,000 \text{ M}^{-1} \text{ cm}^{-1}$) around 600 nm, an EPR spectrum (see Fig. 1. 4.) featuring unusually small A_{\parallel} values, and relatively high reduction potential (generally in the +300 to +500 mV range vs. +150 mV for Cu^{+2} [aq] samples) (Malkin, 1970; Malmstrom, 1960; Fee, 1975; Gray, 1980).

The high resolution (1.8 Å) X-ray crystal structure of azurin from *Alcaligenes denitrificans* has been completed (Baker, 1988) (see Fig. 1.5.). The copper atom makes three strong bonds with the thiolate sulfur of Cys¹¹² (Cu-S distance 2.14 Å), and the imidazole nitrogens of His⁴⁶ and His¹¹⁷ (Cu-N distances are 2.08 and 2.00 Å, respectively). The Cu-N distances are quite normal, but the Cu-S distance is distinctly

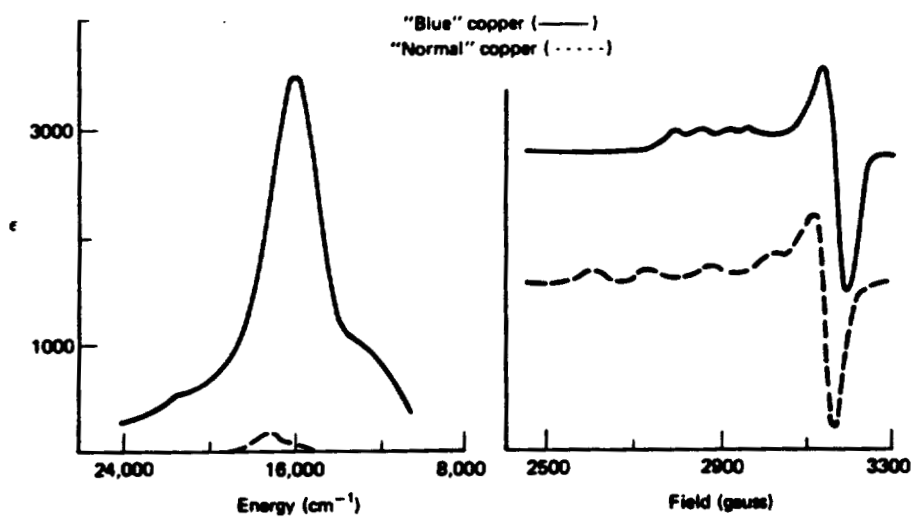


Fig. 1. 4. Comparison of the optical and EPR spectra of a blue copper site and a normal tetragonal copper center.

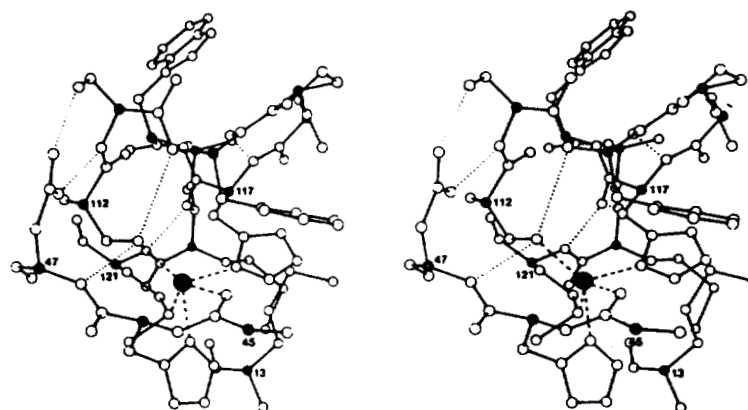


Fig. 1. 5. The copper site in azurin, viewed approximately normal to the trigonal plane through the 3 strongly bound ligands, His⁴⁶, Cys¹¹², and His¹¹⁷. Note the 2 N-H...S hydrogen bonds to Cys¹¹², and the hydrogen bonds made by the conserved Asn⁴⁷ and Ser¹¹³ side-chains (from Baker, 1988).

shorter than is normal for Cu (II)-S bonds, implying a stronger-than-usual interaction. Two much longer axial approaches to copper, from the main-chain carbonyl oxygen of Gly⁴⁵ (Cu-O distance 3.13 Å) and the thioether sulfur of Met¹²¹ (Cu-S distance 3.11 Å) could be described as very weak bonds, completing a distorted, axially elongated trigonal bipyramid.

The crystal structures of plastocyanin from poplar leaves (*Populus nigra var. italica*) and a green alga (*Enteromorpha prolifera*) have been solved by molecular replacement (Colman et al, 1978; Collyer et al, 1990). The Cu site lies about 6 Å from the surface at one end of the molecule. The Cu sites of *E. prolifera* and *poplar* have closely similar dimensions, forming distorted tetrahedrons. Like other type I copper proteins, the copper site of plastocyanin also has two tightly bound His ligands (His³⁷ and His⁸⁷) with the Cu-N distances at 1.89 and 2.17 Å for *E. prolifera* but 2.04 and 2.10 Å for *poplar*, respectively. The Cu-S (Cys⁸⁴) distances are 2.12 and 2.13 Å for *E. prolifera* and *poplar*, respectively; the Cu-S (Met⁸⁷) distance is relatively shorter (2.92 Å for *E. prolifera* and 2.90 Å for *poplar*) than that in azurin (see Fig. 1.6.).

1.2.2. The type II Copper Proteins

In contrast to the type I copper proteins, the type II copper proteins usually have no intense absorbance in the visible region, except galactose oxidase having a tyrosinate to copper charge transfer band at 420 nm. Dopamine β-hydroxylase, superoxide dismutase, galactose oxidase, and amine oxidases belong to this class. They have typical visible absorption spectra of low-molecular-weight copper complexes. The EPR parameters also resemble those of simple tetragonal copper complexes (Fig. 1. 4.). $|A_z|$ values are in the

order of $0.015 - 0.020 \text{ cm}^{-1}$. It is, therefore, likely that copper is coordinated in a tetragonal geometry. Type II copper generally coordinates to nitrogen and oxygen donor atoms. Unlike the type I copper proteins, the non-blue copper proteins have little similarity in their redox potentials.

The structure of bovine erythrocyte Cu, Zn superoxide dismutase has been determined to 2 Å resolution (Tainer et al, 1982). At the active site, Cu (II) and Zn (II) lie 6.3 Å apart; the Zn is buried, while the Cu is solvent-accessible with about 3.9 Å^2 of surface exposed to a 1.4 Å radius probe. The side-chain of His⁶¹ forms a bridge between the Cu and Zn and is coplanar with them (Fig. 1.7.). The Cu ligands, His⁴⁴, His⁴⁶, N_{ε2} of His⁶¹, and His¹¹⁸, form an uneven tetrahedral distortion from a square plane. The Cu has a fifth axial coordination position exposed to solvent. Zn ligands, N_{δ1} of His⁶¹, His⁶⁹, and His⁷⁸, and the O atom of Asp⁸¹ show tetrahedral geometry with a strong distortion toward a trigonal pyramid having the buried Asp⁸¹ at the apex. The Cu-N and Zn-N bond lengths of the liganding His averaged 2.1 Å, while the Zn to O of Asp⁸² bond length averaged just 2 Å. Both the side-chains and main-chains of the metal-liganding residues are stabilized in their orientation by a complex network of hydrogen bonds.

Ito et al (Ito et al, 1991) have determined the crystal structure of galactose oxidase at 1.7 Å resolution. The region around the cupric ion is extremely rich in aromatic side chains. The copper site has five ligands in square pyramidal coordination (see Fig. 1. 8.). Tyr²⁷², His⁴⁹⁶, His⁵⁸¹, and an acetate ion form an almost perfect square with respective distance from the copper of 1.94, 2.11, 2.15, and $2.27 \pm 0.15 \text{ Å}$. The fifth, axial ligand (Tyr⁴⁹⁵) is 2.69 Å away. Tyr²⁷² is covalently bound at C_ε to the sulfur atom of Cys²²⁸. This bond seems to have partial double-bond character with C_β of Cys²²⁸ lying in the

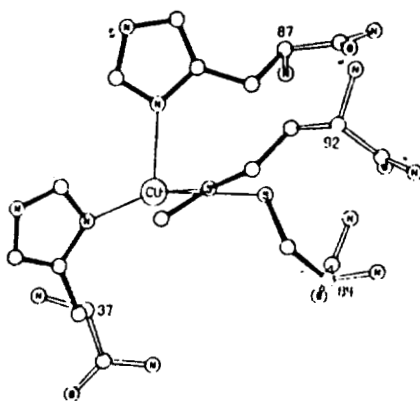


Fig. 1.6. Stereo drawing of the copper-binding site in plastocyanin, showing the four ligand residues (His³⁷, His⁸⁷, Cys⁸⁴, and Met⁹²) (from Colman et al, 1978).

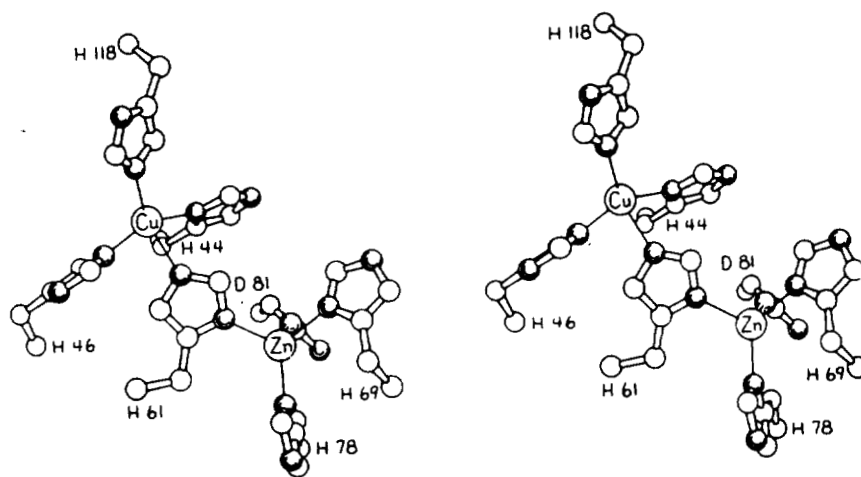


Fig. 1.7. The stereo drawing of Cu/Zn SOD. Nitrogen and oxygen atoms are shaded (from Tainer et al, 1982).

same plane as the ring of Tyr²⁷², suggesting an extended aromatic system. The indole ring of Trp²⁹⁰ is stacked on this "pseudo side chain", with its six-member ring located exactly above the sulfur atom. The electron-density map strongly suggests that Tyr²⁷² exists as a free radical. The unusual bond between Cys²²⁸ and Tyr²⁷² probably plays an essential part in the catalytic mechanism. The sulfur might assist delocalization of the free radical with the stacking Trp aiding its stabilization. The crystal structure of galactose oxidase strongly suggests the involvement of the Tyr²⁷² free radical as the secondary cofactor rather than PQQ.

Copper containing nitrite reductase (NIR) is a trimer containing one type I copper and one type II copper per monomer. The 2.3 Å X-ray structure of NIR (Godden et al, 1991) shows that the type I Cu and the type II Cu are 12.5 Å apart and are bound by adjacent residues in the sequence. There are three domains per monomer, and all four ligands (His⁹⁵, Cys¹³⁶, His¹⁴⁵, and Met¹⁵⁰) to the type I Cu come from domain 1 residues (see Fig. 1.9.). The ligands to the type II Cu are found between domain 1 of one subunit in the trimer and domain 2 of a second subunit, so that, all six metals are bound by the trimer. The type II Cu is bound by two His from domain 1 (His¹⁰⁰ and His¹³⁵), one His from domain 2 (His³⁰⁶), and one water ligand. The geometry of the type II Cu site is nearly a regular tetrahedron, whereas the type I Cu could be better described as a flattened tetrahedron or twisted square plane.

1.2.3. The type III copper proteins

The type III copper proteins contain one or more coupled, EPR-nondetectable binuclear copper sites, which include tyrosinase and hemocyanin, as well as part of blue-oxidases

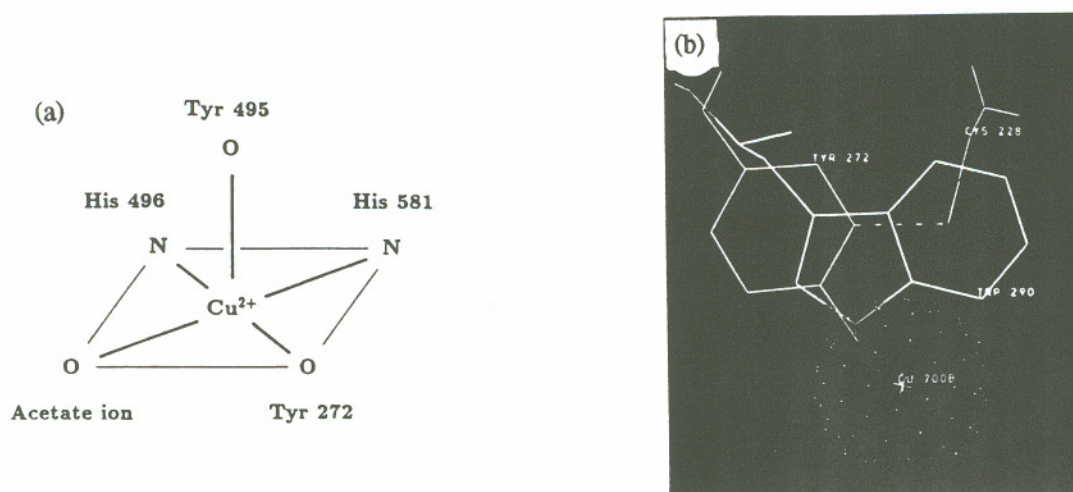


Fig. 1.8. The copper site of galactose oxidase. (a) At pH 4.5, Tyr²⁷², His⁴⁹⁶, His⁵⁸¹ and an acetate ion form an almost perfect square. This square is distorted in PIPES buffer (pH 7.0), where the acetate ion is replaced by a water molecule 2.8 Å from the copper. (b) The stereo view of the unusual thioether bond between Tyr²⁷² and Cys²²⁸ and Trp²⁹⁰ stacking over it (from Ito et al, 1991).

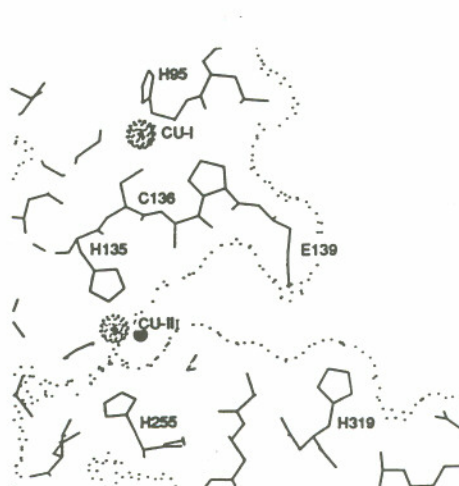


Fig. 1.9. Stereo drawing of the active site in nitrite reductase (from Godden et al, 1991)

(laccase, ceruloplasmin, and ascorbate oxidase). A type III copper center has an absorption band in the 330 nm region but lacks an EPR spectrum, due to the close proximity of two copper (II) ions resulting in strong exchange coupling, and hence the unpaired electron spin is not available to interact with the applied magnetic field to produce the EPR signal. Like the type I copper proteins, the type III copper proteins have relatively high redox potential (tyrosinase $E^* = 360$ mV, laccase $E^* = 434$ mV). Each of the type III copper proteins has different functions. The hemocyanins reversibly bind oxygen (1 O₂ per 2 Cu), but tyrosinase is a monooxygenase that hydroxylates organic substrates (Makino, 1973); this enzyme further functions as a two-electron oxidase, with both coppers being reduced at the same potential in the resting states (Makino, 1974).

For arthropdan hemocyanins, X-ray diffraction techniques have revealed the three-dimensional structure (Gaykema et al, 1984; Volbeda and Hol, 1989). The distance between the two copper ions is 3.8 Å, with an error of ~ 0.4 Å. Copper A is liganded by three His side-chains: His¹⁹⁴, His¹⁹⁸, and His²²⁴. Copper B is liganded in a quite similar manner; two His residues, His³⁴⁴ and His³⁴⁸, also three residues apart, and the third ligand, His³⁸⁴. Many α helices surround the two copper centers; it appears possible to superimpose the "Cu-B helical pair" onto the "Cu-A helical pair"; the three His ligands of Cu-A are superimposed onto the three His ligands of Cu-B with a deviation of 1.0 Å for the C $^{\alpha}$ atoms (see Fig. 1.10.). This implies that the two sites arose from a gene duplication. The oxygen binds at hemocyanin in the $\eta^2-\eta^2$ manner (Magnus and coworkers, Conference of "Copper Proteins" in Baltimore, 1992).

The multicopper oxidases (laccase, ascorbate oxidase, and ceruloplasmin) contain all three types of copper centers. The type III copper centers in laccase and ceruloplasmin seem to

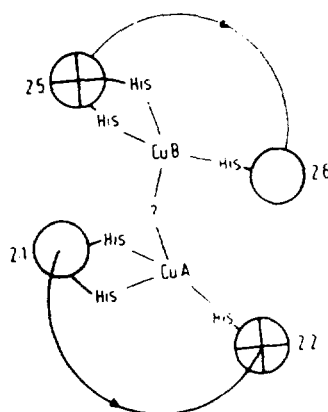


Fig. 1. 10. Schematic view of the active center of arthropodan hemocyanin. Circles represent α -helices (from Volbeda & Hol, 1989)

be in a tetragonal, rather than tetrahedral environment (Dooley, 1979; Dawson, 1979). If not accounting for nitrite reductase, ascorbate oxidase is the only blue oxidase whose crystal structure is available, which has been refined to 2.5 Å resolution (Messerschmidt et al, 1989). The monomer of ascorbate oxidase has three domains connected by three disulfide bonds. The first is from Cys⁸³ to Cys⁵³⁹ linking domain 1 with domain 3. The second one is found in domain 2 between Cys¹⁸¹ and Cys¹⁹⁴. The third one is from Cys²¹ to Cys²⁰² connecting domain 1 with domain 2. Domain 3 contains a type I copper ion in tetrahedral configuration liganded by His⁴⁴⁰, His⁵¹³, Cys⁵⁰⁸, and Met⁵¹⁸ with the Cu-ligand distances at 2.2 Å, 2.0 Å, 1.9 Å, and 2.9 Å, respectively. Domain 2 is not involved in copper binding at all. Between domain 1 and domain 3, there is a trinuclear copper site that includes one type II copper and one pair of type III coppers. Type II and type III coppers form a triangle with the distance between the type II copper and two type III copper at 3.9 and 4.0 Å, respectively. The type I copper is 12.0 and 12.4 Å away from the type III coppers and 14.8 Å away from the type II copper. The distance between two type III coppers is 3.4 Å. The pair of type III coppers, which are bridged by OH⁻ or H₂O (Messerschmidt et al, 1992) have 2 × 3 His ligands (His¹⁰⁸, His⁴⁵¹, and His⁵⁰⁷;

His⁶⁴, His¹⁰⁶, and His⁵⁰⁹), forming a trigonal antiprism with a staggered configuration of imidazoles (see Fig. 1.11.). The type II copper has two His ligands (His⁴⁴⁹ and His⁶²), but is expected to coordinate a third ligand, OH⁻ that points away from the copper, or O₂⁻ that bridges to two type III coppers during the turnover (Messerschmidt et al, 1992).

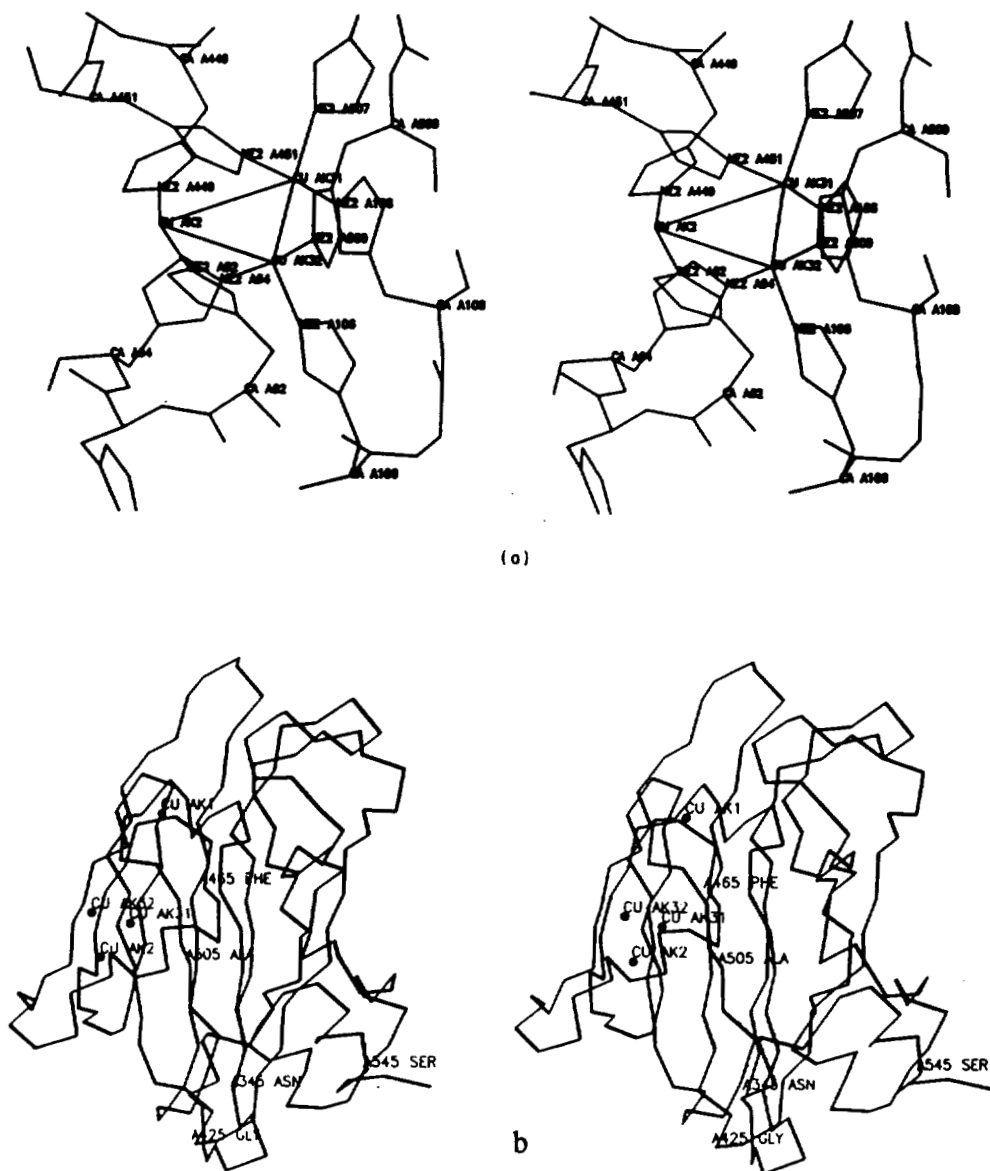


Fig. 1. 11. Stereo drawing of the trinuclear copper site plus ligands of the ascorbate oxidase atomic model. (a) The trinuclear site; (b) Stereo drawing of a subunit (Messerschmidt et al, 1989).

1. 3. Properties of DBH

1.3.1. Protein Structure

Dopamine β -hydroxylase is found either in a soluble or a membrane-bound form, and the water-soluble form from bovine adrenal medulla has been studied most extensively. DBH is a glycoprotein with a molecular weight of 290, 000 daltons (Ljones et al, 1976). There is general agreement that the molecular weight of the monomer is about 77, 000 daltons, but the native enzyme exists as a pair of disulfide bridged dimers, each with molecular weight about 150, 000 daltons (Villafranca, 1981). Margolis (Margolis et al, 1984) has analyzed the sugar content of DBH in detail and found each enzyme tetramer contains an average of six oligosaccharide chains, indicating heterogeneity of glycosylation in each subunit. Joh (Joh and Hwang, 1987) and Speedie (Speedie et al, 1985) have demonstrated the presence of three distinct protein bands (75, 72, 69 Kd) on SDS-PAGE gels run under reducing conditions. With regard to N-terminal sequence analysis, several investigators have reported the presence of at least two types of subunits, one of them contains extra three N-terminal amino acids (Joh and Hwang, 1987; Skotland et al, 1977). In addition to heterogeneity in subunit structure, there is potential for dissociation of the tetrameric enzyme into two dimers (150 Kd) as well as for a possible higher-order oligomerization. Goldstein's group (Park et al, 1976) have detected three different, noninterconverting molecular weight pools of active enzyme from human pheochromocytoma (dimer, tetramer, and octamer). Rosenberg and Lovenberg (Rosenberg and Lovenberg, 1977) have identified only two active, noninterconverting enzyme species (dimer and tetramer, representing 20 - 25% and 70 - 75% of total plasma DBH activity, respectively).

In recent studies of DBH derived from bovine chromaffin granules, Saxena et al (Saxena et al, 1985) reported a pH-dependent dissociation of enzyme. But Klinman's group (Stewart and Klinman, 1988) have characterized the kinetic properties of the tetrameric and dimeric forms of DBH by direct determination of apparent V_{max} and K_m parameters at low (0.1 $\mu\text{g} / \text{ml}$) and high (1 mg / ml) protein concentrations presumed to approximate to exclusive populations of dimer and tetramer, respectively. Significantly, the kinetic properties of the enzyme are very similar at these concentration extremes.

1.3.2. Copper Centers

Although DBH was recognized as a copper containing protein for many years, it was proposed to contain only one copper per subunit. Because of the overall reaction stoichiometry of two electrons per mole of product (see scheme 1. 1.), it was difficult to envisage a satisfactory reaction mechanism for the electron transfer from the reductant to the product. This dilemma was resolved in 1984, with the major breakthrough reported independently by Klinman's group (Klinman et al, 1984) and Villafranca's group (Ash et al, 1984). They found out that DBH activity correlated with the presence of two coppers per subunit. These studies differed in enzyme turnover with dopamine using rapid mixing (Klinman) vs enzyme inhibition by a mechanism-based inhibitor (Villafranca); they were similar in that high concentrations (milligram levels) of enzyme were employed. The correlation of copper with enzyme activity indicated that DBH required two copper per subunit for turnover (Klinman et al, 1984; Ash et al, 1984). Recently the XAS (X-ray absorption spectroscopy) study of both the oxidized and reduced forms of the enzyme containing eight copper atoms per tetramer was reported (Scott et al, 1988). But the concept of two coppers per subunit was challenged by Ljones and coworkers (Syvertsen

et al, 1986). They determined the copper binding constant in DBH using a Cu^{2+} -selective electrode. A stoichiometry of three to four high-affinity sites and four low-affinity sites for Cu^{2+} per enzyme tetramer was evident. The first group of four Cu^{2+} seemed to have about 10^4 higher affinity than the next group of four coppers. The authors, therefore, proposed that the second copper site of each subunit was an adventitious one.

In order to solve the copper environment, measurement of DBH EPR and EXAFS (extended X-ray absorption fine structure) spectra becomes necessary. Though the preliminary EPR spectra reported by Villafranca (Villafranca, 1981) suggests a change in the g_{\parallel} region, neither Skotland (Skotland et al, 1980) nor Klinman & Brenner (Klinman & Brenner, 1987) have observed significant differences between spectra obtained from the enzyme containing one or two coppers per subunit, with the exception of some broadening in the g_{\parallel} region for the enzyme containing two coppers per subunit. This result supports either a structural similarity between copper sites or a statistical binding of copper, such that both sites are populated independent of the ratio of copper to enzyme (or most probably a combination of both features). Studies of EPR power saturation as a function of temperature and copper occupancy indicate there is no difference between enzyme that has one or two coppers per subunit (Klinman, 1987). In contrast to the above results, Blackburn et al (Blackburn et al, 1984) have found that CN^- leads to changes in the EPR spectrum attributed to the formation of a new Cu (II) species with lower g-value, together with a species that resembles native enzyme. When the CN^- / Cu (II) ratio is higher than 1.0, some partially resolved superhyperfine splitting is apparent in the g_{\perp} region. The spectral changes increase as the cyanide-to-copper ratio becomes higher. These changes appear to be fully developed between 2.0 and 2.5 equiv. of CN^- per copper atom. Further addition of CN^- produces no significant change in the relative

intensity of the two signals. These results suggest that the catalytic centers of DBH do not act independently, but are located within the tetrameric molecule such that CN^- binding at one copper influences the electronic structure and / or redox properties of another.

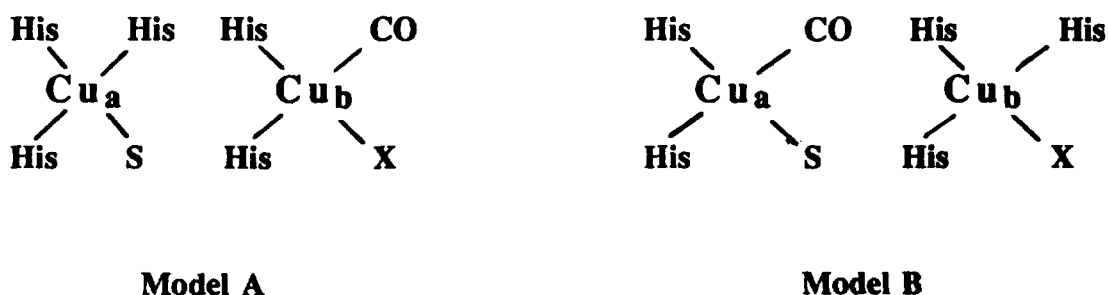
Spin-Echo studies of the Cu (II) binding sites in DBH (Skotland, 1980; Villafranca et al, 1982) have shown that DBH is a typical type II copper protein. The spin Hamiltonian parameters obtained by EPR spectroscopy for fully active DBH containing eight Cu (II) / tetramer ($g_{\perp} = 2.07$, $g_{\parallel} = 2.27$, and $A_{\parallel} = 0.0150 \text{ cm}^{-1}$) are consistent with tetragonal coordination of four nitrogen or mixed nitrogen / oxygen equatorial metal ligation (Peisach and Blumberg, 1974). The electron spin-echo envelope modulation (ESEEM) technique is used to characterize the magnetic interactions between Cu (II) and weakly coupled nuclei around the copper centers to identify and to define the structure of the metal ion binding sites (Kevan, 1979; Mims and Peisach, 1981). Identical results are obtained for DBH containing either eight or four coppers per tetramer, indicating that the copper binding sites are identical. The spectrum of DBH is identical with those obtained from Cu (II)-imidazole model complexes (Mims and Peisach, 1978) and from several Cu (II) proteins (Mims and Peisach, 1979; Kosman et al, 1980; Avigliano et al, 1981). Furthermore, the ESEEM data of DBH are similar to those of copper-imidazole complex with four ^{14}N contribution (McCracken et al, 1987).

An earlier EXAFS (extended X-ray absorption fine structure) study of oxidized DBH containing only four copper per tetramer indicated that Cu (II) bound to four imidazole groups at 2.01 \AA with one or two oxygen atoms at 2.30 \AA (Hasnain et al, 1984). In a later study, the Fourier-transformed spectra of the EXAFS raw data from reduced DBH showed a bifurcated first coordination shell containing two or three N (O) ligands around

1.93 Å and one sulfur - containing ligand around 2.30 Å (Scott et al, 1988). The newest EXAFS results by Blackburn et al (Blackburn et al, 1991) showed that oxidized DBH had 2.5 coordinated histidines and 1.5 oxygen atoms, with an overall 4-coordinate copper site. The Cu-(imid) distance was found to be 1.99 Å, and the Cu-O distance was 1.94 Å. These distances were within the normal range for Cu (II)-imidazole and Cu (II)-O (aq). Although the data did not rule out coordination of anionic oxygen - donor ligands derived from endogenous carboxylate or phenolate groups, a site composed of histidine and water or OH⁻ ligands was suggested. The structure of the reduced copper centers seemed to be very controversial. Villafranca et al (Blumberg et al, 1989) failed to detect any contribution from sulfur or chlorine in their reduced DBH EXAFS data, and asserted that there was little structural change on reduction. However, both Blackburn and Scott (Blackburn et al, 1991; Scott et al, 1988) found that for the reduced enzyme, the imidazole coordination number did not change (within experimental error), but the O-donors were replaced by 0.5 sulfur per copper. There was evidence for the presence of an additional weak interaction at one or both copper atoms. Because DBH contained no free sulfhydryl groups, and there was no reported spectroscopic evidence for a Cu (II) - thiol or thiolate interaction in the oxidized enzyme, it was proposed that the sulfur ligand was derived from methionine. The average coordination at each copper was, therefore, between 3 and 3.5. One Cu (I) in the reduced enzyme was close to 3 - coordinate, two His ligands and one sulfur from methionine with bond length at 2.25 Å ; the other Cu (I) had three His ligands.

In this lab, the measurement of the stoichiometry of CO binding to DBH seems to establish the structural and mechanistic inequivalence of the two Cu (I) centers, because CO selectively binds only one of two copper centers per subunit (Blackburn et al, 1990;

Pettingill et al, 1991). Based on all these data, Blackburn proposed two models for the active site of the CO adduct for the reduced enzyme involving different coordination at the two Cu (I) sites: model A, $[\text{Cu}_a(\text{His})_3\text{S} \cdots \text{Cu}_b(\text{His})_2\text{COX}]$, or model B, $[\text{Cu}_a(\text{His})_2\text{SCO} \cdots \text{Cu}_b(\text{His})_3\text{X}]$, where X is a weakly binding ligand or a histidine. To decide which model is correct is going to be investigated and is the main task in this dissertation.



1.3.3. Kinetic Studies

For an unknown protein, kinetic studies of the time course for reduction and reoxidation of an enzyme usually are performed, providing some insight into the inter-relationship between observed enzyme forms with catalytic function. DBH can hydroxylate a large number of compounds (see Table 1.1.), and tyramine is one substrate for DBH, forming a β -hydroxylated product, octopamine (see Scheme 1.2). Results of kinetic studies with tyramine as a substrate are similar to those obtained with dopamine as a substrate. Since catechol can reduce the enzyme-bound Cu (II) (Levin and Kaufman, 1961), tyramine is usually used as the substrate for kinetic studies (see Scheme 1.2.). In the early substrate binding studies, Goldstein et al (Goldstein et al, 1968) reported when tyramine was the variable substrate, the Lineweaver-Burk plots were linear and parallel to each other. A similar pattern was obtained with ascorbate as the variable substrate. Thus tyramine and

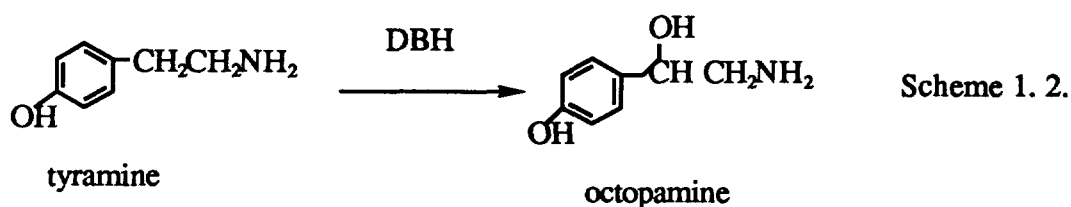


Table 1.1. Substrates for DBH

Substrates	Reaction	Reference		
<i>p</i> -tyramine	hydroxylation	Villafranca,1981		
β -phenethylamine				
dopamine				
<i>m</i> -tyramine				
<i>O</i> -tyramine				
<i>p</i> -methoxyphenethylamine				
α -methyl- <i>p</i> - tyramine				
β -methyl- <i>p</i> -tyramine				
<i>N</i> -methyl- <i>p</i> -tyramine				
γ -phenylpropylamine				
<i>p</i> -hydroxybenzylcyanide				
<i>S</i> -octopamine			ketonization	May et al, 1981
phenyl-2-aminoethyl sulfide			sulfoxidation	May & Phillips, 1980
phenyl-2-aminoethyl selenide	selenoxidation	May et al, 1987		
<i>N</i> -phenylethylenediamine	<i>N</i> -dealkylation	Wimalasena & May, 1987		
<i>N</i> -methyl- <i>N</i> -phenylethylenediamine	<i>N</i> -dealkylation	<i>ibid</i>		
1-phenyl-1-aminomethylethene	epoxidation	May et al, 1983		
3-amino-2-(3-hydroxyphenyl)prene	alkyne oxidation	Padgette et al,1985		

ascorbate obeyed a Ping-Pong mechanism, in which binding of the first substrate (ascorbate) to the enzyme was followed by the release of a product (dehydroascorbate) from the enzyme before a second substrate (tyramine) bound to the enzyme. On the other hand, when dopamine was the variable substrate and the oxygen concentration saturated, the double-reciprocal plots were linear and intersected at one point on the ordinate. The intersecting initial velocity patterns suggested a sequential mechanism in which both substrates (dopamine or tyramine and oxygen) must add to the enzyme before a product was released. The reaction rates of each step suggested that regardless which of these two substrates (oxygen or dopamine) was added first, both steps reached equilibrium rapidly, and the interconversion of the central ternary complexes most likely represented the rate-limiting step.

The pH dependence of $V_{\max} / K(\text{DM})$, $V_{\max} / K(\text{O}_2)$ (Ahn and Klinman, 1983; K_{DM} : Michaelis constant of dopamine, K_{O_2} : Michaelis constant of O_2) shows a bell shaped curve with slopes of -1 and 1 on either side of the maximum, which signifies the presence of at least three ionization states for DBH which may represent binary or ternary enzyme-substrate and enzyme-product. From the curve of V_{\max} vs. pH, Ahn and Klinman have found that there are two pK_a for the DBH reaction, $\text{pK}_{a1} = 4.8 - 4.9$ and $\text{pK}_{a2} = 5.4 - 5.6$. The ionization of at least two residues is required to account for this pH dependence.

It seems to suggest binary complexes $E_{\text{B2}}^{\text{B1}} \text{S}$, $E_{\text{B2}}^{\text{B1H}} \text{S}$, and $E_{\text{B2H}}^{\text{B1H}} \text{S}$ (enzyme•substrate

complexes with no amino acid, one amino acid, and two amino acids protonated, respectively) (the mechanism see Fig.1.12. from Brenner and Klinman, 1989). The finite limiting values of V_{\max} at high and low pH require that two ionization states of the ternary enzyme-product complex be catalytically viable. The kinetic mechanism, at pH 4.5, is

ordered with water dissociation 9.2-fold faster than norepinephrine dissociation from the ternary-complex so that the release of water from the enzyme ternary-complex precedes the release of norepinephrine (Klinman et al, 1980). At pH 5.2 and 6.0, the kinetic mechanism is completely random, having approximately equal rates for water and norepinephrine dissociation. Above pH 6.0, the kinetic mechanism is once again ordered, but with preferential release of norepinephrine. Catalysis requires the protonated form of an enzyme-bound residue ($pK = 5.6 - 5.8$), suggesting an acid-catalyzed activation of oxygen to generate a reactive intermediate. Subsequent cleavage of the C - H bond at β -carbon of substrate may be mediated either directly by an intermediate reduced-dioxygen species or by an active site residue.

1.3.4. Mechanism-based inhibitors

Mechanism-based inhibitors or suicide substrates are inhibitors that themselves are unreactive until they interact with a specific enzyme active site. The inactivation of DBH by the acetylenic mechanism-based inhibitor, 1-phenyl-1-propene, which forms a benzyl free radical by hydrogen abstraction (Colombo and Villafranca, 1984) (Mechanism see Scheme 1.3.), is most likely accomplished by alkylation of an amino acid residue at the active site. Similar DBH inhibition by 2-bromo-2-(*p*-hydroxyphenyl)-1-propene, which is a substrate analogue, shows that inactivation of DBH arises only when DBH is incubated with analogue, reducing agent, and oxygen (Colombo et al, 1984). Authors suggest that two groups at the active site of the enzyme are likely to be involved. A base acts as a nucleophile, and an acid protonates the allene or vinyl ketone. The enzyme-bound intermediate or product may rearrange to an electrophilic species, leading to the formation of a stable adduct. The kinetic data suggested that enzyme inactivation by another mechanism-based inhibitor, 3-phenylpropene, proceeds by hydrogen atom

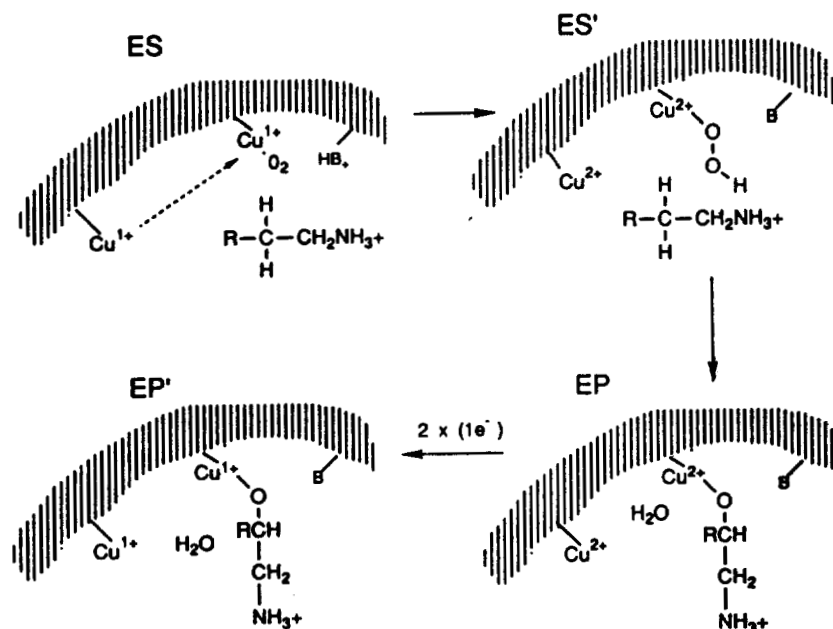
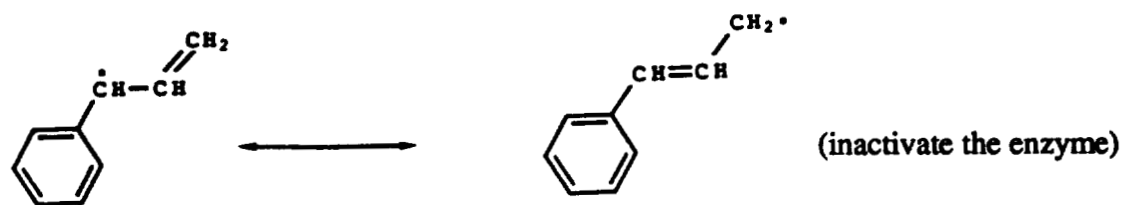


Fig. 1.12. Postulated DBH mechanism involving distinct copper sites with separate functions (from Brenner and Klinman, 1989)



Scheme 1.3. The mechanism of DBH inhibition by mechanism-based inhibitors

abstraction and formation of a benzyl radical which then partitions between hydroxylation and inactivation of DBH.

[³H]-6-Hydroxybenzofuran and [¹⁴C]-phenylhydrazine are mechanism-based inhibitors of DBH (Farrington et al, 1990). Phenylhydrazine inactivates DBH by reducing Cu (II) to Cu (I), resulting in the formation of a N-centered radical cation (phenylhydrazine) intermediate. The intermediate may then break down to a carbon-centered radical (R·) from the enzyme. Both inhibitors label a unique tyrosine, Tyr⁴⁷⁷, but [¹⁴C]-phenylhydrazine also labels a unique histidine, His²⁴⁹. His²⁴⁹ is a possible copper ligand and Tyr⁴⁷⁷ may be an active residue. By isolation of a modified nonradio-labeled peptide, authors have found that there is an amino acid deleted from the peptide. This amino acid has a large UV peak but without radioactive label. It is Arg⁵⁰³ putatively modified during inactivation of DBH by two inhibitors. The chemical nature of modified Arg⁵⁰³ is unknown. The stoichiometry of inactivation of 6-OH-benzofuran has been shown to be 0.5 / active site of DBH. Because enzyme loses an Arg residue after inactivation of DBH with either 6-OH-benzofuran or phenylhydrazine, the mechanism of DBH inactivation may involve oxidation of an amino acid active site.

The inactivation of DBH by two additional mechanism-based inhibitors (DeWolf et al, 1988, 1989) demonstrates that two other amino acid residues can be covalently modified. These residues are not His²⁴⁹ and Tyr⁴⁷⁷, but His³⁹⁸ and Tyr²¹⁶. Both His²⁴⁹ and His³⁹⁸ are in a sequence commonly found in copper-binding sites, His-X-His, and thus are candidates as ligands for the copper ions.

1.3.5. The primary structure of dopamine β -hydroxylase

The primary amino acid sequence of soluble bovine DBH has been obtained recently by peptide mapping and sequencing (Robertson et al, 1990). The comparison of bovine amino acid sequence with that derived from *bovine* (Lamouroux et al, 1987) and *human* cDNA (Lewis et al, 1990) is shown in Fig. 1.13. The full length of *human* DBH cDNA encodes 603 amino acids, including a 25 residue signal-peptide. The complete bovine gene codes for a polypeptide of 597 amino acids, but the mature enzyme contains 578 amino acids. 19 amino acids represent signal peptide sequences which are thought to be proteolytically cleaved and are absent in the peptide maps. 561 of the 597 amino acids have been confirmed by protein sequencing (Robertson et al, 1990). N-terminal sequence analysis of the bovine enzyme indicates that two different N-termini exist, one of which is 3 amino acids longer than the other and begins with the sequence Ser-Ala-Pro (Talor et al, 1989). The bovine peptide sequence has five differences from the sequence derived from the bovine cDNA, and four of the differences could be derived from a single base change in the DNA. The bovine sequence is 85 % identity to that derived from the human cDNA. There are four consensus sites (50, 170, 552, 597) for glycosylation in the bovine peptide sequence. However, only two, at the position 170, 552, have been tested positive for glycosylation by the phenol-sulfuric acid test (Dubois et al, 1956). In the human enzyme, there is a consensus site at 330, not at 597.

Analysis of the amino acid composition of bovine DBH suggest there are 13-16 Cys/monomer (Skotland and Ljones, 1979) comparing with 16 for the human sequence (Lamouroux et al, 1987; Rossenberg and Lovenberg, 1986). Two Cys in the human enzyme are replaced with Arg in the bovine enzyme. At the position 553, the human cDNA derived sequence has a Lys, and the bovine cDNA derived sequence has an Arg.

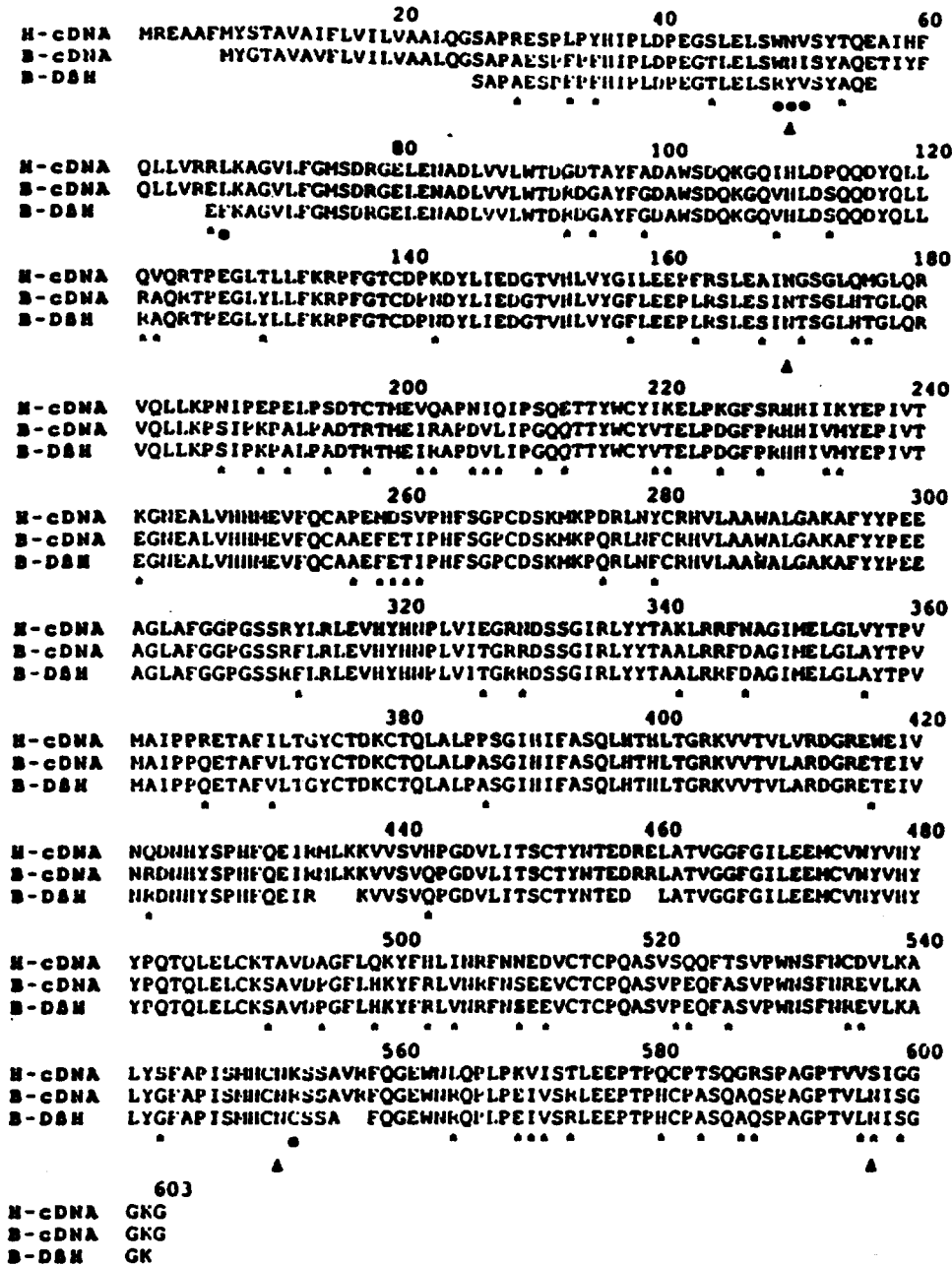


Fig. 1. 13. Primary Amino Acid Sequence of Bovine Dopamine β -Hydroxylase Fifty-nine Peptides from the Bovine Enzyme were Aligned with the Corresponding Sequences Derived from the Human cDNA (H-cDNA) and the Bovine cDNA (B-cDNA). The gaps represent peptides that could not be identified in our peptide maps or sequences that could not be read from peptides that overlapped that region. Stars (*) represent differences between the bovine sequence and the human sequence, while filled circles (●) represent differences between the bovine cDNA derived sequence and the bovine peptide sequences. Triangles (▲) represent consensus sites for glycosylation. Chemical assays confirmed glycosylation at amino acids 170 and 552.

Since spin-echo EPR and EXAFS data have demonstrated copper coordination to 3-4 histidines for each copper in DBH, there should be 6 - 8 His at the active site of each DBH monomer. All the 21 His residues predicted by the bovine cDNA have been identified. Five regions in the bovine sequence, including positions 230 (His-His), 248 (His-His-Met), 319 (His-X-His), 398 (His-X-His), and 425 (His-X-X-X-His), provide contiguous or closely spaced His residues for potential Cu-ligands. Met²⁵⁰ could also be a Cu-ligand with S as the coordination atom.

DBH is strikingly similar to an important enzyme, peptidylglycine α -amidating monooxygenase (PAM) as well as significantly homologous to the first 92 amino acids of DBH and the entire sequence of NADH : ubiquinone oxidoreductase. PAM catalyzes the C-terminal amidation of a variety of hormonal peptides and is dependent upon copper, ascorbate, and molecular oxygen for the enzymatic activity (Eipper et al, 1983; Eipper and Mains, 1988). PAM is a key regulatory enzyme in neuropeptide biosynthesis; like DBH, it exists in both soluble and membrane-bound forms. PAM is a monomer with one or two copper(s) per monomer, consisting of total 976 amino acid residues (including a 25 residue signal sequence, a putative 10 residue propeptide, an 831 residue catalytic / intragranular domain, and a 25 residue transmembrane domain with an 86 residue cytoplasmic tail).

Based on the slightly larger DBH section of 295 residues aligned with 270 residues from PAM, the number of identical positions is 27 % with 52 % structural conservation by the exchange of similar residues in positions of nonidentity (see Fig. 1.14.) (Southan and Kruse, 1989). Several lines of evidence indicate that the similar section between these two enzymes represents a common catalytic domain. Out of 7 Cys residues in PAM, 5

are, allowing for small gaps, in identical or similar positions as in DBH. This implies some conserved pattern of intra-chain disulfide formation. Two histidine clusters are also conserved at positions 102 (HHM) and 238 (HXH) in PAM relative to the positions 250 (HHM) and 398 (HXH) in human DBH that are probable Cu (II) ligands. The HHM cluster in DBH and PAM also supplies the potential sulfur ligand from Met for the coppers in these two enzymes. Direct evidence for a ligand motif of type H-X-H in copper type II proteins comes from the 3-dimensional structure of the copper binding site in superoxide dismutase (Tainer et al, 1982). Both enzymes contain additional potential ligand clusters but at different positions. These would include HYH at the position 319 - 321 in DBH and an unusual Met / His cluster at the position 345 in PAM. Since the EXAFS data indicates Met is a possible ligand to copper in DBH, this unusual Met / His cluster in PAM may supply the Met ligand to copper center rather than Met¹⁰⁴. On the basis of both primary structures and biochemical functions, DBH and PAM are proposed to be members of a new protein family of type II copper monooxygenases.

1. 4. Anion Binding to Copper Proteins


Since type II copper proteins have no optical absorbance, conclusions regarding the role of the Cu (II) site have to be based largely on inhibition experiments with anions, such as cyanide, azide, and thiocyanate, which are known, from electron paramagnetic resonance (EPR) studies, to interact strongly with the "nonblue" copper atoms. An intense azide to copper charge-transfer transition near 400 nm permits the optical detection of complexation between Cu (II) and azide (see Fig. 1.15.). SCN⁻ also produces a ligand to metal charge-transfer transition, but with much lower intensity. CN⁻ has very strong affinity for Cu (II) centers in enzymes, but lacks a charge transfer band. Azide-Cu

complexes are then the easiest to investigate. A series of stable, structurally characterized Cu (II)-azide model compounds have been synthesized. There are three possible binding modes for a single azide coordinating to Cu (II) center: terminal, μ -1, 3, or μ -1, 1 geometry.

Azide and SCN^- are known to bind to most type II copper proteins terminally. Some model compounds, $[\text{Cu}(\text{dien})\text{H}_2\text{O}]^{2+}$, $[\text{Cu}(\text{terpy})\text{H}_2\text{O}]^{2+}$, and $[\text{Cu}(\text{Me}_5\text{dien})\text{H}_2\text{O}]^{2+}$, can coordinate to N_3^- anion through the displacement of H_2O from the equatorial position on Cu (II). In each case, the other three equatorial positions are occupied by strongly bound nitrogen atoms from a tridentate ligand, diethylenetriamine, 2, 2', 2'' - terpyridine, or 1, 1, 4, 7, 7 - pentamethyldiethylenetriamine, respectively. Difference spectra (Cu (II)- N_3^- complex - Cu (II)- H_2O complex) show that λ_{max} values for the azide to copper (II) charge transfer transitions of $[\text{Cu}(\text{dien})]^{2+}$, $[\text{Cu}(\text{terpy})]^{2+}$, and $[\text{Cu}(\text{Me}_5\text{dien})]^{2+}$ are at 346, 348, and 375 nm, respectively (see Table 1.2.). Comparisons of λ_{max} values of LMCT (ligand to metal charge transfer) transitions of the type II copper proteins with that of these model compounds will provide information about the structure of copper centers, because perturbation of a square-planar structure toward tetrahedral or trigonal bipyramidal will shift the azide to copper (II) charge-transfer transition to lower energy (longer λ_{max}). The LMCT band of the laccase type II Cu (II)-azide complex (405 nm) is observed at considerably longer wavelength than those of the square planar $[\text{Cu}(\text{dien})\text{N}_3]^+$ (Morpurgo et al, 1973) and $[\text{Cu}(\text{terpy})\text{N}_3]^+$ (Holwerda et al, 1982), while close to the bands for $[\text{Cu}(\text{Me}_5\text{dien})\text{N}_3]^+$ (375 nm) (probably intermediate between square and trigonal pyramidal) (Felthouse et al, 1978) and $[\text{Cu}(\text{Me}_6\text{tren})\text{N}_3]^+$ (385 nm) (Coates et al, 1979) (probably trigonal bipyramidal) (DiVaira and Orioli, 1968). Hence, the half-filled metal orbital which correspond to the LUMO (lowest unoccupied molecular orbital) for the

Table 1.2. Spectroscopic Properties of Cu-azido Complexes

Cu-N-N-N	
compounds	λ_{\max} of the absorption band
[Cu(dien)N ₃] ⁺ dien = diethylenetriamine	346 nm from Morpurgo et al, 1973
[Cu (terpy) N ₃] ⁺ terpy = 2, 2', 2'' - terpyridine	348 nm from Holwerda et al, 1982
[Cu (Me ₅ dien) N ₃] ⁺ Me ₅ dien = 1, 1, 4, 7, 7-pentamethyldiethylenetriamine	375 nm from Felthouse et al, 1978
[Cu (Me ₆ tren) N ₃] ⁺ Me ₅ dien = 2, 2', 2'' -tris (N, N-dimethylamino)triethylamine	385 nm from Coates et al, 1979
[Cu (Et ₄ dien) N ₃] ⁺ Et ₄ dien = 1, 1, 7, 7-tetraethyldiethylenetriamine	388 nm IR 2062 cm ⁻¹ from Pate et al, 1989
[Cu (py ₂) N ₃] ⁺ py ₂ = bis[2-(2-pyridyl) ethyl]amine	395 nm IR 2041 cm ⁻¹ from Pate et al, 1989

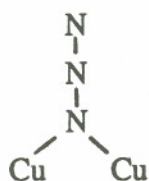
[Cu (L'-O- N ₃) ⁺	395 nm
L'-O = 2 - [N, N-bis(2-pyridylethyl)amino]methylphenol	IR 2039 cm ⁻¹
	from Pate et al, 1989
Type II copper in laccase	405 nm
	from Holwerda et al, 1982
amine oxidase from bovine plasma	385 nm
	from Dooley and Cote, 1985
SOD (bovine superoxide dismutase)	375 nm
	from Dooley and McGuirl, 1986
met-apo Hemocyanin (from arthropdan)	415 nm
	from Himmelwright et al, 1980
	
[Cu ₂ (L-Et) N ₃] ²⁺	365, 420 nm
L-Et =N, N, N', N' -tetrakis[2-(1-ethylbenzimidazolyl)]	IR 2025 cm ⁻¹
2-hydroxy -1, 3-diaminopropane	from Pate et al, 1989

$[\text{Cu}_2 (\text{bpeac}) \text{N}_3]^{2+}$	376, 435 nm
$\text{bpeac} = 2, 6\text{-bis-}[\text{bis}[2\text{-(1-pyrazolyl)ethyl}]\text{amino}]\text{-}p\text{-cresol}$	IR 2038 cm^{-1}
	from Pate et al, 1989

Hemocyanin

half-met (from Arthropodan)	400, 480 nm
	IR 2039 cm^{-1}
met-Hc	380 (Busycon), 500 (Limulus), 420 (cancer)
	from Solomon, 1981

met-tyrosinase (from Neurospora)	360 nm, 420 nm
	from Solomon, 1981



$[\text{Cu}_2 (\text{N}_6\text{O}) \text{N}_3]^{2+}$	413 nm
$\text{N}_6\text{O} = 2, 6\text{-bis}[\text{bis}[2\text{-(1-pyrazolyl)ethyl}]\text{aminomethyl}]\text{-}p\text{-cresol}$	from Pate et al, 1989

$[\text{Cu}_2 (\text{L-O-}) \text{N}_3]^{2+}$	417 nm
$\text{L-O-} = 2, 6\text{-bis}[\text{N, N-bis}(2\text{-pyridylethyl})\text{aminomethyl}]\text{phenol}$	from Pate et al, 1989

CT (charge transfer) transition is expected to decrease in energy as the structure distorts towards trigonal, tetragonal, or tetrahedral configuration.

Anion binding will also change the EPR spectra of type II copper proteins. EPR spectra of SOD- N_3^- , SOD- F^- , SOD- CN^- (Rotilio et al, 1972; Fee and Gaber, 1972), and SOD- SCN^- (Bertini et al, 1980) show that the rhombic symmetry of the bovine enzyme, which results from the binding of copper to three strong His ligands and the fourth weaker His ligand, becomes axially symmetric after binding to N_3^- , CN^- , and F^- ions. Because the affinity of anions for Cu (II) in SOD is comparable to that of strong ligands, anions can replace the fourth, weaker ligand, yielding a nearly square planar site. EPR spectra of DBH containing CN^- showed a new signal reflecting the formation of the complex of CN^- -Cu (II) DBH (Obata et al, 1987; Blackburn et al, 1984) (Fig.1.16.). An excess of CN^- in the enzyme solution caused a substantial reduction of Cu (II) to Cu (I); therefore, there were two components upon CN^- binding to DBH. From combination of EPR and ^1H

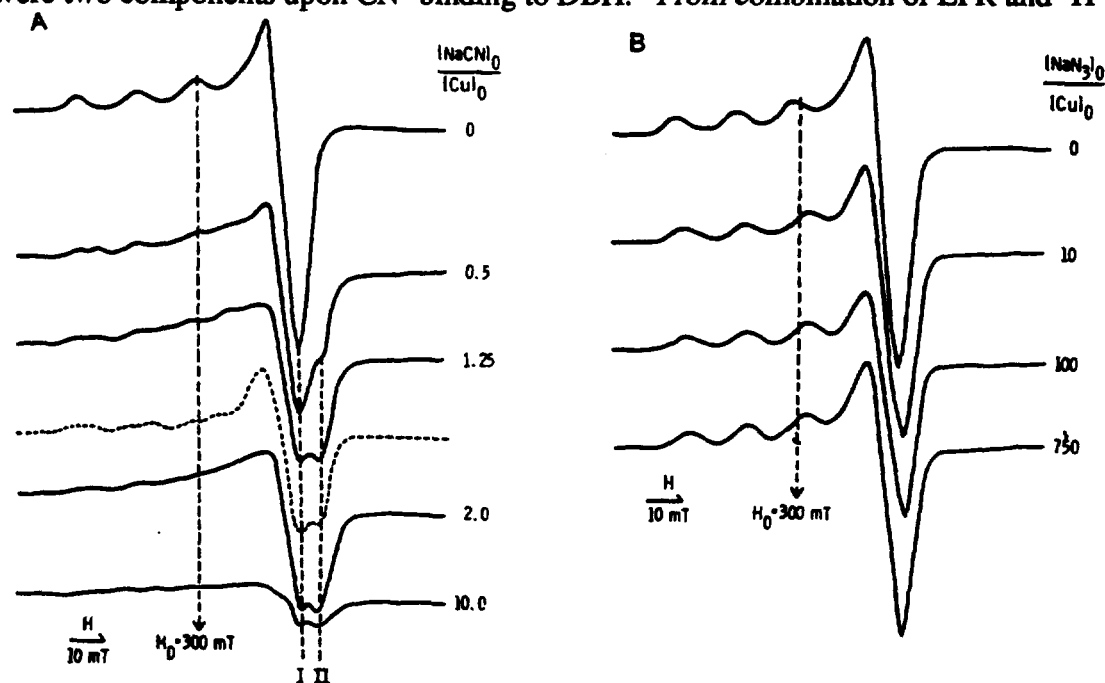


Figure 1. 16. (A) Change of EPR spectra of ^{63}Cu -dopamine β -hydroxylase solution with increase of the $[\text{NaCN}]_0 / [\text{Cu}]_0$ ratio. The dashed line is the spectrum simulated on the basis that the solution consisted of equal proportions of component I and component II. (B) Change of EPR spectra of ^{63}Cu -dopamine β -hydroxylase solution with increase of the $[\text{NaN}_3]_0 / [\text{Cu}]_0$ ratio (Obata et al, 1987).

NMR relaxation studies, Obata suggested (Obata et al, 1987) that component I represented a Cu (II) site with two water molecules and component II represented a Cu (II) site that had lost one water molecule as the result of ligation of one CN^- . In the case of N_3^- ligand, no reduction of Cu (II) was observed over the whole range of the ligand concentration. The A_{\parallel} (hyperfine splitting constant) value was larger in the Cu (II)- CN^- complex than in the native site, but smaller than in the Cu (II)- N_3^- complex, although the g_{\parallel} values were smaller in both complexes than in the native site.

In this study, EPR, IR, and CD spectra have been used extensively. Electron Paramagnetic Resonance (EPR) can only be applied to species having one or more unpaired electrons. This covers a fairly wide range of substances, including free radicals, biradicals, and many transition metal compounds. EPR spectra provide information about numbers of unpaired electrons and the electronic structure of the magnetic species. In the presence of a magnetic field, B_0 , a molecule or ion having one unpaired electron has two electron spin energy levels, given by: $E = g\mu_B B_0 M_s$, where μ_B is the Bohr magneton, M_s is the electron spin quantum number (+ 1/2 or - 1/2) and g is a proportionality factor, equal to 2.00230 for a free electron. For radicals this factor is normally very close to the free-electron value, between 1.99 and 2.01, but for transition metal compounds spin-orbit coupling and zero-field splitting. It is the transitions between such energy levels, induced by the application of an appropriate frequency radiation, that are studied by EPR. The frequencies required depend on the strength of the magnetic field.

Vibrational spectroscopy has been extensively used because it is a tool for identifying and measuring concentrations of samples without needing to know anything about how or why the spectra arise. For a molecule as composed of massive particles (atoms) joined by

the connections with the bonding electrons, its motions can be calculated classically using Newton's Laws of Motion $F(x) = -kx$, where x is a displacement from equilibrium, and k is the force constant. The vibrational motions that involve no overall translation or rotation of the molecule can be resolved into various oscillations about the equilibrium structure. The characteristic vibration frequency is $\nu = 1/2\pi \sqrt{k/\mu}$, where μ is a deduced mass for the particular motion.

Circular Dichroism (CD) has been employed increasingly to gain insight into the details of the coordination of metals with proteins and to characterize the properties and structures of anion complexes of copper proteins. CD measures the differential absorption of polarized light, therefore, measures the existence of molecular symmetry as well as the details of the coordination geometry of metals and their immediate environment. The primary, secondary, tertiary, and quaternary protein structure, the amino acid side chains which serve as metal ligands, the nature and environment in three-dimensional space, symmetry, charge, polarity, water etc. must all be considered.

The aim of this dissertation is to study the structures of copper centers through anion-binding to DBH and to understand the catalytic role of Cu in "non-blue" copper proteins. Both spectroscopic (including UV / vis, IR, EPR, and CD) and kinetic methods are used in these studies. The half-apo DBH that contains only one copper per subunit (only Cu_b) has been prepared successfully for the first time. In this study, the comparison of spectroscopy between fully reconstituted DBH (2 coppers / subunit) and half-apo DBH (1 copper / subunit) were made; therefore, the environments of two copper centers in each subunit were investigated. DBH inhibition by anions, N_3^- and SCN^- , has been examined so that some insight into the mechanism of the DBH reaction can be obtained.

CHAPTER II

DBH PREPARATION AND CHARACTERIZATION

2. 1. Isolation and Preparation of DBH

Bovine adrenal glands were collected from a local slaughterhouse, placed on ice, and dissected to remove the medulla tissue. Every attempt was made to process the tissue as quick as possible. The medullas were quick-frozen in liquid nitrogen immediately after dissection and stored without thawing until use. The medullas (250 g) were pulverized at 77 K in a Waring blender cooled with liquid N₂ previously; the powder was added to 750 ml of 20 mM potassium phosphate buffer, pH 7.5, containing 0.5 mM phenylmethylsulfonyl fluoride (PMSF) and 50 µg / ml catalase. The suspension was then stirred until the ice was just melted, and during this process the temperature was not allowed to rise above 2 °C. The crude suspension was homogenized at 12,000 rpm for 3 min by using a Brinkman PT 3000 homogenizer fitted with a PT-DA 3020 / T generator. This homogenate was centrifuged at 27,000 g for 60 min. The pellet was discarded, and the supernatant was filtered through two layers of cheesecloth. Solid ammonium sulfate was slowly added into the solution to a final concentration of 0.106 g / ml, and the suspension was stirred for 60 min at 4 °C. It was then centrifuged at 27,000 g for 90 min; the pellet was discarded, and the supernatant was filtered through cheesecloth again. After slowly adding a further 0.106 g / ml solid ammonium sulfate, the suspension was stirred for 60 min at 4 °C and the suspension was centrifuged at 27,000 g for 100 min. The

supernatant was discarded, and the pellet was dissolved in 150 ml of 50 mM potassium phosphate buffer, pH 7.5. The solution was then homogenized at 5,000 rpm with the Brinkman PT 3000 homogenizer. Homogenization should be done very carefully to avoid making too much foam. The homogenate was dialyzed overnight against 2 liters of 50 mM potassium phosphate buffer, pH 7.5, to remove excess ammonium sulfate and to allow complete dissolution of enzyme. The dialyzed sample was then centrifuged at 150,000 g for 60 min to remove membranous material and filtered once more through cheesecloth to remove lipid floating on the surface of the supernatant.

5 ml Concanavalin A (ConA) - sepharose 4B (Sigma) was packed in a 0.9 * 3.5 cm column washed with Milli-Q water to remove anti-bacterial reagent (NaN_3) in ConA and equilibrated with 30 - 50 ml potassium phosphate buffer, pH 7.5. Then, the supernatant described above was applied to the ConA-Sepharose 4B column at a flow rate of 20 ml / hour. The column was washed overnight with 50 mM potassium phosphate containing 150 mM sodium chloride, pH 7.5, to elute nonspecifically bound proteins and was then given a final wash with 40 ml of chloride-free 50 mM potassium phosphate buffer, pH 7.5. The bound glycoproteins including DBH were eluted at room temperature with 90 ml of the same buffer containing 5 % α -methylmannoside.

The eluant from ConA was concentrated to approximately 5 ml or less, centrifuged to remove any particulate matter, and injected via a superloop onto a Zorbax GF-450 XL high-resolution gel-filtration column (Du Pont) attached to a Pharmacia LKB Biotechnology Inc. fast-protein liquid chromatography system (FPLC). The FPLC was programmed to allow the injection of the sample from the superloop, the elution of the enzymes from the column, and the collection of DBH automatically. The column was

pre-equilibrated with 200 ml 50 mM potassium phosphate buffer, pH 7.5. The eluant was monitored by UV absorbance at 280 nm. The UV spectrophotometer was also connected to the FPLC system. DBH was eluted at a retention volume of approximately 40 ml as the second sharp reproducible peak among a total of four peaks (see Fig. 2.1.). The purified enzyme was sterilized and stored in liquid N₂. The purified enzyme was tested by the native gel electrophoresis, displaying a single band.

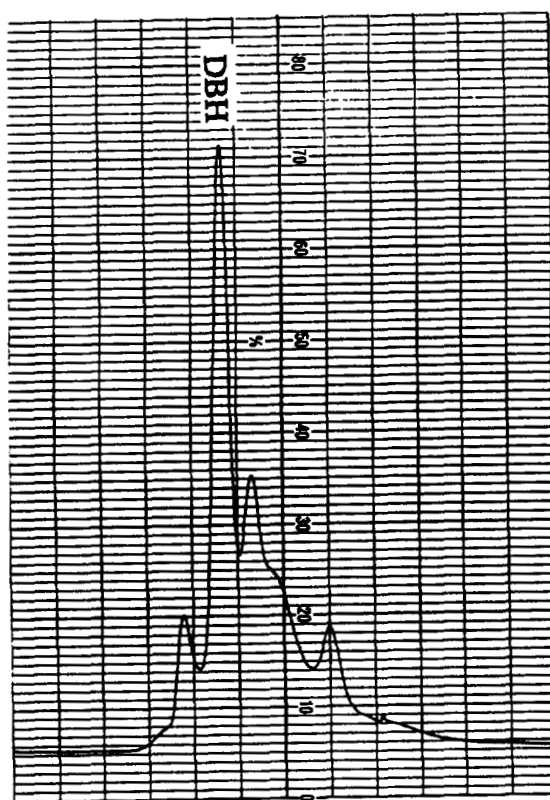


Fig. 2.1. The eluents from FPLC. The second band is DBH peak.

2. 2. Protein Concentration Measurement

Protein concentration was determined by UV spectrophotometry. $A^{1\%}_{280} = 1.24$ (Skotland and Ljones, 1977).

2. 3. Enzyme Activity Measurement

Enzyme activity was determined from the rate of O_2 consumption of the enzyme catalyzed reaction measured by a Clark oxygen electrode (Rank Brothers, Bottisham, Cambridge) connected with a Cole Parmer strip-chart recorder. The electrode was inserted into a thermostated cell with 3 ml - 6 ml capacity, which was also equipped with a magnetic stirrer. A stock solution of tyramine (20 mM) and catalase (0.1 mg / ml) (Sigma, 1860 units / ml) was dissolved in air-saturated, 200 mM acetate buffer, pH 5.0. Catalase was used to remove H_2O_2 produced by the autooxidation of ascorbate. 5 ml of this solution was pipetted into the cell, and a solution of diluted DBH (10 - 50 μ l) was added. The assay solution was allowed to equilibrate at 25 °C for 2 min. 50 μ l of 1 M ascorbate was injected into the chamber to initiate the reaction, giving a final ascorbate concentration of 10 mM. The electrode was calibrated with 99.9 % Ar ($[O_2] = 0 \mu$ M) and air-saturated buffer ($[O_2] = 236 \mu$ M) (Hodgman et al, 1963). The specific activities of preparations used in the study, as determined by this assay, varied between 18 and 24 units (μ mol O_2 consumption / min) per mg protein (calculation see equation 2.1.). However, our assay conditions were different from those used by other groups, since we have chosen 25 °C (rather than 37 °C) as the temperature for routine measurements. The specific activities of our preparations were also assayed under the conditions used by Colombo and co-workers (Colombo et al, 1987; 37 °C, 200 mM acetate at pH 5.00, 10 mM fumarate, 15 mM tyramine, 20 mM ascorbate, 5400 units of catalase). It was unclear from the reports in the literature what value these authors used for the concentration of dissolved O_2 in solution at 37 °C. We have calculated a value of $[O_2]$ at 37 °C for 176 μ M from the tables of solubilities of dissolved gases given by Hodgman et al (Hodgman et al, 1963). Using this value, our specific activities were 2 times greater than those measured under their conditions at 37 °C.

$$\text{specific activity} = \frac{\text{oxygen consumption } (\mu\text{M} / \text{min}) \cdot \text{total volume of assay solution (ml)} \cdot 1000}{\text{enzyme added (ml)} \cdot \text{enzyme concentration (mg / ml)}} \\ (\mu\text{mol} / \text{mg min})$$

Equation 2. 1.

2. 4. Copper Content Analysis

Copper concentration was analyzed by a Varian Techtron AA-5 flame atomic absorption spectrophotometer. A series of $\text{Cu}(\text{NO}_3)_2$ solutions, concentration ranging from 3 μM to 25 μM , prepared with analytical accuracy were used as copper standards. The DBH was diluted to the copper concentration in the range of 3 μM to 25 μM for the measurement. The copper lamp was turned on at 3 mA current and warmed up for at least 30 min; the slit was adjusted to 100 μm , wavelength was at 324.65 nm. After igniting the gas mixture of acetylene and air, the copper samples were sucked into the flame of the AA (atomic absorption) through a plastic tube which was soaked in Milli-Q water before using. By comparing the magnitude of DBH signal with that of copper standards, the copper concentration of enzyme was estimated. The calculation of the number of copper per enzyme was shown in equation 2.2.

$$\text{The number of Copper / enzyme} = \frac{\text{Copper concentration } (\mu\text{M})}{\text{DBH concentration (mg/ml)} / 0.29 \text{ (mg / nmol)}}$$

Equation 2. 2.

2. 5. Copper Reconstitution

As isolated, DBH contained approximately four copper atoms per tetramer, and was more than 50 % in the Cu (I) form as determined by double integration of the EPR spectra. Samples for spectroscopic measurements were routinely reconstituted to seven or eight copper atoms per tetramer via addition of a 20-fold excess of $\text{Cu}(\text{NO}_3)_2$ into the enzyme tetramer in 50 mM potassium phosphate buffer, pH 7.5, followed by several cycles of washing with the same phosphate buffer, in a Centriprep 30 concentrator (Amicon). The enzyme was finally concentrated to the concentration that was needed for different experiments.

2. 6. Preparation of Fully Oxidized DBH:

Purified DBH was oxidized with 50 equivalents $\text{K}_3\text{Fe}(\text{CN})_6$ for 5 min and washed exhaustively by ultrafiltration in a centriprep 30 concentrator (Amicon) with 50 mM phosphate buffer to remove $\text{K}_4\text{Fe}(\text{CN})_6$ and excess $\text{K}_3\text{Fe}(\text{CN})_6$. The percentage of Cu (II) in the protein was measured by comparing the copper concentration through flame atomic absorption with that determined from double integration of the EPR spectra. EPR spectra were measured by a Varian E109 EPR Spectrometer. The temperature of the cavity was stabilized at - 150 °C by a Varian Variable Temperature Controller.

CHAPTER III

THE FULLY OXIDIZED DBH-N₃⁻ COMPLEX

3. 1. Introduction

As described in chapter I, studies of anions (N₃⁻, CN⁻ and SCN⁻) binding to type II copper proteins can provide much useful information about structures of copper centers and mechanisms of catalytic reactions. In this chapter, the characterization and interpretation of UV / vis, CD, and IR spectroscopy of the azido-DBH complex will be described via comparison with other type II copper proteins and relevant inorganic Cu (II)-azido complexes.

Many type II copper proteins (SOD, amine oxidase, type II center of laccase, galactose oxidase) have an intense N₃⁻ to Cu charge transfer band around 400 nm that is one of the most important features of N₃⁻ - Cu complexes. At the same time, the CD spectrum of the DBH-azido complex seems to be unique among non-blue copper protein-azido complexes. Since CD spectra reflect the symmetry of a molecule, analysis of the CD spectra will supply information about the configuration of the copper centers in the DBH-azido complex. IR spectra shows that N₃⁻ vibrational antisymmetric stretching frequencies shift after binding to DBH; the magnitude of the shift depends on the environment of the

copper centers.

We have also measured thermodynamic data on azide coordinating to DBH; ΔH , ΔS , and ΔG provide information on the properties of the N_3^- binding process and of the ligand dissociation process. The results of all these experiments point to the conclusion that the two copper centers of each subunit are inequivalent structurally and functionally.

3. 2. Experimental Methods

3. 2. 1. Azide to DBH Charge Transfer Transition

A Perkin Elmer λ -9 spectrophotometer was used to monitor the absorbance change of the DBH - azide complex. The fully oxidized DBH was centrifuged at 7,000 rpm for 3 min. to remove the protein precipitate formed during the sample preparation. 1 ml DBH (around 1 - 5 mg / ml) contained in a 1.0 cm path-length sample cuvette was scanned between 500 - 300 nm as the protein background because only a single beam was used. Then DBH was titrated with 5 μ l, 0.05 M — 20 μ l, 5 M azide, equilibrated for 5 min, and scanned again between 500 - 300 nm. This process was repeated until the spectrum showed no further change. 0.25 μ mol to 100 μ mol of azide was added into the system each time. The difference spectra were obtained by subtracting the absorbance of fully oxidized DBH from that of the DBH-azide complex. The data were corrected for the protein dilution and protein losses due to protein precipitation during the titration.

3. 2. 2. CD Spectra of DBH- N_3^- and SOD- N_3^- Complexes.

CD spectra were measured with a JASCO J-500 A spectropolarimeter (Dr. H. P.

Bachinger group, Shriners Hospital, Portland, Oregon) interfaced to a computer. A round thermostated cell with a 1 ml capacity and 1 cm pathlength was used. The temperature during the data collection was kept at 20 °C. The DBH CD spectrum was obtained by subtracting the scan of 50 mM potassium phosphate buffer, pH 7.5, from the scan of DBH (around 5 mg / ml in the same potassium phosphate buffer). The CD spectrum of the DBH-N₃⁻ complex was obtained by subtracting the CD scan of fully oxidized unliganded DBH from that of the DBH-N₃⁻ complex. A similar procedure was applied to the SOD-N₃⁻ complex.

3. 2. 3. DBH-azide infrared spectra

Infrared spectra were measured by a Perkin-Elmer 1800 FTIR spectrophotometer interfaced to a Perkin - Elmer 7500 computer. The IR cell employed rectangular CaF₂ windows (McCarthy Scientific Co.) separated by a 0.025 mm Teflon spacer (McCarthy Scientific Co.). The whole assembly was confined within a thermostated copper block. CaF₂ windows were cleaned with concentrated permanganic acid (two to three crystals of KMnO₄ dissolved in 5 - 10 ml of 98 % H₂SO₄) to oxidize surface organic contaminants before use. Samples of about 15 µl were injected into the cell through a septum with a syringe.

Because NaN₃ has a strong IR signal at 2048 cm⁻¹, the DBH-azide IR spectra can be obtained only through the difference spectra of the azido-DBH complex and free azide. The following technique was developed in order to obtain accurate difference IR spectra. For the low azide concentration DBH samples, 0.1 ml of fully reconstituted, oxidized DBH (about 2 mM in copper) was added to an equivalent amount of azide. It was then

washed by ultrafiltration with a 50 mM phosphate buffer in a Centricon-30 concentrator to remove free azide, and azide IR spectra were monitored until free azide IR peaks were quite small. The IR spectra of filtrate and retentate were recorded, and the DBH-azide spectrum was obtained from the difference spectra of the filtrate and the retentate. When the DBH sample was titrated with a large excess of azide dissolved in the 50 mM phosphate buffer, pH 7.5 to make the DBH-azide sample with high azide concentration, the free azide was removed slowly by ultrafiltration in a Centricon 30 concentrator as the procedure described for preparing low azide concentration sample. The spectra of the filtrate and the retentate were recorded again. 200 scans were accumulated for every spectrum of both sample and blank. During the scan, the temperature of the cell was maintained at 10 °C with an external water bath. The same procedure was applied to SOD, whose final copper concentration was about 4 mM.

3. 3. Results and Discussion

3. 3. 1. The absorption spectrum of azide - Cu (II) charge transfer transition

The optical spectrum of azido-DBH at room temperature is presented in Fig. 3. 1. A single intense band was observed at 385 nm, which may be assigned as an azide to Cu (II) charge-transfer transition. The extinction coefficient, $\epsilon = \Delta A / CL$ ($C = \text{Cu}$ molar concentration; $L = \text{cuvette pathlength in cm}$), at room temperature was $3,100 \text{ M}^{-1}\text{cm}^{-1}$, which was normalized to the copper concentration in the protein.

Azido-Cu (II) complexes generally display an intense absorption band in the near

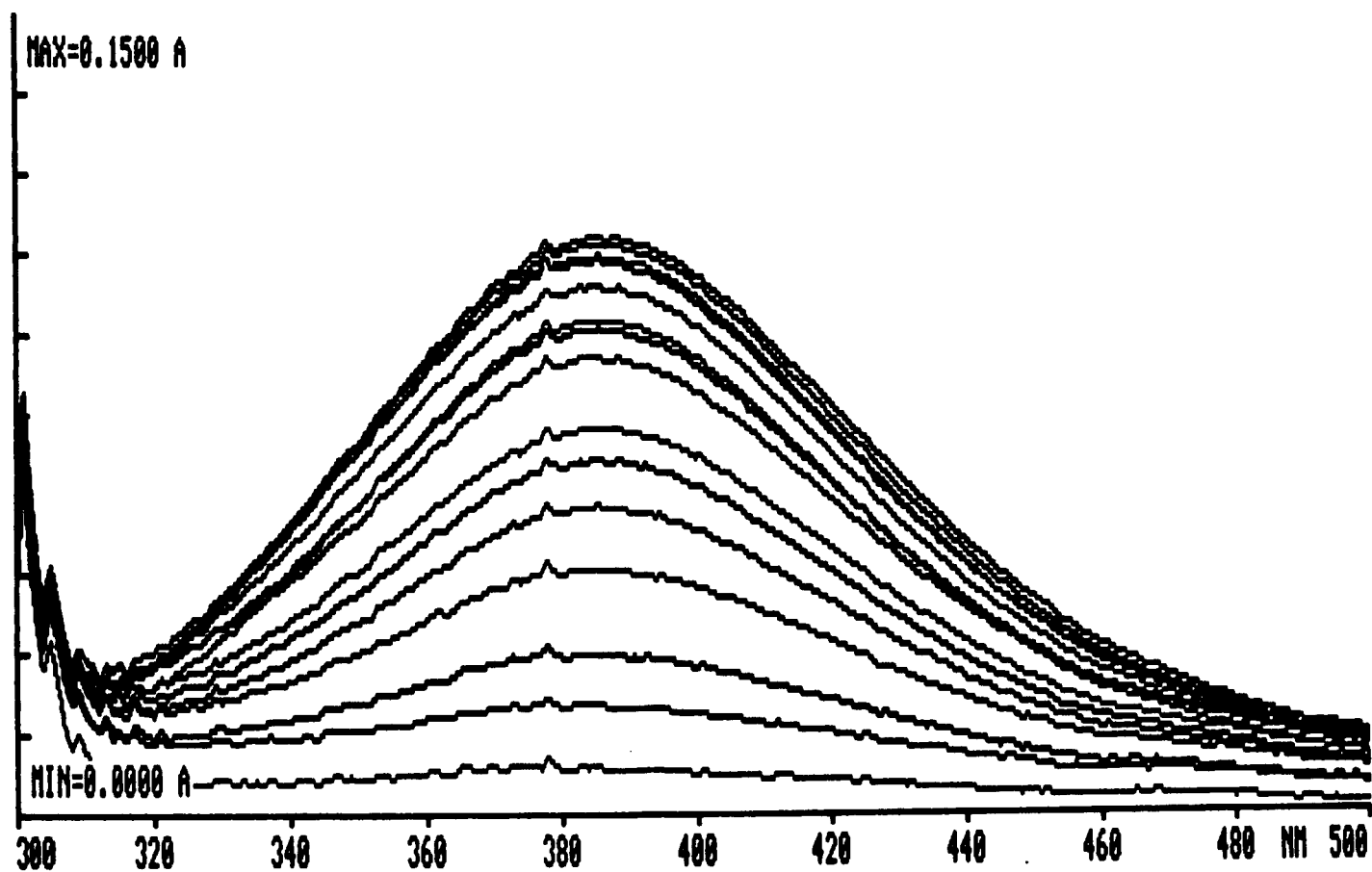
DBH - N₃ titration

Fig. 3. 1. Absorption spectra of the azido complex of fully oxidized dopamine β -hydroxylase at the room temperature. The enzyme concentration was about 1 mg / ml in 50 mM phosphate buffer, pH.7.5. Azide concentrations from bottom to top are 0 mM, 0.25, 1.24, 6.16, 11.03, 15.85, 40.05, 64.01, 87.74, 134.53, 203.05, 291.47, 376.70, 458.90 mM

ultraviolet region. There are three structurally distinct modes of copper (II) - azide coordination in which a single azide may be bound in a terminal (Ziolo et al, 1972; Karlin et al, 1987 a), μ -1, 3 (McKee et al, 1981; Sorrell et al, 1985), or μ -1, 1 (Karlin et al, 1987 b; Sorrell, 1986; Kahn et al, 1983) geometry (see Table 1.2.). Absorption, resonance Raman, and infrared spectroscopy have been used to identify spectral features of azide bound to copper (II) in model compounds with all three geometries (Pate et al, 1989). The absorption bands around 400 nm have been assigned by Raman excitation profiles to azide to copper charge transfer transitions. Absorption spectra for each of these complexes (from Pate et al, 1989) are shown in Fig. 3.2. The terminally bound azide shows an intense band around 350 - 400 nm (ϵ around $2000 \text{ M}^{-1} \text{ cm}^{-1}$, see Fig. 3. 2.a). The absorption spectra of the bridging μ -1, 3 azide-copper complexes reveal the presence of an intense charge-transfer band near 375 nm (ϵ around $2300 \text{ M}^{-1} \text{ cm}^{-1}$) with an associated shoulder near 440 nm (ϵ is about $1200 \text{ M}^{-1} \text{ cm}^{-1}$, see Fig. 3. 2. b). A Gaussian analysis resolves these features into two charge transfer bands at 365 nm

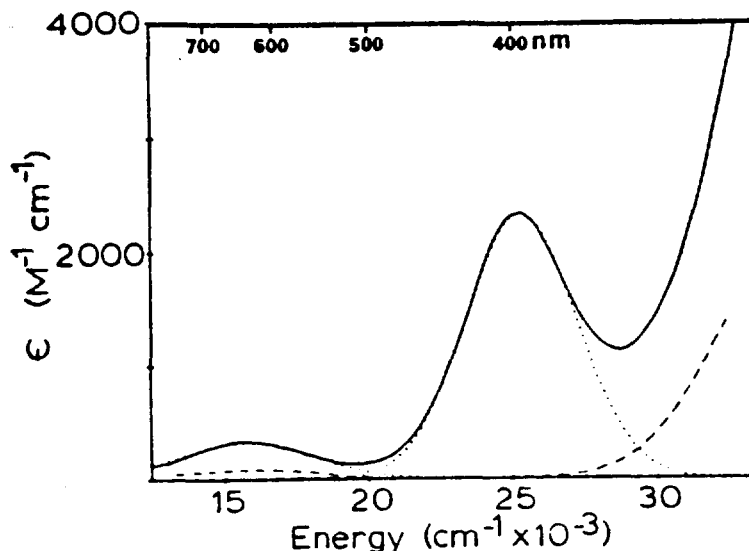


Fig. 3. 2. a Absorption spectra of terminally bound azide-Cu complexes: $[\text{Py}_2\text{-Cu-(NO}_3\text{)(N}_3\text{)}]$ (—); $[\text{Py}_2\text{-Cu-(NO}_3\text{)}]$. Gaussian components of the azide complexes are indicated by (...) (from Pate, 1989).

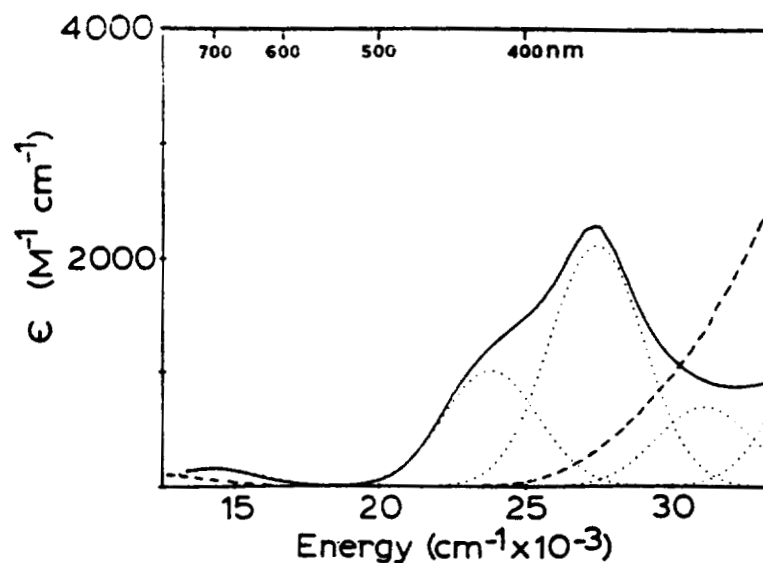


Fig. 3. 2. b Absorption spectra of acetone nitrile solutions of $[\text{Cu}_2(\text{L-Et})(\text{N}_3)][\text{BF}_4]_2$ (—) and $[\text{Cu}_2(\text{L-Et})(\text{OAc})][\text{ClO}_4]_2$ (---). Gaussian components of the azide complex are indicated by (···).

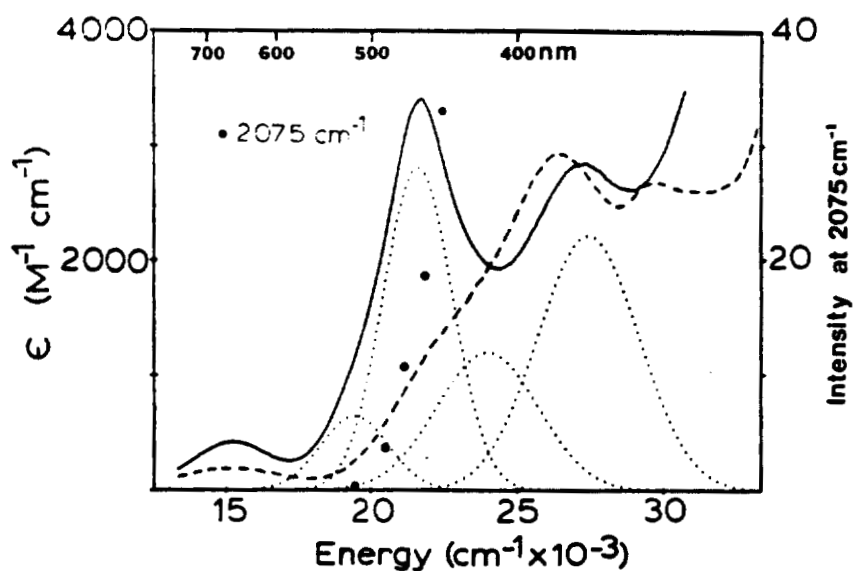


Fig. 3. 2. c Absorption spectra of an acetone nitrile solutions of $[\text{Cu}_2(\text{L-O-})(\text{N}_3)][\text{PF}_6]_2$ (—) and $[\text{Cu}_2(\text{L-O-})(\text{OH})][\text{PF}_6]_2 \cdot \text{THF}$ (---). The resonance Raman profile of the 2075-cm^{-1} feature is denoted by (●). Gaussian components of the azide complex are indicated by (···). The scale at right indicates the relative intensity of the asymmetric intraazide stretch.

(27400 cm^{-1} , $\epsilon = 2100 \text{ M}^{-1} \text{ cm}^{-1}$) and 420 nm (23800 cm^{-1} , $\epsilon = 1000 \text{ M}^{-1} \text{ cm}^{-1}$) for $[\text{Cu}_2(\text{L-Et})(\text{N}_3)][\text{BF}_4]_2$. μ -1,1 bridged Cu (II) complexes exhibit an intense charge-transfer band at 460 nm ($\epsilon \approx 3000 \text{ M}^{-1} \text{ cm}^{-1}$) and other unresolved features at higher energy (Fig. 3. 2. c).

Although two azide to copper (II) charge-transfer transitions are predicted for a terminal copper (II) azide complex (Himmelwright et al, 1980), a comparison of the spectroscopic features of model compounds with those of non-azide analogs reveals only one observed charge-transfer band around 400 nm. The 400 nm band is assigned as the $\Pi_{\sigma\text{nb}}$ -to-copper (II) charge-transfer transition (see Fig.1.15.). The comparison of the CT band of azido-DBH to the model compounds suggests that azide binds to Cu (II) terminally. The optical spectrum of the azide - SOD complex, which is known to originate from a terminal monomeric Cu (II) - azide adduct also exhibits a single CT band at 375 nm (Dooley and McGuirl, 1986; Bertini et al, 1985), providing further evidence for terminal azide coordination in DBH.

As described in Chapter I, the wavelength of azide to Cu (II) charge transfer is affected by the configuration of copper centers (see Table 1.2.). The perturbation of a square-planar structure toward a tetrahedral or trigonal bipyramidal structure will cause a wavelength shift to lower energy (longer λ_{max}) of LMCT transition. Square planar molecules, $[\text{Cu}(\text{dien})\text{N}_3]^+$ and $[\text{Cu}(\text{terpy})\text{N}_3]^+$, have LMCT transitions at 346 and 348 nm, respectively; but $[\text{Cu}(\text{Me}_5\text{dien})\text{N}_3]^+$ (see Table 1.2.), which has a configuration between square planar and trigonal pyramidal, has a LMCT band at 375 nm; a trigonal bipyramidal molecule, $[\text{Cu}(\text{Me}_6\text{dien})\text{N}_3]^+$ has an absorption band at 385 nm, which is the same as the λ_{max} of the DBH-azide complex. It may indicate that the copper centers in the DBH-

azide complex do not display a square planar coordination; or it can be said that they are closer to a tetragonal or trigonal bipyramidal configuration than that in the SOD-azide complex (375 nm) (Dooley and McGuirl, 1986 a). In native DBH, the copper center is thought to be in a tetragonal geometry (Stewart and Klinman, 1988) which may be retained in the azide adduct.

The value of the extinction coefficient of azide to Cu (II) charge transfer transition ($3,100 \text{ M}^{-1}\text{cm}^{-1}$) indicates that azide binds to Cu (II) equatorially in the azido-DBH complex. EPR and optical titration of model compounds (Himmelwright et al, 1980) have established that $[\text{Cu}(\text{dien})\text{N}_3]^+$ binds one azide in the equatorial plane; the azide to copper CT occurs at 345 nm with an extinction coefficient of $2,600 \text{ M}^{-1} \text{ cm}^{-1}$. Azide binding is pH dependent with $K = 40 \text{ M}^{-1}$ at pH 7.2. Axial coordination of azide has been investigated by the model compound, Cu[2,3,2-tet], which has four amine nitrogens forming an equatorial plane such that azide is forced to bind at the axial position, which causes very low extinction coefficient for the azide-Cu complex. The binding constant can be extremely low as well, on the order of 1 M^{-1} or less, and no intense charge-transfer band is observed.

Non-blue copper proteins, bovine amine oxidase (Dooley and Golnik, 1983; Dooley and Cote, 1985), SOD (Dooley and McGuirl, 1986 a; Bertini et al, 1980; Bertini et al, 1985), galactose oxidase (Ettinger and Kosman, 1981), pig plasma amine oxidase (Barker et al, 1979), and met apo-hemocyanin (Himmelwright et al, 1980), all show a single equatorial azide coordinating at the copper centers and display a similar intense charge-transfer band. Bovine plasma and kidney amine oxidases are dimers and contain two well separated, non-interacting copper ions in each enzyme, confirmed by EPR and NMR measurements

(Barker et al, 1979). Although the two subunits in the bovine enzyme appear to be identical, two groups of workers have reported that the two copper ions in the native enzyme are in different environments (Barker et al, 1979; Kluetz, M. D. and Schmidt, P. G., 1980). However, on adding the inhibitors, azide or cyanide, the two copper centers become identical (Barker et al, 1979). Both coppers appear to be bonded by three nitrogen and two oxygen ligands in a tetragonal array. Two oxygen ligands are apparently water molecules, one at an axial and the other at an equatorial position. Azide and cyanide ions displace the equatorial water molecule (Dooley and Golnik, 1983; Dooley and Cote, 1985). Similarly, the copper center of galactose oxidase in which there are two histidine ligands, two tyrosine ligands (one at the equatorial position and the other at an axial position), and one equatorial water ligand. Azide and cyanide also replace the equatorial water ligand (Ettinger and Kosman, 1981).

The requirement for equatorial coordination of azide to a copper center may be understood in the following way (Dooley and Golnik, 1983; Spira-Solomon and Solomon, 1987). Tetragonal Cu (II) complexes have four ligands with relatively short bond lengths, in approximately planar symmetry; axial ligands (when present) are at a considerably longer distance. In such a complex, the Cu (II) $d_{x^2-y^2}$ orbital located within the equatorial plane contains the unpaired electron. Energies and especially intensities of charge-transfer transitions depend critically on overlap between the electron donor and acceptor orbitals; an $\epsilon > 1000 \text{ M}^{-1} \text{ cm}^{-1}$ requires good overlap and therefore equatorial coordination. Since DBH has a very high ϵ , like other type II copper proteins, DBH is expected to bind azide equatorially.

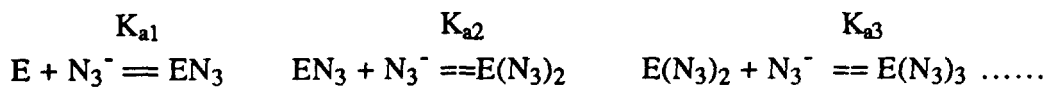
The anion binding constant can be obtained through Hill plot (see equation 3.1.). The Hill

equation is usually used for describing the cooperative behavior of ligands coordination to a protein. In the Hill equation, n is called the Hill constant, R is defined as the fraction of completely liganded enzyme molecules (C_{ES} / C_E°) or the fractional saturation. When the Hill constant, n , is unity, the binding process is noncooperative, in which the first ligand binding does not affect binding of the second, third, and fourth ligand; each ligand binds to an enzyme independently. If $n > 1$, the ligand binding becomes positively cooperative. In this case, the binding of the first ligand will increase the binding constant of the second ligand, and the second ligand will accelerate the third ligand binding. If $0 < n < 1$, the ligation of ligands exhibits negative cooperativity, which means that the first ligand will destabilize the second ligand binding. The second ligand has a smaller binding constant than the first one. The maximum value for n is the number of binding sites per enzyme molecule. In practice, the Hill constant, n , is usually smaller than the number of binding sites. It also gives a measurement of cooperativity — the farther n is from 1, the larger the cooperativity.

$$\log K_a + n \log C_s = \log y \quad \text{Equation 3.1.}$$

$$\text{where } y = \frac{C_{ES_n}}{C_E^\circ - C_{ES_n}} = \frac{R}{1 - R}$$

$$C_s = C_{\text{azide}^\circ} - n[\text{DBH}(\text{N}_3)] \approx C_{\text{azide}^\circ} \quad \text{when azide concentration is large excess}$$



$$K_a = (K_{a1} K_{a2} K_{a3} \dots K_{an})^{1/n}$$

Figure 3. 3. shows a Hill plot for azide binding to DBH. K_a , obtained from the intercept of the Hill plot is 240 M^{-1} , which represents the average equilibrium constant of every bound azide molecule at DBH. The Hill constant, n , is 0.69 at room temperature, indicating that the binding of azide to DBH exhibits negative cooperativity. A Hill constant less than 1 indicates that the coordination of N_3^- ion to the Cu (II) center of DBH is a negative cooperative process; therefore, there must be more than one N_3^- binding site in each enzyme molecule. The binding of the first N_3^- ion inhibits the binding of the second ion due to either a conformational change of the enzyme or an interaction between these anion molecules.

Some non-blue proteins, such as SOD (Dooley and McGuirl, 1986 a), amine oxidase (Dooley and Golnik, 1983; Dooley and Cote, 1985; Barker et al , 1979), or galactose oxidase (Ettinger and Kosman, 1981), have only one Cu (II) center per subunit, and azide binding is noncooperative; they all exhibit linear Scatchard plots. Because they have only one Cu (II) center per subunit, there is no interaction between copper centers, whereas DBH has two copper centers per subunit that may be close enough to interact with each other.

3. 3. 2. CD spectra of DBH-azide and SOD-azide complexes

The circular dichroism (CD) spectrum of fully oxidized native DBH is shown in Fig. 3.4.a. There is no significant dichroism in the region of 700 - 300 nm. Bovine SOD displays a positive CD band at 352 nm (see Fig. 3.5.a, also see Fig. 3.6. from Fee and Valentine, 1977), which is assigned to histidine to copper charge transfer transition. The band around 600 nm is assigned to d-d transition.

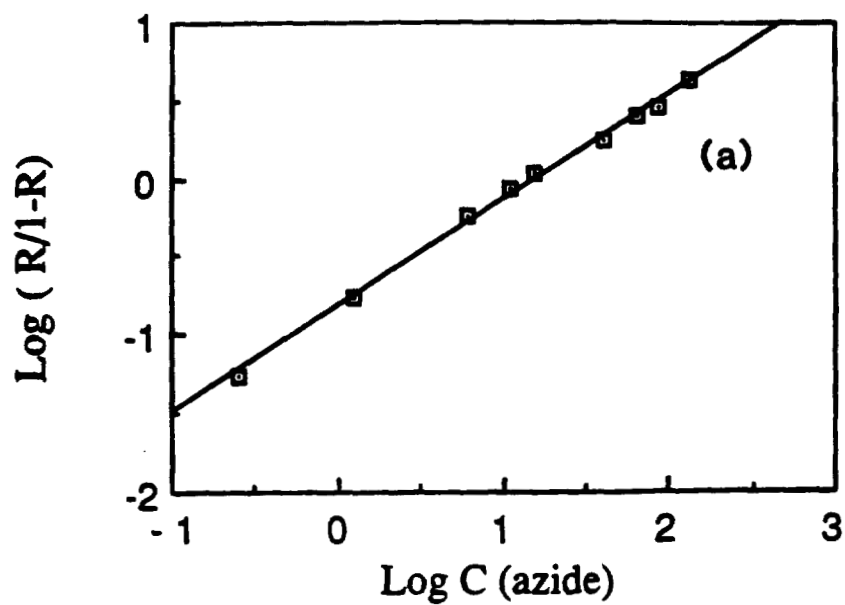


Fig. 3. 3 Hill plot for titration of dopamine β -hydroxylase with azide at room temperature.

Conditions were as given in Figure 3. 1. $R = (A - A_0) / (A_{\infty} - A_0)$. $C =$
concentration of azide.

Unlike other type II copper proteins, DBH lacks both charge transfer transitions and d-d transitions from 550 to 700 nm. Another type II copper protein, beef plasma amine oxidase, shows Cu (II) ligand field CD transitions at 660 (positive) and 800 (negative) nm, along with an organic cofactor band at 410 nm (positive) (Dooley and Cote, 1985). Galactose oxidase also displays d-d transitions at 600 nm (negative) and 800 nm (positive) (Ettinger, 1974). Another band near 445 nm in the galactose oxidase CD spectrum is possibly derived from a combination of d-d transitions, imidazole to copper charge transfer, and tyrosine-to-copper charge transfer (Amundsen et al, 1977; Solomon et al, 1976; Ito et al, 1991). The intense positive band at 314 nm is apparently another charge transfer transition involving O from tyrosine (Amundsen et al, 1977). The lack of CD absorbance in the visible region for DBH may indicate different symmetries between the copper centers in DBH and in other type II copper proteins. The copper centers in DBH are either in more asymmetric configuration than other non-blue copper proteins or their d-d bands appear at a longer wavelength than 700 nm. SOD has four His ligands, and one of them bridges to the Zn atom. Amine oxidases are thought to contain three His ligands and one H₂O at the equatorial positions and one H₂O at the axial position (Dooley and Cote, 1985). On the other hand, galactose oxidase has two His ligands, one H₂O, and a tyrosine ligand at the equatorial positions, and one tyrosine at the axial position (Ito et al, 1991). It seems that the ligands at a copper site do not affect the symmetry very much; but the protein conformation probably plays a more important role on the symmetry of an active site. Since DBH lacks phenolate-to-Cu (II) charge transfer bands in the CD spectra similar to those exhibited by galactose oxidase, it is impossible for DBH to contain an O-ligand from tyrosinate, but some other ligands (an O-type ligand from an amino acid other than tyrosinate) may exist.

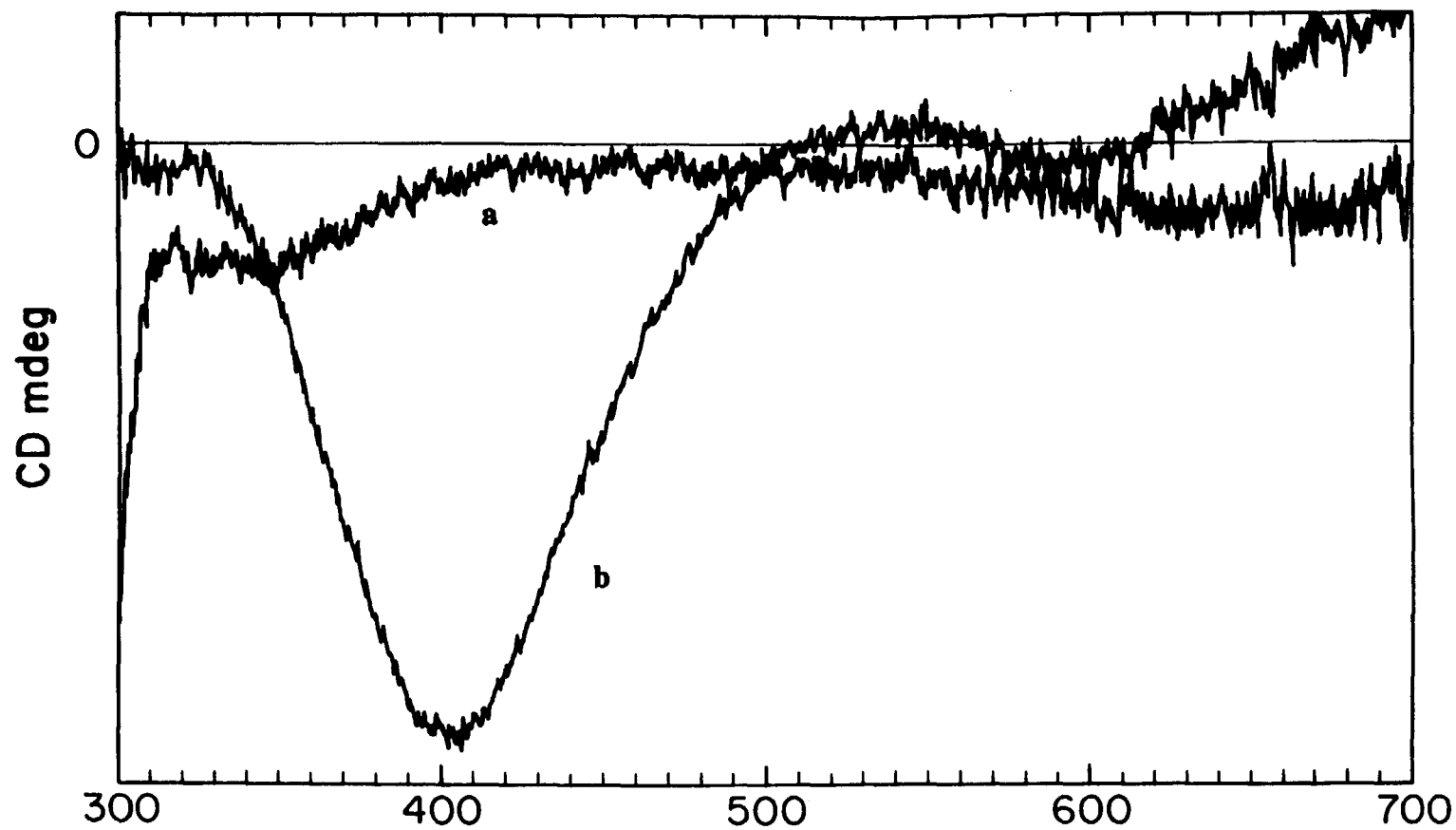


Fig. 3. 4. CD spectra at 20 °C of fully oxidized dopamine β -hydroxylase (protein concentration is about 5 mg / ml) (a) and the DBH-azide complex in the presence of 700-fold azide (b). The temperature during the data collection was kept at 20 °C. The scan speed was 20 nm/min; step resolution 0.1 nm; sensitivity 1 mdeg/cm; time constant 2 sec.; beam width 1.0 nm; the number of scans 2.

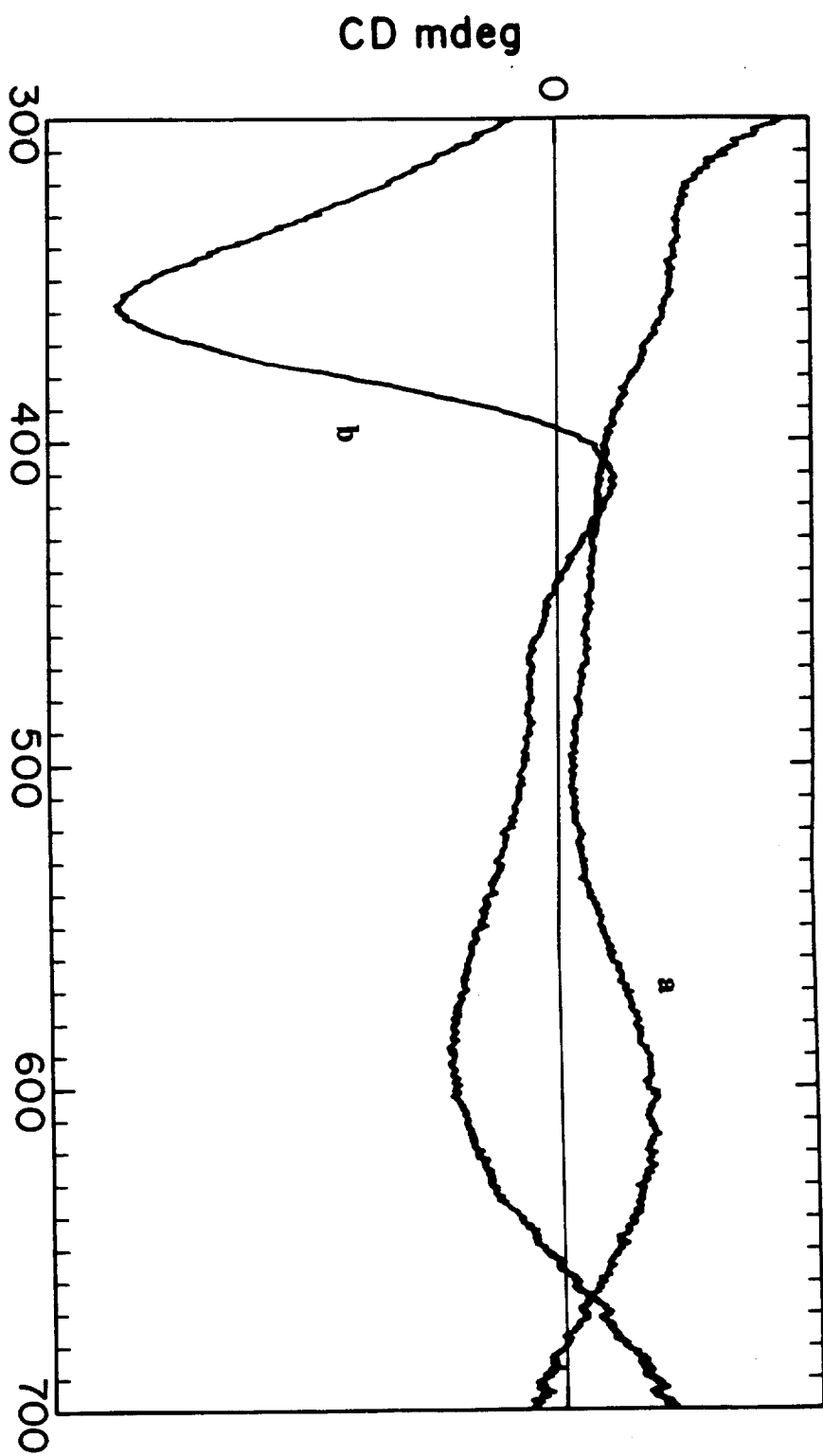


Fig. 3. 5. CD spectra at 20 °C of superoxide dismutase (in 2 mM copper concentration) (a) and the superoxide dismutase-azide complex in the presence of 50-fold azide (b). The temperature during the data collection was kept at 20 °C. The scan speed was 20 nm/min; step resolution 0.1 nm; sensitivity 1 mdeg/cm; time constant 2 sec.; beam width 1.0 nm; the number of scans 2.

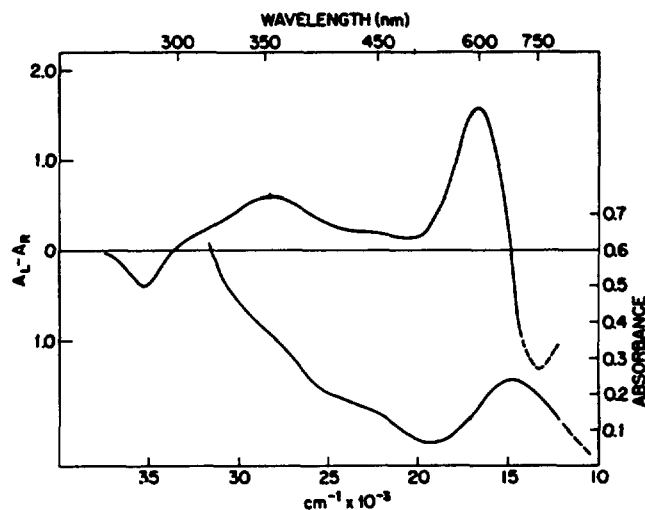


Fig. 3.6. Optical and circular dichroism spectra of bovine superoxide dismutase. [Reprinted with permission from Michelson, McCord, and Fridovich, eds., *Superoxide and Superoxide Dismutases*, Academic Press, London, 1977. Copyright by Academic Press (London), Ltd.]

Fig. 3.4.b. is the CD spectrum of the DBH- N_3^- complex. A single broad, negative CD band ($\Delta \epsilon = \epsilon_{\text{left}} - \epsilon_{\text{right}}$) is observed at 405 nm. It is unique among N_3^- to type II copper protein charge transfer transitions. The SOD- N_3^- CD spectrum (see Fig. 3.5.b.) shows that there are two absorption bands in the LMCT region at 365 nm (negative) and 405 nm (positive), as well as a ligand field transition at 595 nm (negative). It is very hard to assign these LMCT bands because of overlapping transition. If both bands belong to N_3^- to copper charge transfer transitions, the single band observed from the absorption spectrum (at 375 nm) must split into two bands, one positive and one negative, suggesting that there are two different transitions for N_3^- to copper charge transfer transition, one of them producing the positive CD band and the other producing the negative CD band. But all previous reports have inferred that only one N_3^- can bind a copper site and the two copper centers in the enzyme are in identical environments; furthermore, the 365 nm band also appears in the native SOD CD spectrum at the same position with a positive sign. Thus, the SOD- N_3^- complex probably possesses only one N_3^- to copper charge transfer

transition, and, consequently, there should be one CD band around 405 nm. The 360 nm, negative band should still belong to the histidine ligand to copper charge transfer transition that changes its sign because of the binding of N_3^- , suggesting a change in configuration of the Cu centers upon the binding of N_3^- .

Moffitt and Moscowitz have studied intensively the parallelism between the spectra of absorption and of optical activity (Moffitt and Moscowitz, 1959). Two cases are considered: 1. This class includes naturally asymmetric chromophores and certain special cases of symmetric chromophores in which the transition leading to absorption is forbidden electrically but allowed magnetically. The induced asymmetry is then so strong that it produces both a high ϵ -value and a very marked circular dichroism. Under these conditions, assuming that the optical activity can be measured, both the wavelengths corresponding to the maxima or minima and the band widths for natural and dichroic absorption are identical. 2. The chromophore is symmetric but in an asymmetric environment. The transition is electrically forbidden. Under these conditions, the wavelength at the absorption maxima is shorter than that at the circular dichroic maxima or minima, and the bandwidth of circular dichroic absorption is smaller than that of natural absorption. Differences in wavelength maxima between CD and absorption spectra need not necessarily require the presence of two transitions of which only one is active in the absorption spectrum. Nonetheless, this possibility is not excluded, and circular dichroism curves in which two active transitions of opposite sign occur side by side are frequently encountered.

That the CD maximum of azido-DBH occurs at about 20 nm longer wavelength than the UV / vis maximum appears to be the result of an asymmetric environment in the protein.

The optical activity of N_3^- -Cu (II) DBH is not proportional to the absorption of natural light. The wavelength and sign of CD spectra are very sensitive to the configuration of a chromophore, which is a good tool to study conformation of N_3^- -DBH and azido-SOD complexes.

Because the chromophore including the copper centers and N_3^- in the N_3^- -SOD complex is symmetric itself, the wavelength at the CD maximum is supposed to be longer than that of the absorption maximum (375 nm) (Dooley and McGuire, 1986). This is the major reason that the 365 nm band in azido-SOD CD spectra is assigned to the histidine-to-copper charge transfer transition. It leaves the 405 nm band as a single N_3^- to copper charge transfer transition that exhibits a 30 nm red shift from that in the absorption spectrum. Due to the intense negative His to copper charge transfer transition at 365 nm, this band not only becomes small and narrow, but λ_{max} may shift to longer wavelength too much—the actual λ_{max} may be around 400 nm or 390 nm. The negative band at 595 nm is assigned to the d-d band. The interesting fact is that both the His to Cu (II) charge transfer transition and the d-d band flip their signs from positive to negative upon the coordination of azide; as the consequence, azide must alter the configuration of the copper centers.

CD spectra of amine oxidase- N_3^- complexes are very similar to that of SOD- N_3^- . In the CD spectrum of native amine oxidase, there are two bands at 410 nm (negative, cofactor to copper charge transfer transition) and 610 nm (positive, d-d band); however, in CD spectra of amine oxidase- N_3^- complexes, the 410 nm band shifts to 480 nm but keeps the negative sign, and the d-d band (610 nm) shifts to 680 nm but reverses the sign to negative (see Fig. 3. 7., from Dooley and Cote, 1985). There is a new band at 400 nm

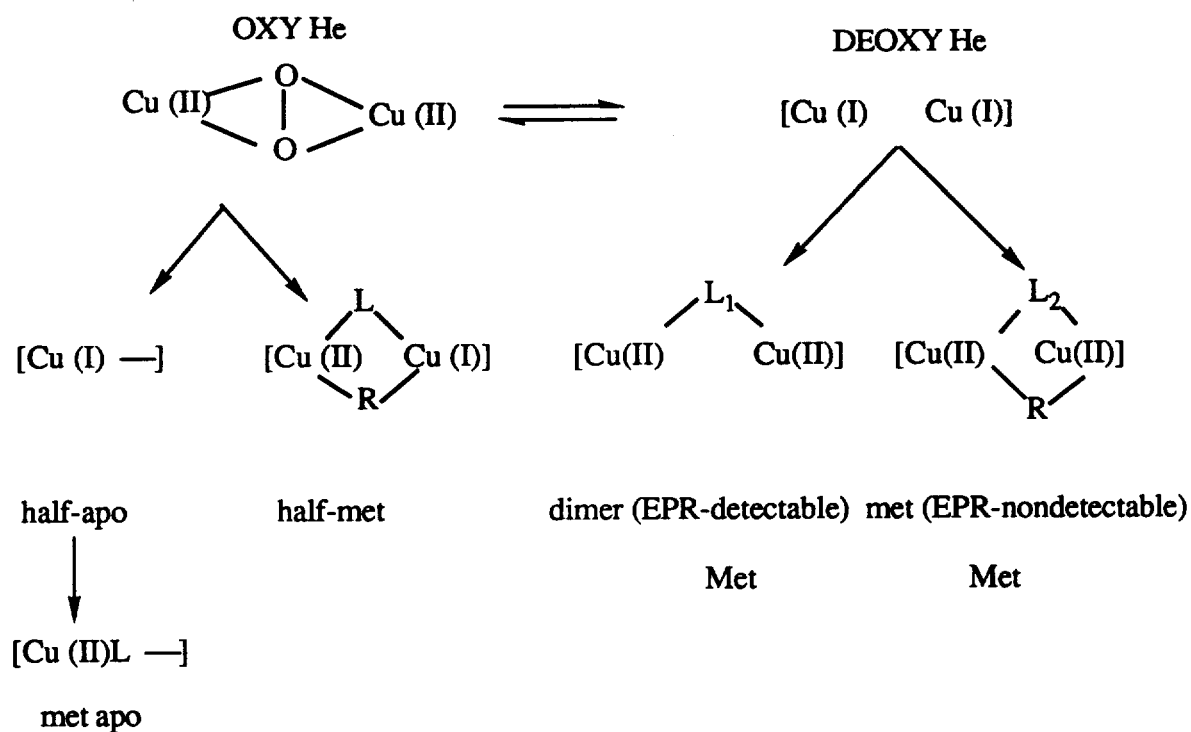
(positive) assigned to the N_3^- to copper charge transfer transition. SOD- N_3^- and amine oxidase- N_3^- complexes display very similar d-d transition and N_3^- -to-copper charge transfer transitions — both exhibit positive LMCT and negative d-d transitions (Dooley and Cote, 1985). Therefore, they probably behave very similar towards the coordination of N_3^- at the copper centers, but exactly opposite to the properties of DBH. The CD spectra indeed indicate there are some differences between DBH and other type II copper proteins.

On the other hand, the CD signal of the DBH- N_3^- complex is very similar to some type III copper protein - N_3^- complexes, such as hemocyanin, tyrosinase, and type II copper depleted laccase. The met-hemocyanin- N_3^- complex (met-hemocyanin: oxidized form of hemocyanin) displays a single negative CD band at 440 nm for Mollusc and 425 nm for Arthropod, in which N_3^- forms the μ -1, 3 bridged Cu- N_3^- complex (Solomon, 1981). Similar results are obtained for the met-tyrosinase-azide complex (Himmelwright et al, 1979; see Fig. 3.8., from Pate et al, 1989). However, the met apo-Mollusc homocyanin- N_3^- complex (definition of met apo homocyanin see Scheme 3.1., from Himmelwright et al, 1980) also displays a single negative CD band around 400 nm, although N_3^- binds to the copper center terminally (Solomon, 1981). For the DBH- N_3^- and the Mollusc met-apo hemocyanin- N_3^- complexes, their copper centers probably are in a similar configuration in the presence of azide, and N_3^- attaches to the coppers in the same way or in the same direction. Laccase contains all three type copper centers, in which the type I copper is not able to coordinate to N_3^- . The type II copper depleted laccase- N_3^- complex displays a single negative CD band around 450 nm; however, the CD spectrum of the azide adduct of native laccase that contains a type II copper center exhibits an extra positive feature at the shorter wavelength than 400nm. It seems that the type II copper

$-N_3^-$ centers always generate positive CD bands except in DBH and met-apo hemocyanin, and the type III copper $-N_3^-$ centers produce negative CD bands.

The sign of CD spectra is usually decided by the optical configuration of a chromophore. Some CD spectra of metal-amino acid model compounds provide a hint about the relationship between CD and absorption spectra of metal complexes. One typical example is the $[Co^{2+}(L\text{-ala})_3]$ complex that consists of 4 isomers including two geometrical isomers (fac and mer) and two optical isomers (Δ and Λ) (see Fig. 3.9, from Douglas and Yamada, 1965). In these complexes, the donor atoms of an amino acid are nitrogen and oxygen. The symbols "fac" (facial) and "mer" (meridinal) are used, respectively, to designate an isomer in which three N atoms (or three O atoms) occupy the corners of one octahedral face, cis-cis or cis-trans, respectively. The CD and the visible-UV absorption spectra of all four isomers have been obtained by Denning and Piper (see Fig. 3.10) (Denning and Piper, 1965). The geometric isomers (mer- Λ and mer- Δ , or fac- Λ and fac- Δ) have almost identical absorption spectra but reversed CD spectra. But CD spectra of a pair of optical isomers (mer- Λ and fac- Λ , or fac- Δ and mer- Δ) are consistent in shape, the band position, and sign (see Fig. 3.10.); the only deviation is intensity.

Considering the similar absorption and the reversed CD spectra of DBH- N_3^- and bovine plasma amine oxidase- N_3^- complexes (see Table 3.3), their copper centers are probably in a parallel relationship as those optical isomers of model compounds—azide coordinates to copper centers of DBH and of beef plasma amine oxidase in the opposite directions, although they have comparable copper structures. Azide, then, binds to DBH in the same way that it coordinates to met-hemocyanin, met apo-hemocyanin, met-tyrosinase, and type II copper depleted laccase.



Scheme 3.1. Hemocyanin derivatives

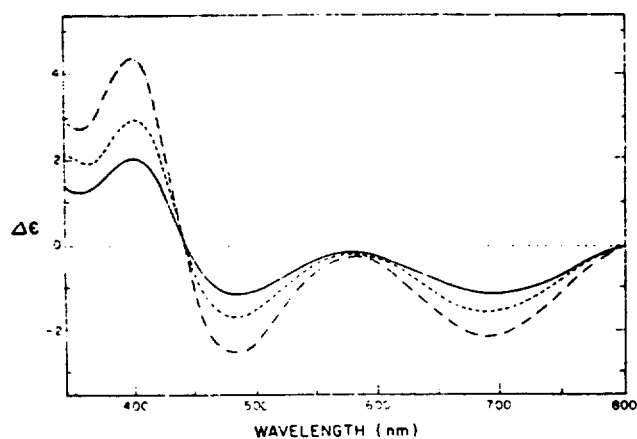


Fig. 3.7. CD spectra obtained by digitally subtracting the resting amine oxidase spectrum from spectra of the enzyme in the presence of azide at various concentrations. Azide concentrations were (—) 25 mM, (- -) 50 mM, and (...) 185 mM (from Dooley and Cote, 1985).

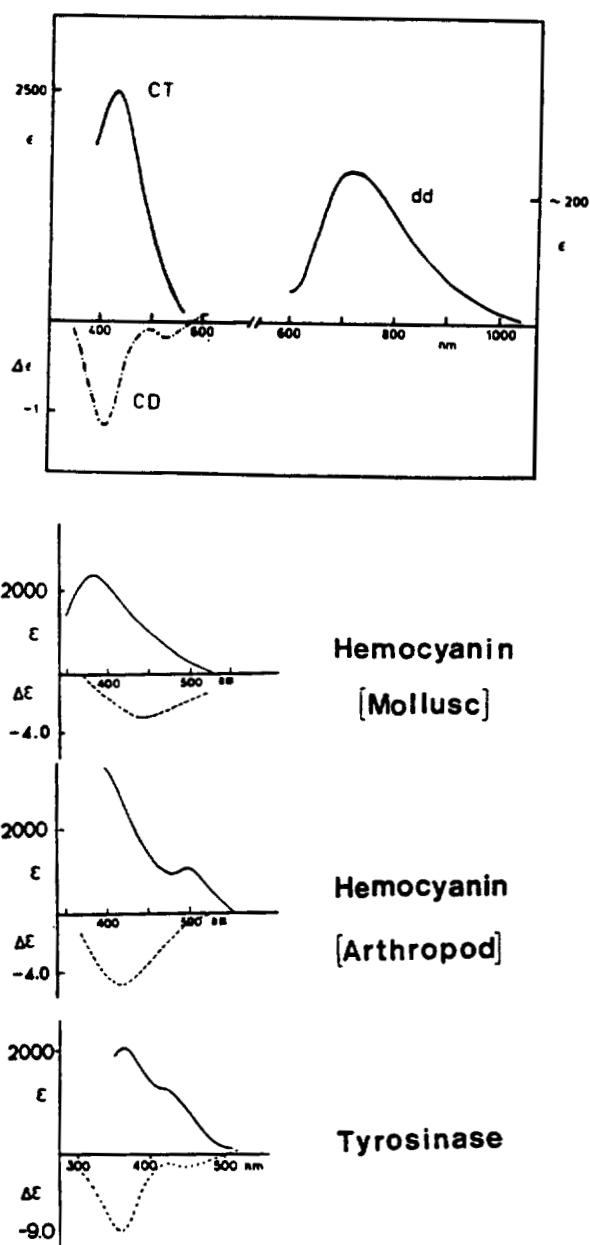


Fig. 3. 8. Absorption (solid line) and circular dichroism (dot line) spectra of Met Apo-hemocyanin-azide (top); met azide mollusc hemocyanin (*Busycon*) (second from top); met azide arthropod hemocyanin (*Limulus*) (third from top); met azide tyrosinase (*Neurospora*) (bottom) (from Pate et al, 1989).

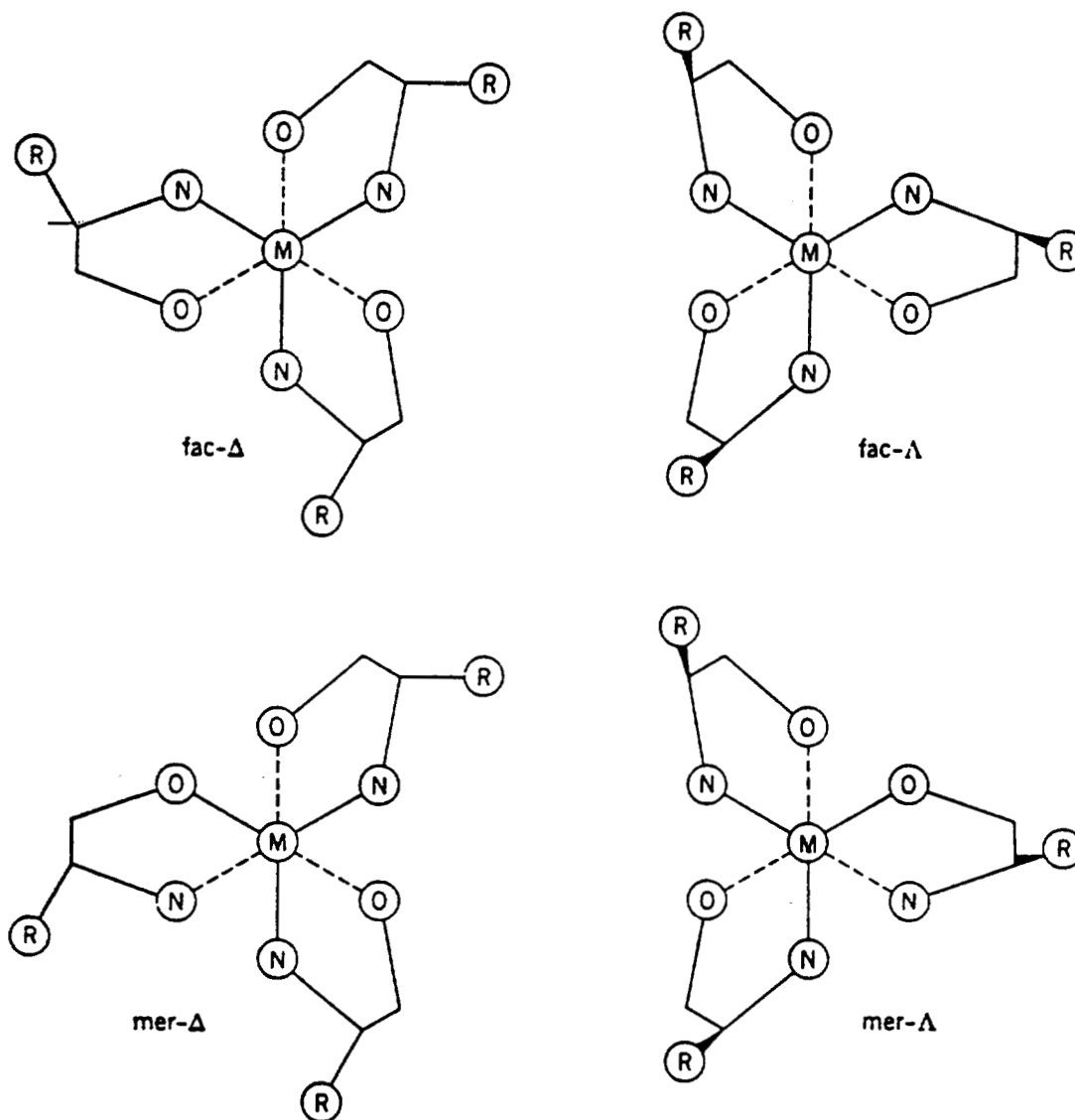


Fig. 3. 9. Four isomers of a tris-(L- α -amino acidato) complex. The substituents R are equatorial in the fac- Δ and mer- Δ isomers, and axial in the fac- Λ and mer- Λ isomers (from Douglas and Yamada, 1965).

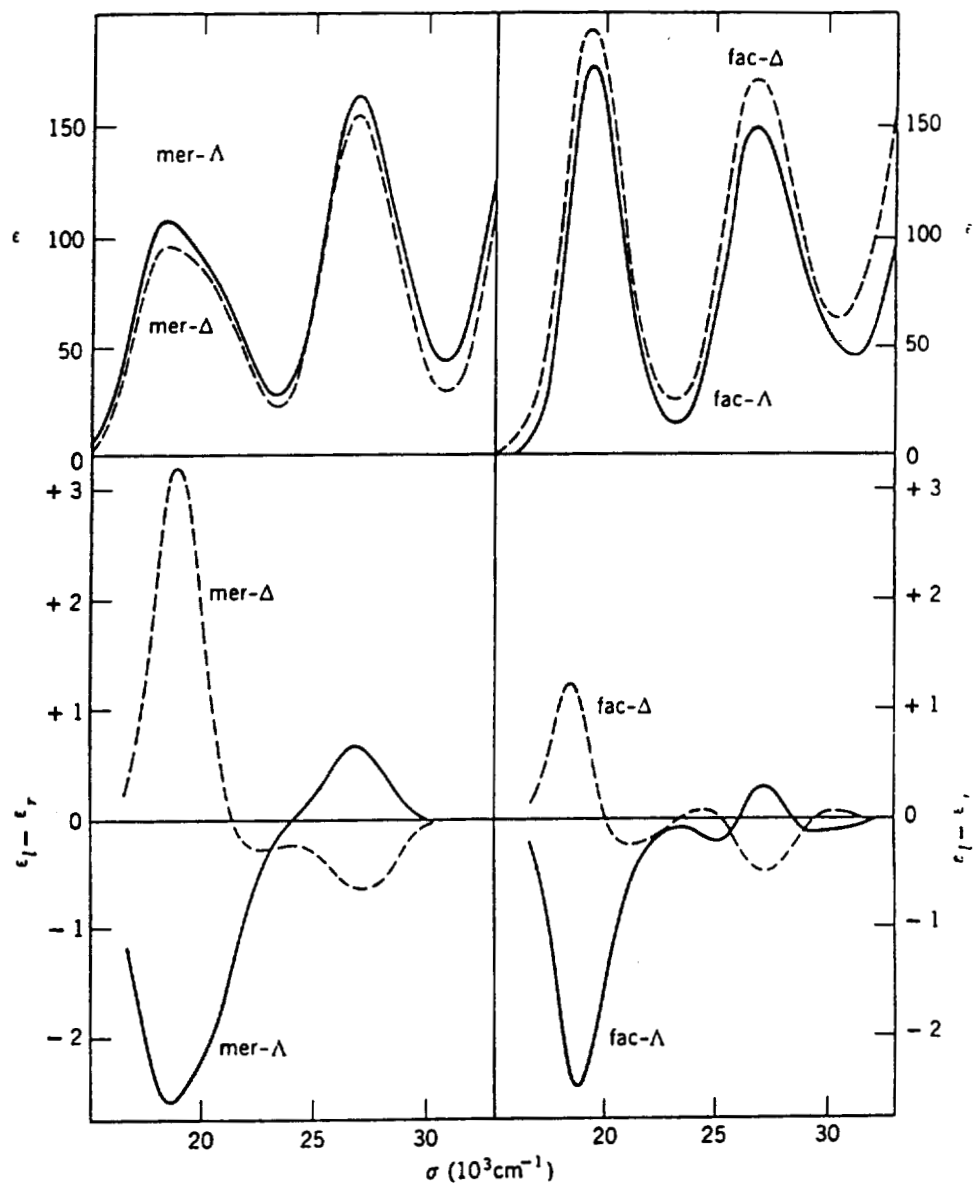


Fig. 3.10. The CD and absorption spectra of four isomers of $[\text{Co}(\text{L-Ala})_3]$ (from Denning and Pipper, 1965).

Table 3. 3. Comparison of optical properties between DBH-azide and beef plasma amine oxidase-azide complexes

	absorption band (nm)	ϵ ($M^{-1} \text{ cm}^{-1}$)	CD band (nm)	sign of CD band
DBH-azide	385	3100	405	negative
amine oxidase- azide complex	385	3200	400	positive
SOD-azide complex	375	1300	400	positive

3.3.3. IR spectra of DBH-azide and SOD-azide complexes:

IR spectra for the azido-complexes of DBH and SOD are shown in Figure 3.11. NaN_3 has a single strong IR peak at 2048 cm^{-1} due to the asymmetric stretch of the azide moiety ($\text{N} \leftarrow \text{N} \leftarrow \text{N}$). DBH-azide has a single peak at 2062 cm^{-1} at low azide concentration (about 1: 1 N_3^- to Cu ratios before washing out free N_3^-), which is very similar to the single peak of SOD-azide (2059 cm^{-1}). When the azide concentration is increased to azide to copper ratio larger than 100 : 1, the DBH-azide peak is broadened, suggesting the presence of a second peak around 2046 cm^{-1} . Further increase in azide concentration does not produce more IR peaks, but causes the intensity of the second peak (at 2046 cm^{-1}) to increase. The wavenumber of the first band is higher than that of free azide, and

the wavenumber of the second band is slightly lower than that of free azide. In a relevant control experiment, apo-DBH does not show any IR signal of protein-bound azide.

The vibrational spectra of three types of azide-Cu (II) model compounds (terminal, μ -1, 1, and μ -1, 3) have been published by the Solomon group (Pate et al, 1989) (see Fig. 3.12.). Terminal mononuclear copper (II) azide model complexes exhibit a single band in the 2040 - 2060 cm^{-1} region (Fig. 3. 12. b). The IR or resonance Raman spectra of μ -1, 3 azide-Cu(II) complexes have a single peak in the 2025 cm^{-1} region. One μ -1, 3 complex, $[\text{Cu}_2(\text{bpeac})(\text{N}_3)] [\text{ClO}_4]_2$, displays an IR peak at 2038 cm^{-1} (Fig. 3.12.a). The crystal structure of $[\text{Cu}_2(\text{bpeac})(\text{N}_3)] [\text{ClO}_4]_2$ shows that the $\text{N}_1 - \text{N}_2$ bond length in the azide is shorter than that of the $\text{N}_2 - \text{N}_3$ (1.14 vs. 1.21 Å) which may contribute to the broadening. μ -1, 1 azide compounds exhibit a single azide related peak at 2065 - 2075 cm^{-1} (Fig. 3. 12. c). The information content of the vibrational data (see Table 3.4) would provide a lot of structural information about the environment of copper centers (full names of model compounds are in Table 1.2.).

Although the energy of the intra-azide vibrational stretch correlates well with the geometric mode of azide binding, it does not result from a simple mass effect of the coupled vibrational unit, but from inequivalence of two intraazide bonds (Dori and Ziolo, 1972). This inequivalence is reflected in the difference between the force constants $k(\text{N}_1 - \text{N}_2)$ and $k(\text{N}_2 - \text{N}_3)$. A rationale for inequivalence within the bound azide is provided by considering the ground-state electronic structure of the coordinated azide in terms of contributions from the two resonance structures in Fig. 3.13. The N-N bond length would also be expected to reflect this asymmetry. The resonance structures in Fig. 3.13. (from Pate et al, 1989) indicate that as the amount of single-triple character within azide

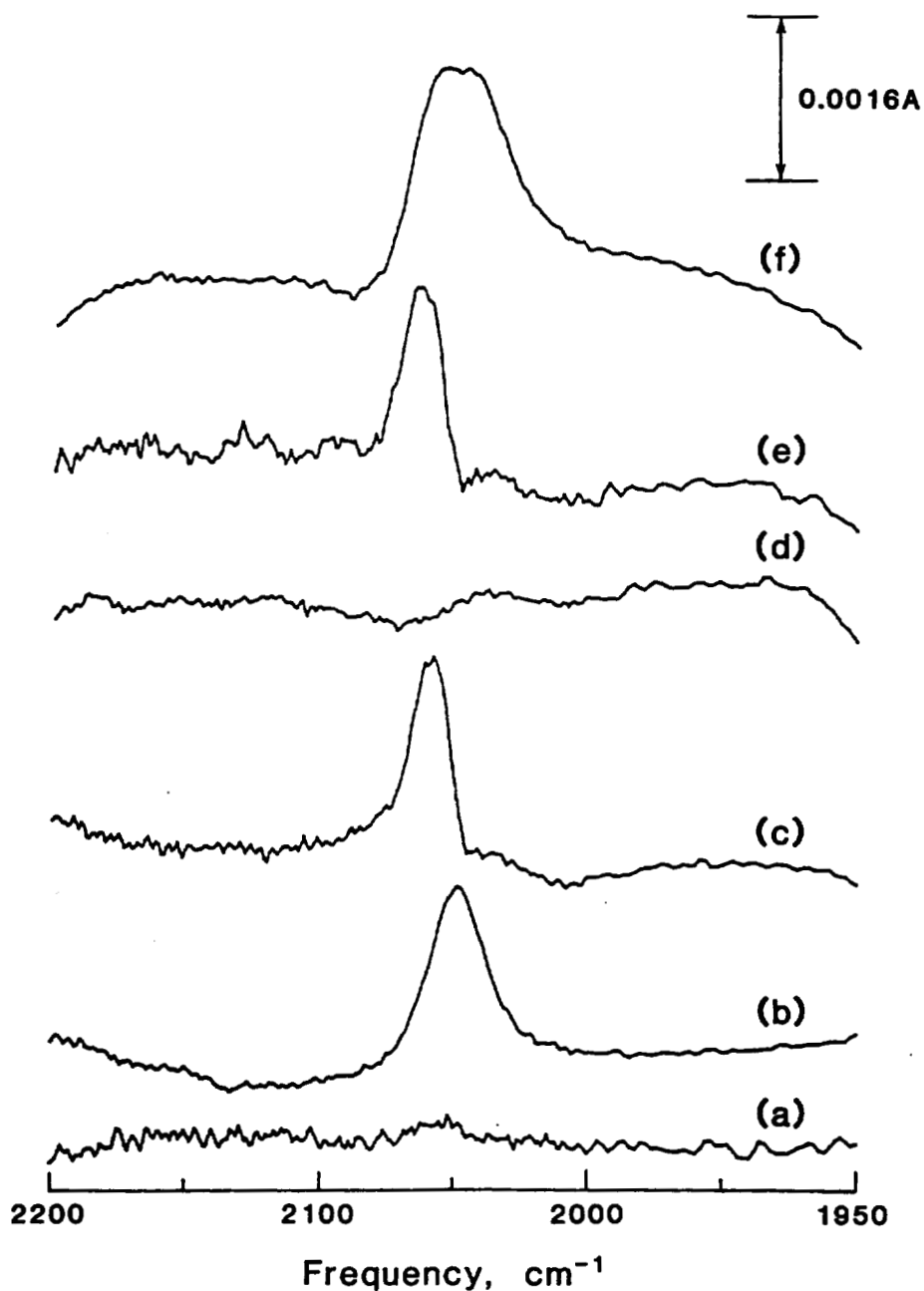


Fig. 3. 11. Fourier transfer infrared spectra in the region $2200 - 1950 \text{ cm}^{-1}$ for the azide complexes of bovine Cu/Zn superoxide dismutase and dopamine β -hydroxylase. (a) difference spectrum of the retentate-filtrate for a 10 mM solution of sodium azide (protein-free) after ultrafiltration in a centricon 30. (b) 0.5 mM sodium azide. (c) the azido complex of Cu/Zn superoxide dismutase (8 mM in Cu) in sodium borate buffer, pH 8.1. (d) apo-DBH treated with a 10-fold excess of azide. (e) the azido complex of DBH at low azide concentration (Cu to azide ratio 1 : 1). (f) the azido complex of DBH at high azide concentration (Cu to azide ratio 1 : 500). The DBH was approximately 2 mM in total copper, in 50 mM phosphate buffer, pH 7.5, for all experiments.

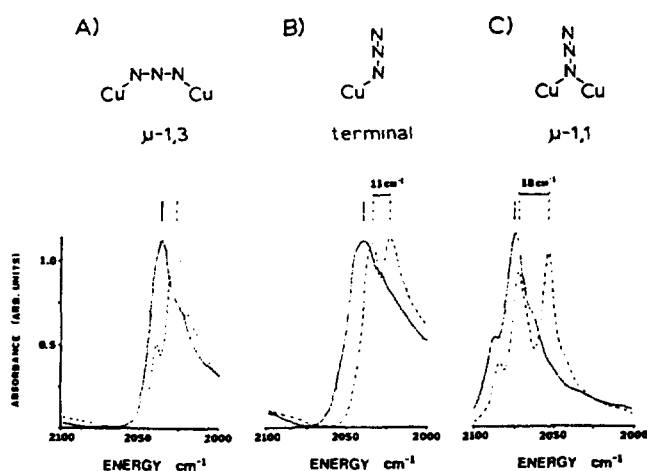


Fig. 3.12. Infrared spectra of Nujol mulls of (a) $[\text{Cu}_2(\text{bpeac})(\text{N}_3)][\text{ClO}_4]_2$, (b) $[\text{Cu}(\text{L}'\text{-O})(\text{N}_3)]$, and (c) $[\text{Cu}_2(\text{L-O})(\text{N}_3)][\text{PF}_6]_2$ prepared with $^{14}\text{N}^{14}\text{N}^{14}\text{N}$ (—) and $^{14}\text{N}^{14}\text{N}^{15}\text{N}$ (- -) (from Pate et al, 1989).

Table 3.4. Vibrational frequencies and calculated force constants of the asymmetric intraazide stretch of isotopically labeled copper azide model complexes.

	vibrational frequencies (cm^{-1})			force constants ($\text{mdynes}/\text{\AA}$)		
	$^{14}\text{N}_3$	$^{15,14}\text{N}_3, ^{14,15}\text{N}_3$	$\Delta \text{ cm}^{-1}$	$k(\text{N1N2})$	$k(\text{N2N3})$	$k_{\text{int}}(\text{NN})$
$\begin{array}{c} 123 \\ \text{NNN} \\ \text{Cu} \end{array}$						
$[\text{Cu}(\text{Et}_4\text{dien})\text{N}_3\text{Br}]$ (R)	2062	2048, 2054	6	11.8	14.0	1.29
$[\text{py}_2\text{-Cu}(\text{NO}_3)(\text{N}_3)]$ (IR)	2041	2025, 2033	8	11.5	14.2	1.49
$[\text{Cu}(\text{L}'\text{-O})(\text{N}_3)]$ (IR, R)	2039	2022, 2033	11	11.2	14.5	1.56
$\begin{array}{c} 123 \\ \text{NNN} \\ \text{Cu} \quad \text{Cu} \end{array}$						
$[\text{Cu}_2(\text{L-Et})(\text{N}_3)]^{2+}$ (IR, R)	2025	2013, 2013	0	12.6	12.6	1.36
$[\text{Cu}_2(\text{bpeac})(\text{N}_3)]^{2+}$ (IR)	2038	2026, <2028	<2	12.5	12.8	1.25
$\begin{array}{c} \text{N3} \\ \text{N2} \\ \text{N1} \\ \text{Cu} \quad \text{Cu} \end{array}$						
$[\text{Cu}_2(\text{N}_6\text{O})(\text{N}_3)]^{2+}$ (IR, R)	2065	2045, 2062	17	10.2	15.5	1.49
$[\text{Cu}_2(\text{L-O})(\text{N}_3)]^{2+}$ (IR, R)	2075	2055, 2073	18	10.1	15.7	1.46

*Structure not yet available.

Both Fig.3. 12. and Table 3.4. are from Pate et al, 1989

increases, the bond length should become more inequivalent, with $N_1 - N_2 > N_2 - N_3$. The terminal bound azide has a predicated inequivalence of about 0.05 - 0.07 Å (see Table 3.4., from Pate et al, 1989).

The calculated N-N force constants provide insight into differences in the bond order within azide. A comparison of calculated N-N force constants for an single (F_2 , 4.45 mdyne / Å), double (O_2 , 11.39 mdyne / Å), or triple azide bond (N_2 , 22.41 mdyne / Å) indicates that the N-N force constants in the $\mu-1, 3$ complexes are similar to those expected for a two double bond structure. As the intra-azide bonds become more inequivalent in the terminal and $\mu-1, 1$ structures, the bond orders acquire greater single-triple character. However, the largest inequivalence (the $\mu-1, 1$ complex) still corresponds to approximately only 60 % resonance form A.

The 2048 cm^{-1} IR band of NaN_3 is associated with the azide antisymmetric stretch, ν_{as} , and its energy depends only on the configuration of the bonded azide (Agrell, 1971) — that is, on the degree of its symmetry. Thus, the larger the difference between the two N-N distances, the higher is the energy of ν_{as} (Dori and Ziolo, 1973). In the case of a metal bound azide, azide is asymmetric, and the long N-N distance always occurs between the middle nitrogen and the nitrogen coordinating to the metal. Spectroscopic

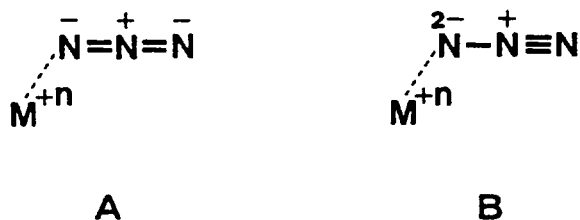


Fig. 3. 13. The resonance structures of the bound azide

measurements of metal-azide complexes suggest that the metal-azide bond is largely covalent. The larger the π interaction between the p orbital on N_1 and the d orbitals on the metal, the larger will be the difference between the two N-N distances. Consequently, the larger this π interaction, the higher ν_{AS} is.

The antisymmetric stretch of SOD-azide is at 2059 cm^{-1} , about 11 cm^{-1} higher than that of free azide. It is the copper attachment to azide that causes the inequivalence of the two nitrogen-nitrogen bonds. The N_1-N_2 bond becomes weaker and longer because of the positive charge of Cu (II). The N_2-N_3 becomes stronger and shorter. The first IR band of DBH-azide (2062 cm^{-1}) is close to that of SOD-azide and indicates that the bond lengths of azide in these two complexes should be very similar. Therefore, the environment of one Cu center in DBH is probably comparable to that in the azido-SOD complex. SOD has a single copper center per subunit; each copper center has 4 His ligands, and one of them bridges between Cu and Zn centers. Azide substitutes one of the equatorial His ligands other than the bridging His 61 (Fee et al, 1981). In addition, the model compound, $[\text{Cu}(\text{Et}_4\text{dien})\text{N}_3\text{Br}]$ which has an almost identical azide antisymmetric stretch frequency (2062 cm^{-1}), is composed of three N ligands and one azide ligand at the equatorial position (Pate et al, 1989). Correspondingly, the copper centers of the oxidized DBH-azide complex probably also have 3 His ligands and one azide ligand. Since azide most possibly substitutes an equatorial water molecule rather than one of the His ligands, as mentioned previously, one of the Cu (II) centers in the oxidized form of DBH before binding to an azide molecule should have three His and one equatorial water as ligands. The second IR band of the DBH-azide complex at the high azide concentration has a relatively lower frequency (around 2045 cm^{-1} , a number that may be little too high because of the overlap of two different peaks). This may represent another type of copper

center with a different environment from the first copper center. It is very possible that this second type of copper center has different internal ligands resulting in different electron densities at the copper and consequent changes in the bond distances within the azide molecules. Solomon's copper model compounds (Pate et al, 1989) that have a terminal bound azide, $[\text{Cu}(\text{Et}_4\text{dien})\text{N}_3\text{Br}]$, $[\text{py}_2\text{-Cu}(\text{NO}_3)\text{N}_3]$, and $[\text{Cu}(\text{L}'\text{-O-})(\text{N}_3)]$, have azide vibrational frequencies of 2062, 2041, 2039 cm^{-1} , respectively (see Table 3.4.). When Cu has all N ligands, the azide IR stretching frequency is relatively higher, around 2060 cm^{-1} . But as oxygen acts as a ligand, the ν_{AS} becomes lower. The second IR peak of the DBH-azide complex is quite comparable to that of $[\text{Cu}(\text{L}'\text{-O-})(\text{N}_3)]$, in which three N and one O serve as ligands (L'-O- = 2-[N, N-bis (2-pyridylethyl) amino] methylphenol). It is reasonable to assume that in the azido-complex of DBH, the second copper center of DBH may have 2 nitrogen ligands from His and one oxygen type ligand. Since the second IR azido-DBH band appears only at the relatively high azide concentration, azide bound at the different copper centers causes both the different azide binding affinity at the copper center and the different azide vibrational frequency. Because the oxygen atom can supply more electron density to the copper center than nitrogen can, the Cu (II) becomes less positively charged, and the Cu-N bond is relatively weaker. As a consequence, the N-N bond length becomes less uneven, which gives a relatively lower azide antisymmetric stretching frequency. The different electron density of two copper centers in each subunit may affect their redox potential during turnover, and therefore, affect the electron transfer from the reductant, ascorbate. The measurement of IR spectra of azido-DBH indicates the two copper centers in each subunit have different endogenous ligands, different affinities of anion binding, and probably different redox potentials.

Klinman et al have postulated a mechanism (Miller and Klinman, 1985; Klinman et al,

1990; Brenner et al, 1989; Stewart and Klinman, 1987), in which two distinct coppers in each subunit perform separate functions and may be fairly distant in space. A reductant site and a substrate binding site are magnetically isolated to catalyze the electron transfer and substrate hydroxylation, respectively. An electron is transferred from the reductant site to the oxygen binding site, allowing a two electron reduction of oxygen to a copper hydroperoxide. Copper hydroperoxide may be competent to hydroxylate bound substrate without further activation. In the final stage of the mechanism, two electrons are added via the reductant copper site to generate the E-Cu (I)•P complex (see Fig.1.12.).

The spectroscopic studies of the azide-DBH complex also suggest the inequivalence of two Cu (II) centers in each subunit. One copper center contains one tightly coordinated oxygen type ligand besides two histidine ligands, and the other copper center contains only histidine ligands and weakly bound water molecules.

3. 4. Conclusions

The two copper sites of each subunit of DBH may not be identical; they have their own functions, but are not independent. The binding of N_3^- caused a very strong negative cooperativity, suggesting an interaction between the copper centers. The N_3^- molecule can replace a water molecule at an equatorial site on the copper center. A conformational change may occur as the temperature is lowered. The azide vibrational antisymmetric stretch in the azide-Cu(DBH) complex has resolved a single band at low azide concentration and two IR bands at high azide concentration, respectively. This strongly supports the conclusion that the environments of two copper centers in each subunit are inequivalent.

CHAPTER IV

THE HALF-APO-DBH-N₃⁻ COMPLEX

4. 1. Introduction

It has been shown, in the previous chapter through azide binding studies, that the two copper centers of each subunit in DBH may not be in the same environment. In order to confirm these results, an effort has been made to prepare half-apo-DBH that contains only one particular copper in each subunit. The CO binding to DBH measurements have been used to test if only one type of copper remains in the enzyme because previous results from this laboratory have proven that the stoichiometry is 0.5 CO / copper center (Blackburn et al, 1990) and hence that CO binds to only one copper center per subunit.

Since CO exhibits competitive inhibition with respect to molecular oxygen (Blackburn et al, 1990), CO and oxygen are expected to bind to the enzyme at the same sites. The electronic structures of O₂ and CO are similar according to the availability of empty Π^* levels and the consequent ability of both ligands to take part in Π - backbonding into the filled d-orbitals on the metal (Nakomota, 1986). Studies of inorganic copper - carbonyl chemistry have established that CO coordinates only to Cu (I) centers (Pasquali and Floriani, 1984). Previous measurements from this laboratory have clearly shown that reduced DBH binds 0.5 molecules of CO / copper.

Formation of a DBH·CO complex has also been investigated by using Fourier transform - infrared spectroscopy. Cu (I) - carbonyls are known to exhibit C-O stretching frequencies due to terminally coordinated CO in the range of 2130 - 2000 cm^{-1} and due to bridging coordinated carbonyls in the range of 2000 - 1850 cm^{-1} . Fig. 4.1. shows the FTIR spectrum of CO-treated, reduced DBH in the 2200 - 2000 cm^{-1} energy range (Blackburn, 1990). No bands are observed in the 2000 - 1850 cm^{-1} region. This result provides direct evidence for the formation of a terminally coordinated Cu (I)-CO complex in the reduced enzyme. Because CO and oxygen bind to only one copper center per subunit terminally, if Cu_b is assumed to be the CO's binding site and Cu_a is not able to bind CO at all, oxygen should also be able to coordinate at the Cu_b center, -but not at the Cu_a center.

Examination of the trends of CO stretching frequencies in inorganic Cu (I) - carbonyl complexes helps to formulate the possible coordination in DBH·CO. The stretching frequency of a π -acceptor ligand, such as CO, coordinated to a metal is dependent on the degree of backbonding from metal d-orbitals into the π^* - antibonding orbitals of CO. Table 4.1. (from Blackburn, 1990) contains details of ligation and $\nu(\text{CO})$ for a number of Cu (I) - carbonyls. In general, $\nu(\text{CO})$ decreases with an increase in the number and basicity of the accompanying ligands. Thus, in compounds 1 and 2, coordination of an additional imidazole group decreases $\nu(\text{CO})$ by 17 cm^{-1} , suggesting that in Cu (I) - imidazole systems three - coordinate carbonyls have CO stretching frequencies some 15 -20 cm^{-1} above their four - coordinate analogous. The π backbonding from Cu (I) (d^{10}) to the empty π^* orbitals on CO is proportional to the ability of the other ligands to donate electron density to Cu (I) and thus offset electron donation to CO.

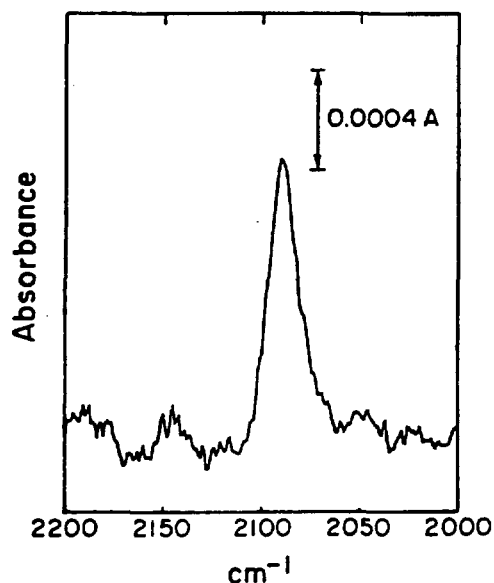


Fig. 4. 1. FTIR spectrum of the CO complex of reduced dopamine β -hydroxylase in the 2200–2000 cm^{-1} range. The enzyme-bound copper concentration was 1.3 mM, 100 mM triethanolamine acetate, pH 7.00 (Blackburn, 1990).

The IR stretching frequency of CO - DBH is 2089 cm^{-1} (Fig. 4. 1.). This value is on the high end of what is expected for carbonyls of Cu (I) model compounds. The 4-coordinate *tris*-imidazole complex $\text{Cu}(\text{timm})\text{CO}^+$ reported by Sorell and Borovick (Sorell and Borovick, 1987) has a $\nu(\text{CO})$ of 2080 cm^{-1} , whereas CO complexes of both molluscan and arthropodal hemocyanins occur at lower frequencies (2063 and 2043 cm^{-1} , respectively) (Fager and Alben, 1972) (see Table 4.2. from Blackburn, 1990). The copper centers in hemocyanins have three histidine ligands after binding to CO, and CO coordinates to both hemocyanins and DBH (at 2089 cm^{-1}) terminally. An increase in $\nu(\text{CO})$ for DBH could be explained by a 4-coordinate Cu(I)-carbonyl in which one of the ligands is a poorer electron donor than histidine. This would occur if the fourth ligand is less basic or is less strongly bound and would also be true for 3-coordinate carbonyls where the fourth ligand is lost.

In the preparation of half-apo DBH, the results of CO binding stoichiometry experiments

Table 4. 1.

Effect of coordination number and basicity on $\nu(\text{CO})$ of some inorganic Cu(I) carbonyls

Complex	Donor atom set ^a	ν_{CO}
1. $[\text{Cu}_2(\text{mb-him})(\text{CO})]^{2+}$	1N (imid), 1N (amino)	2088
2. $[\text{Cu}_2(\text{mb-him})(\text{imid})(\text{CO})]^{2+}$	2N (imid), 1N (amino)	2071
3. $[\text{Cu}(\text{CO})(\text{HBpz}_3)]$	3N (pz)	2083
4. $[\text{Cu}(\text{CO})(\text{bpeap})]$	2N (pz), 10 ⁻ (phenolate)	2074
5. $[\text{Cu}(\text{CO})(\text{bpeaa})]$	2N (pz), 1N (tertiary amino)	2098
6. $[\text{Cu}(\text{CO})(\text{pza})]^+$	2N (pz), 1N (amino)	2089
7. $[\text{Cu}(\text{CO})(\text{pze})]^+$	2N (pz), 1O (ether)	2105
8. $[\text{Cu}(\text{CO})(\text{pzs})]^+$	2N (pz), 1S (thioether)	2123
9. $[\text{Cu}_2(\text{CO})_2(\text{Xyl-o})](\text{PF}_6)_2$	2N (py), 10 ⁻ (phenolate)	2070
10. $[\text{Cu}_2(\text{CO})_2(\text{N4py2})](\text{PF}_6)_2$	2N (py), 1N (amino)	2080
11. $[\text{Cu}_2(\mu\text{-CO})(\text{tmen})_2(\mu\text{-PhCO}_2)]^+$	bridging CO	1926
12. $[\text{Cu}_2(\mu\text{-CO})(\text{tmp})_2(\mu\text{-PhCO}_2)]^+$	bridging CO	1925

^a Abbreviations: imid, imidazole; pz, pyrazole; py, pyridine; Xyl, xylose.

Table 4. 2.

CO-stretching frequencies for carbonyl complexes of copper proteins

Enzyme	$\nu(\text{CO})/\text{cm}^{-1}$
Arthropodal Hc	2043
Molluscan Hc	2063
Cytochrome ba_3 (<i>T. thermophilus</i>)	2054 ^a
Cytochrome caa_3 (beef heart)	2062 ^a
Dopamine β -hydroxylase	2089

^a This value represents the major component.

Table 4.1. and 4.2. are from Blackburn et al, 1990

have been used to assay the distribution of copper centers. It is assumed that Cu_b is the oxygen and CO binding site and Cu_a is the non oxygen binding site. If DBH contains only one copper per subunit (statistically distributed between the two sites), the CO / copper ratio would maintain at 0.5. If all coppers are at the non CO binding site (Cu_a), the CO / copper ratio would be 0; if all coppers are at the CO binding site (Cu_b), the CO / copper ratio would be 1.0. If proportion of DBH molecules contain two coppers per subunit and a proportion of them contains no coppers, the CO / Cu ratio should be maintained at 0.5. The CO / copper stoichiometry measurement is the best method to determine whether prepared DBH is genuine half-apo DBH. The measurement uses a modification (Blackburn et al, 1990) of the method by Zolla and Brunori (Zolla and Brunori, 1983; Zolla et al, 1984).

In this chapter, the successful preparation of half-apo DBH will be described for the first time; the properties of half-apo DBH described below, are quite unique compared with fully metallated DBH. Spectroscopic properties of the half-apo DBH- N_3^- complex are compared with that of the fully reconstituted DBH- N_3^- complex, from which much information about the two copper centers in each subunit is obtained.

4. 2. Experimental Methods

4. 2. 1. Preparation of half-apo DBH

Half-apo DBH, which contains only one particular type of copper in each subunit — either Cu_a or Cu_b but not both, was prepared by the regular method prior to the step of reconstitution with copper. Since it contained around or less than 4 coppers per enzyme

right after the preparation, DBH was usually reconstituted with copper after the preparation but prior to the spectroscopic studies. However, newly prepared DBH before the reconstitution with copper satisfied the definition of half-apo DBH. The copper concentration and the CO / Cu ratio in newly prepared DBH was measured (the CO / Cu ratio was measured by Dr. B. Reedy) by using a modified method developed by Blackburn et al (Blackburn et al, 1990). The CO/Cu ratio of DBH was measured by saturating CO to reduced DBH and buffer-blank (Blackburn et al, 1990). The CO concentrations in DBH and buffer-blank were then measured by titrating into a solution of deoxyhemoglobin. Under these conditions quantitative transfer of CO (DBH-CO - CO in buffer) to the hemoglobin was achieved. The CO concentrations in DBH and blank were determined separately from the absorbance of the resulting carbonmonoxy hemoglobin at 419 nm using an extinction coefficient of $191 \text{ mM}^{-1}\text{cm}^{-1}$. The concentration of CO bound to DBH was calculated from the difference between the CO concentrations in the sample and the buffer. The copper concentration of DBH was determined through the atomic absorption spectra. The activity and the copper content were determined as described in Chapter II.

4. 2. 2. Spectroscopic studies of half-apo DBH

Absorption and CD spectroscopic studies were conducted under the same conditions used for the measurement of fully reconstituted DBH. EPR spectra were obtained as described in Chapter II.

In order to obtain IR spectra of the half-apo DBH-azido complex, an excess amount of azide had to be added (azide : Cu \geq 20). Half-apo DBH was concentrated to 0.2 ml by

ultrafiltration in a Centricon 30 concentrator. After added 20 μl of 1 M N_3^- , the enzyme was concentrated to 0.1 ml in the same Centricon 30 concentrator. IR spectra of both filtrate and retentate were then recorded. The IR spectrum of the half-apo DBH- N_3^- complex was obtained by subtracting the IR spectrum of filtrate from that of retentate.

4. 3. Results

4.3.1. Properties of half-apo DBH

The native enzyme immediately after purification but before reconstitution with copper shows that it contains about or less than 4 coppers / enzyme and a CO / copper ratio of 1.0. The data of several preparations are shown in Table 4.3. Although the copper content in the enzyme after preparation varied from 2.5 to 4.3, the ratio of CO / Cu is consistently found to be 1.0. Therefore, the native enzyme immediately after the preparation must be a mixture of genuine half-apo and fully apo-forms of DBH.

Traditional methods for preparing half-apo enzyme were not able to produce genuine half-apo DBH. If the preparation of half-apo DBH was attempted by removing 4 coppers from fully reconstituted DBH (containing 8 coppers/enzyme), the CO/Cu ratio was 0.5, indicating the presence of mixed copper centers. For DBH prepared with this method, part of the enzyme possessed two coppers per subunit, part possessed no coppers, and part had only one copper but at either one of two sites in every subunit.

If the preparation was started from addition of 4 coppers in apo-DBH (has no copper at all), the same result was obtained—the CO / Cu ratio was 0.5. Then both methods were not successful for preparing real half-apo DBH even though the enzyme contained 4

coppers / enzyme; instead, DBH right after the purification was half-apo DBH itself.

In the DBH preparation, either the GF-450 gel filtration column or the Con A affinity column was the step most likely to remove copper atoms from DBH. Both columns were tested by passing reconstituted DBH through these two columns, followed by the remeasurement of the copper content as well as the CO / copper ratio (see Table 4.4.). The GF-450 column removed about three coppers from DBH, and the CO / copper ratio was 0.5. However, the Con A column removed about 4 coppers from a DBH tetramer and yielded a CO /copper ratio of 0.75. In this case, the Con A column appeared to be the step where most of Cu_a was pulled out from DBH; but the GF-450 column removed copper from both sites (both Cu_a and Cu_b). Other steps in the preparation might also play some roles on the removal of copper from DBH. Thus, Con A column was the most possible step that removed Cu_a and produced real half-apo DBH.

Half-apo DBH exhibited lower activity than fully reconstituted DBH (see Table 4.5.). If half-apo DBH was reconstituted with Cu^{2+} to form fully reconstituted DBH, the activity of the enzyme recovered to the normal level (about or higher than $16 \mu\text{mol} / \text{mg min.}$). Half-apo DBH was about $1/3$ — $1/4$ less active than fully reconstituted DBH. Because half-apo DBH can pick up copper from the activity assay buffer, it was hard to estimate how active half-apo DBH was; however, it was sure that half-apo DBH was not as active as fully reconstituted DBH.

The Cu^{2+} content in half-apo DBH was obtained from EPR spectra; more than 50 % of the total copper was in Cu^+ form (see Table 4. 5.). The Cu^{2+} content increased with time after the preparation, because oxygen in air caused partial oxidation of Cu^+ into Cu^{2+} ;

Table 4.3. Stoichiometry of CO binding to DBH

Preparation	Before Reconstitution		After Reconstitution	
	[Cu] / E	[CO] / [Cu]	[Cu] / E	[CO] / [Cu]
1.	4.3	1.08	8.1	0.45
2.	3.1	1.02	7.0	0.50
3.	2.8	1.03	7.4	0.42
4.	2.5	0.90		

Table 4.4. The copper content of fully reconstituted DBH after column chromatography

	Pass through GF-450 column	Pass through Con A column
copper content (Cu / DBH)	5.4	3.66
CO / Cu ratio	0.46	0.75

Cu^+ was not a very stable form in the enzyme and was very easy to oxidize. The large amount of Cu^+ in native DBH might indicate that Cu^{2+} produced by Cu^+ oxidation during the preparation was easier to dissociate from the enzyme than Cu^+ is. Since most of the Cu_a was pulled out in the preparation, it must be easier for Cu_a to be oxidized than for Cu_b , and their redox potential may not be at the same level, i.e. Cu_a has a lower redox potential than Cu_b , which means that Cu_b can receive an electron from an electron donor more easily during turnover.

4. 3. 2. Absorption spectra of the N_3^- - half-apo DBH complex.

The half-apo DBH was titrated with 1M and 5M N_3^- solutions, and then the absorption spectra were recorded (the procedure was the same as the titration of fully reconstituted DBH). Before the measurement, half-apo DBH was oxidized with $\text{K}_3\text{Fe}(\text{CN})_6$, washed intensively with 50 mM potassium phosphate buffer, pH 7.5, in a centricon 30, and concentrated to around 5 mg / ml. The spectrum looked the same as for the fully reconstituted DBH- N_3^- complex, except was of lower intensity (the spectrum is not shown). Much higher N_3^- concentration (2.5 mM [N_3^-]) was required to produce the absorption band at 385 nm than for the fully reconstituted enzyme (0.25 mM [N_3^-]).

The Hill plot, shown in Fig. 4.2., is linear. The Hill constant, n , is 0.96; the association constant, K_a , is 68 M^{-1} , indicating that the N_3^- binding to half-apo DBH is noncooperative — The first N_3^- bound at the enzyme does not influence the binding of the subsequent N_3^- molecules, in another words, each N_3^- molecules bind to DBH independently without any interaction.

Table 4.5. The activity comparison of fully reconstituted and half-apo DBH right after preparations

Cu ⁺ conc. in half-apo DBH	activity (μmol/mg min)	activity after reconstitution	Cu ⁺ after reconstituted
37.2% after few days	12.6	16.34	
96 %	12.8	19.84	33.2 %
60.5 %	17.3	20.1	

Table 4.6. Comparison of N₃⁻ binding properties in fully reconstituted and half-apo DBH

	ε (M ⁻¹ cm ⁻¹)	K (M ⁻¹)	Hill constant, n
Fully rec. DBH	3,100	240	0.69
Half-apo DBH	1,512	68	0.96

The association constant of half-apo DBH-N₃⁻ (68 M⁻¹), compared with that of fully reconstituted azido-DBH, (240 M⁻¹), is much lower. Cu_b, the oxygen binding site, thus has a lower N₃⁻ affinity than Cu_a. The extinction coefficient ϵ is 1,512 M⁻¹cm⁻¹ (in per molar copper concentration), about half as much as in fully reconstituted DBH (see Table 4.6.).

Since fully reconstituted DBH and half-apo DBH share the same λ_{\max} in the absorption spectra, their copper centers probably have similar Cu (II) coordination. For the half-apo DBH-N₃⁻ complex, the extinction coefficient, ϵ , (Cu_b-N₃⁻) is 1,500 M⁻¹cm⁻¹; the average ϵ for Cu_a-N₃⁻ and Cu_b-N₃⁻ (from the fully reconstituted DBH-N₃⁻ complex) is 3,100 M⁻¹cm⁻¹; ϵ for Cu_a-N₃⁻ would be $2 \times 3100 - 1512 = 4,688$ M⁻¹cm⁻¹, which is three-fold of that for Cu_b-N₃⁻.

4. 3. 3. CD spectra of the half-apo DBH-N₃⁻ complex.

Like in native DBH, there was not any absorption bands in the visible region of the half-apo DBH CD spectrum (Fig. 4. 3.a). The CD spectrum of the half-apo DBH-N₃⁻ complex resembled that of fully metallated DBH-N₃⁻ (see Fig. 4. 3.b and Fig. 4. 4.a) with a broad negative band at 400 nm. Due to the lower copper concentration in the enzyme solutions (105 μ M for half-apo DBH against 185 μ M for fully reconstituted DBH), the intensity appeared lower than that of the fully reconstituted DBH-azide complex. But actually they were almost equal in the molar coefficient of dichroic absorption ($\Delta\epsilon$). Moreover, sign, shape, and wavelength of CD spectra of fully metallated DBH-N₃⁻ and half-apo DBH-N₃⁻ complexes were basically indistinguishable, except for a 5 nm violet shift for the half-apo DBH-azide complex. Of course, the CD

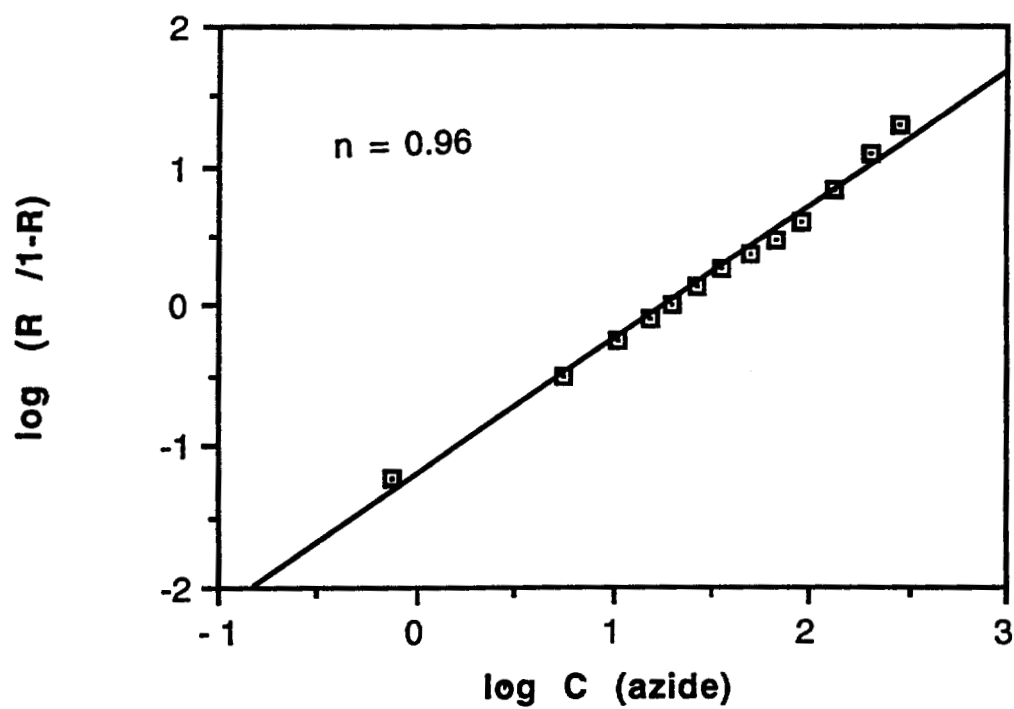


Fig. 4. 2. Hill plot for titration of half-apo DBH with azide at room temperature.

Conditions were as given in experimental section.

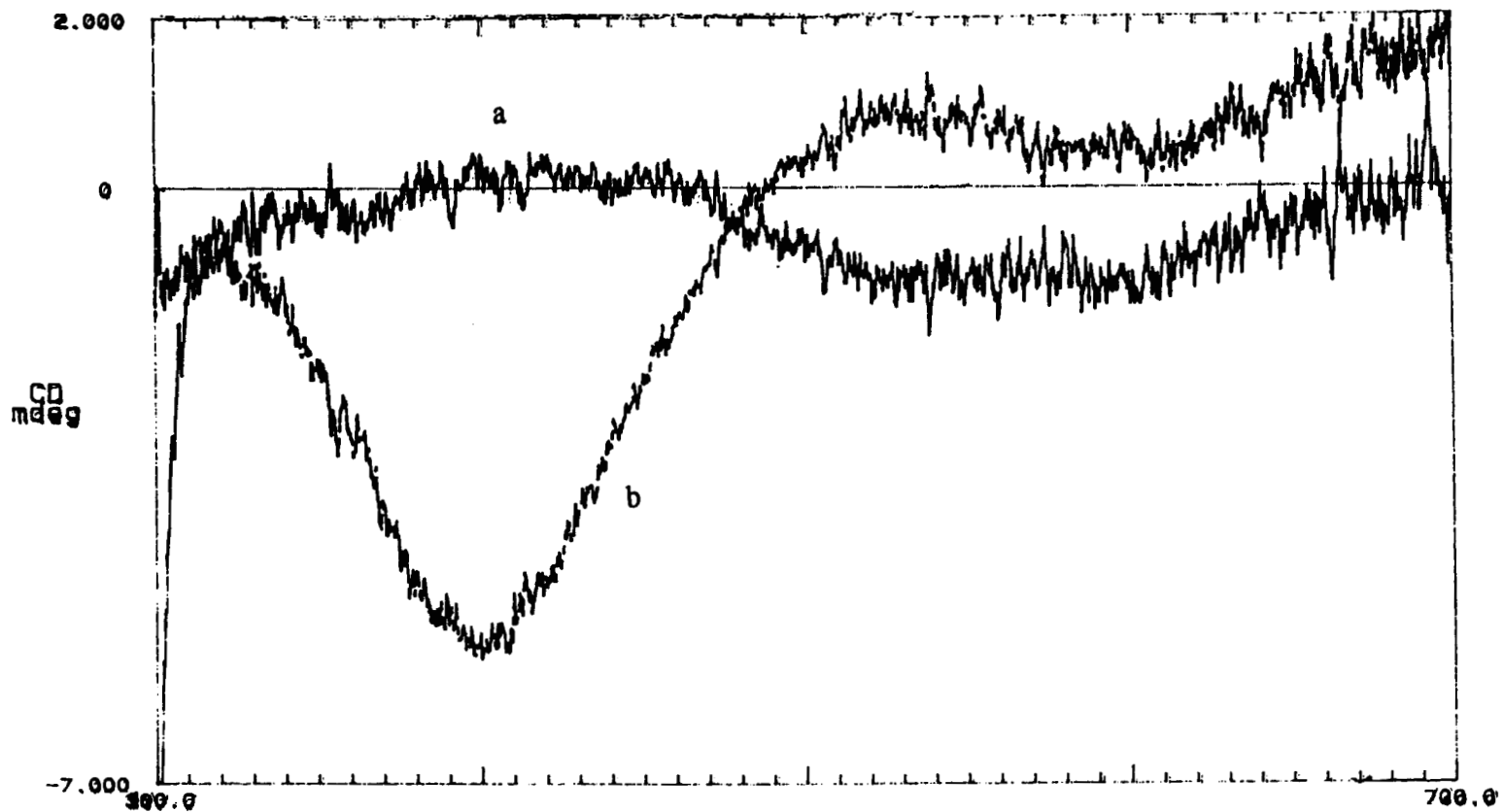


Fig. 4. 3. CD spectra of half-apo DBH (about 5 mg / ml) (a) and the half-apo DBH - azide complex in the presencet of 700- fold azide (b). The temperature during the data collection was kept at 20 °C. The scan speed was 20 nm / min; step resolution 0.1 nm; sensitivity 1 mdeg / cm; time constant 2 sec; BW 1.0 nm; and, the number of scan 2

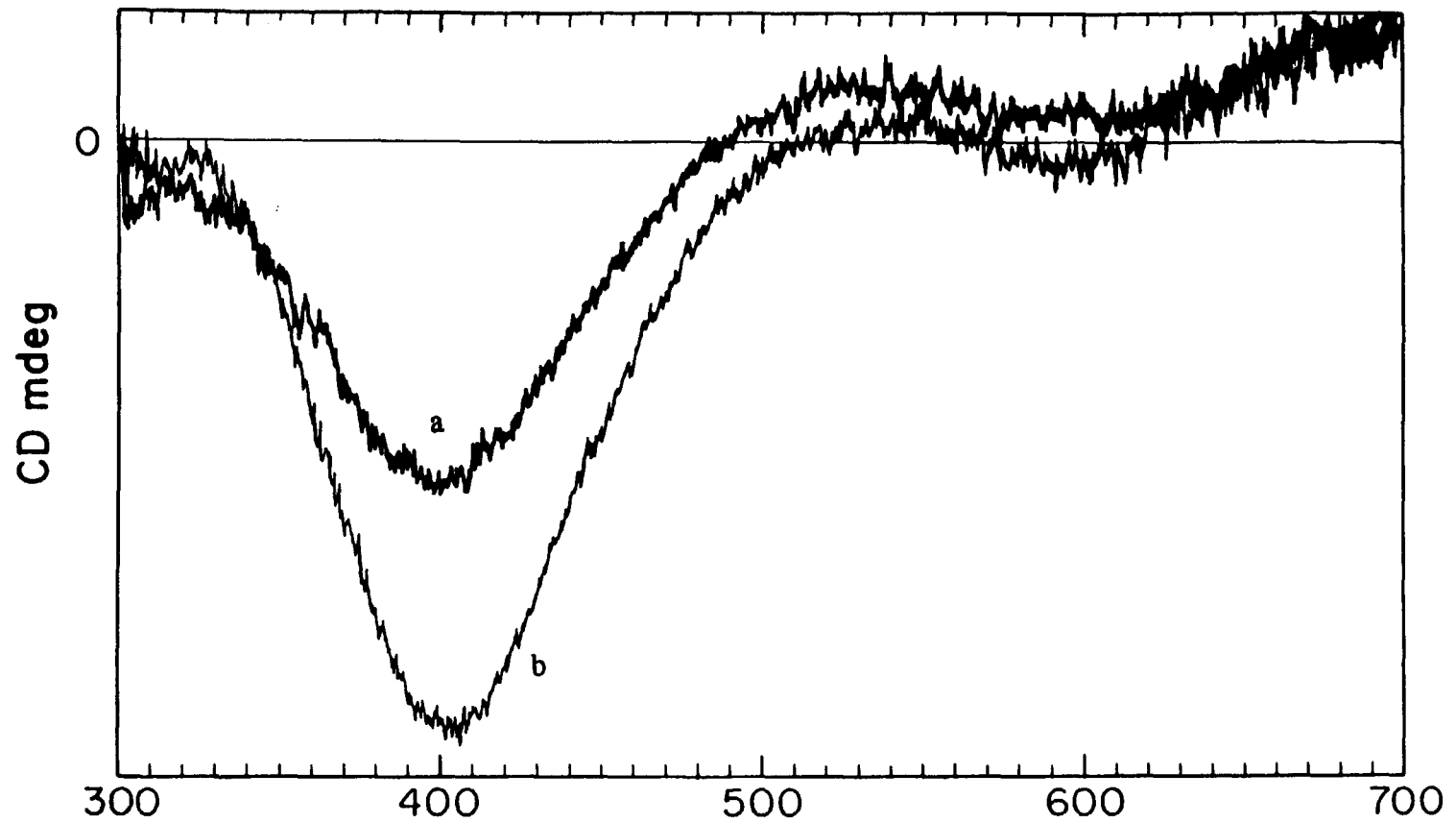


Fig. 4. 4. CD spectra of the half-apo DBH-azide (a) and fully reconstituted DBH-azide complex (b).

Conditions are as described in Fig. 4. 3.

spectrum of the fully metallated DBH-N₃⁻ complex included the signal of Cu_a - N₃⁻ as well as Cu_b - N₃⁻. λ_{\max} of the CD band for Cu_a - N₃⁻ was probably around 410 nm for the reason that λ_{\max} CD for Cu_b - N₃⁻ was at 400 nm and the mean λ_{\max} CD for the mixture of Cu_a - N₃⁻ and Cu_b - N₃⁻ was at 405 nm, and in addition, they had almost identical intensity at the same copper concentration. As a result, the CD bands of Cu_b - N₃⁻ and Cu_a - N₃⁻ should differ by 10 nm. This represents a small, yet probably significant difference.

4. 3. 4. EPR spectra of half-apo DBH

There are no differences in EPR spectra for fully reconstituted and half-apo DBH (see Fig. 4.5. - 4.7.). Figure 4. 5. is the EPR spectrum of half-apo DBH, Fig.4.6. is the EPR spectrum of half-apo DBH oxidized with K₃Fe(CN)₆, and Fig. 4.7. is the EPR spectrum of fully reconstituted oxidized DBH. EPR spectra were measured by a Varian E109 EPR Spectrometer. The temperature of the cavity was stabilized at - 170 °C by a Varian Variable Temperature Controller. The center of the magnetic field was set at 3000 G and the scan range 1000 G. The microwave power was 10 mw, modulation amplitude 20 G, microwave frequency 9.125 GHz, time constant 0.064 second, and scan time 2 minutes. All of EPR spectra look exactly the same, with identical g-value ($g_{\parallel} = 2.27$, $g_{\perp} = 2.07$) and A-value ($A_{\parallel} = 0.0150$), only varying in intensity due to the different Cu²⁺ concentrations.

4. 3. 5. IR spectra of the half-apo DBH-N₃⁻ complex.

The IR spectra of azido-half-apo DBH has a positive band around 2040 cm⁻¹ and an

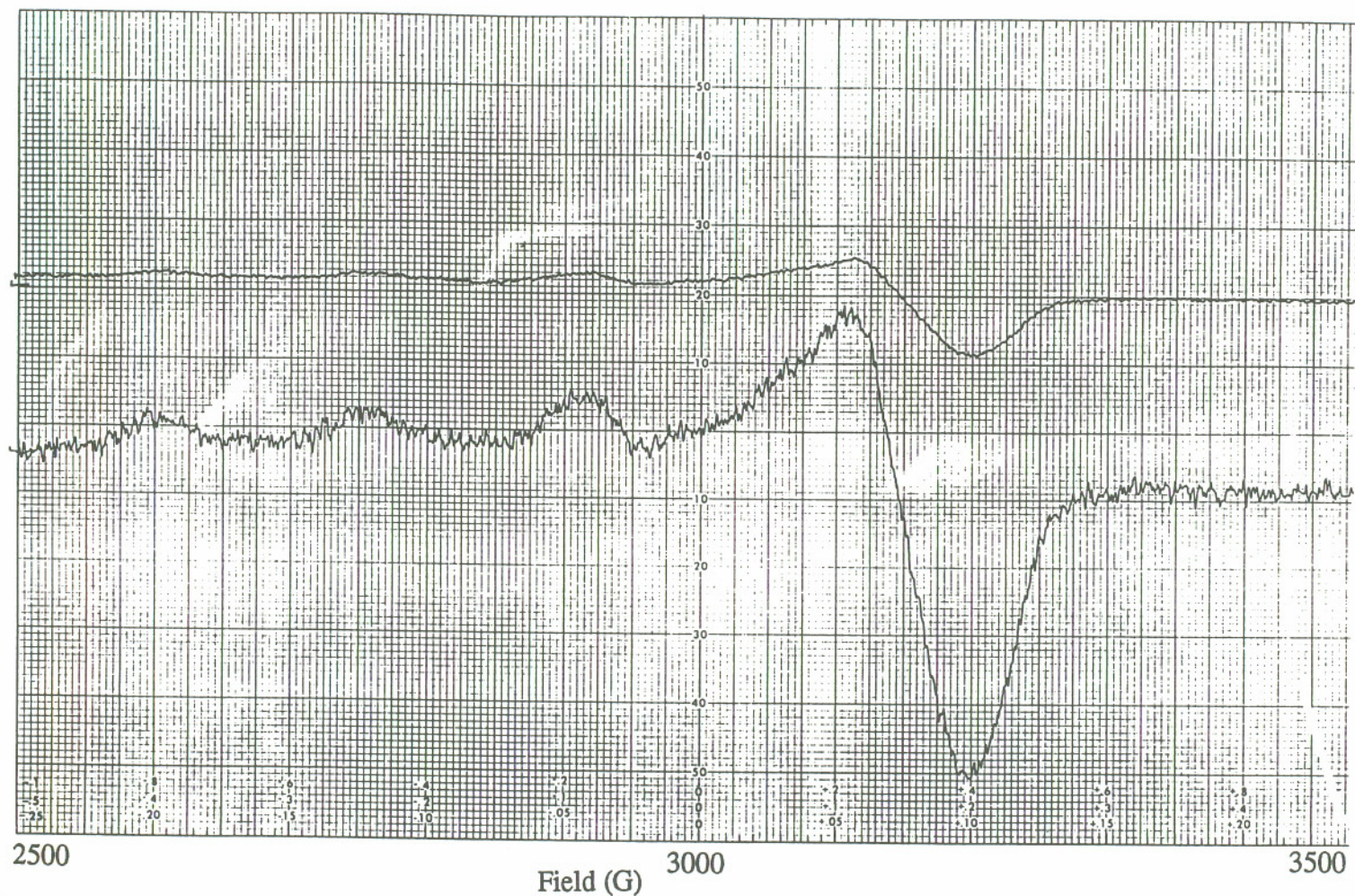


Fig. 4. 5. EPR spectra of half-apo DBH at $-170\text{ }^{\circ}\text{C}$. Two spectra in this figure are from same sample but at different gain. Magnetic field: 3000 G; scan range: 1000 G; Microwave frequency 9.13 GHz; Modulation amplitude 20 G; Microwave power 10 mW; Time constant 0.064 sec; Scan time 2 min.

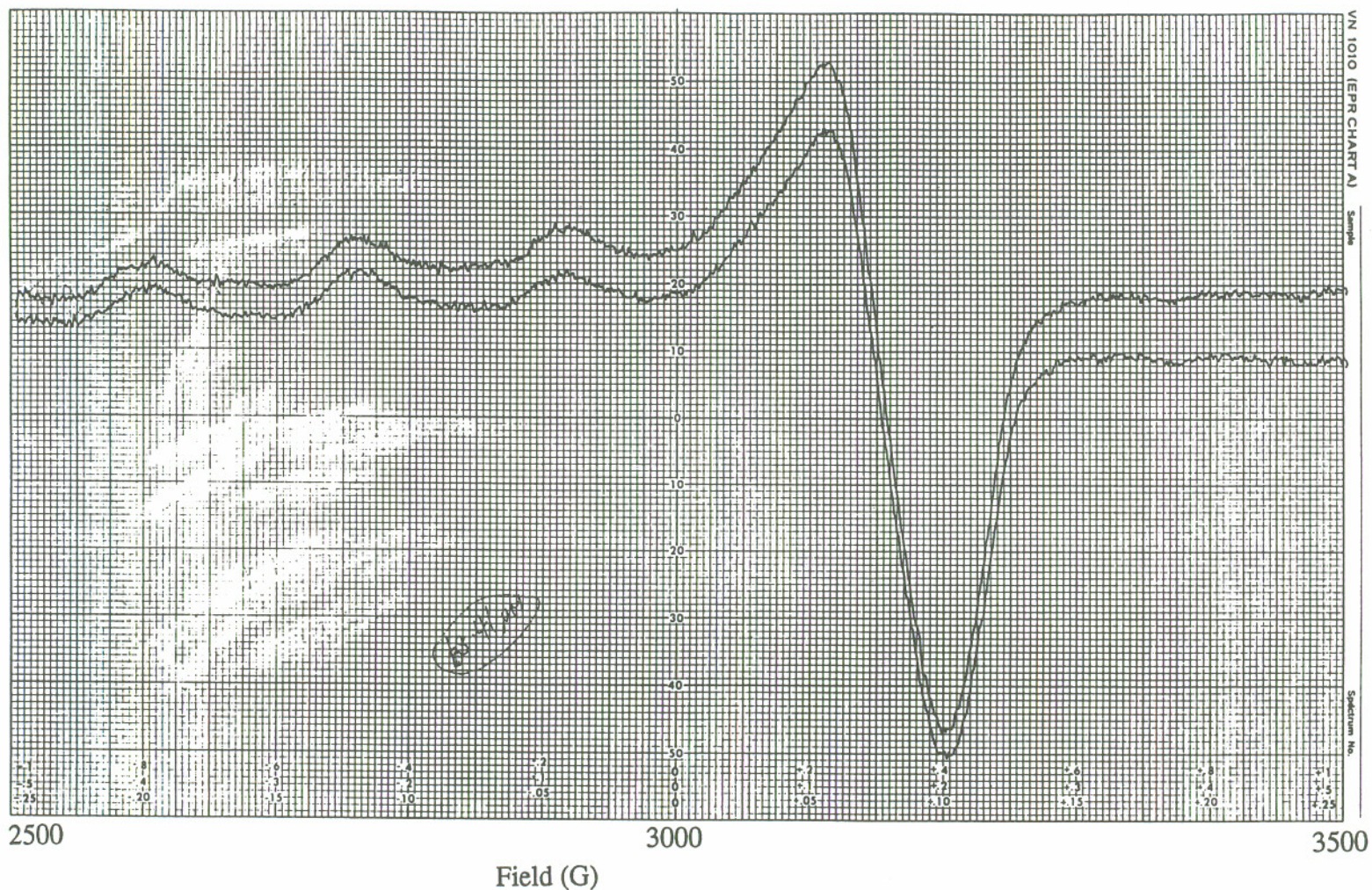


Fig. 4. 6. EPR spectra of oxidized half-apo DBH at -170 °C. Two spectra in this figure are from same sample but at different gain. Magnetic field: 3000 G; scan range: 1000 G; Microwave frequency 9.13 GHz; Modulation amplitude 20 G; Microwave power 10 mW; Time constant 0.064 sec; Scan time 2 min.

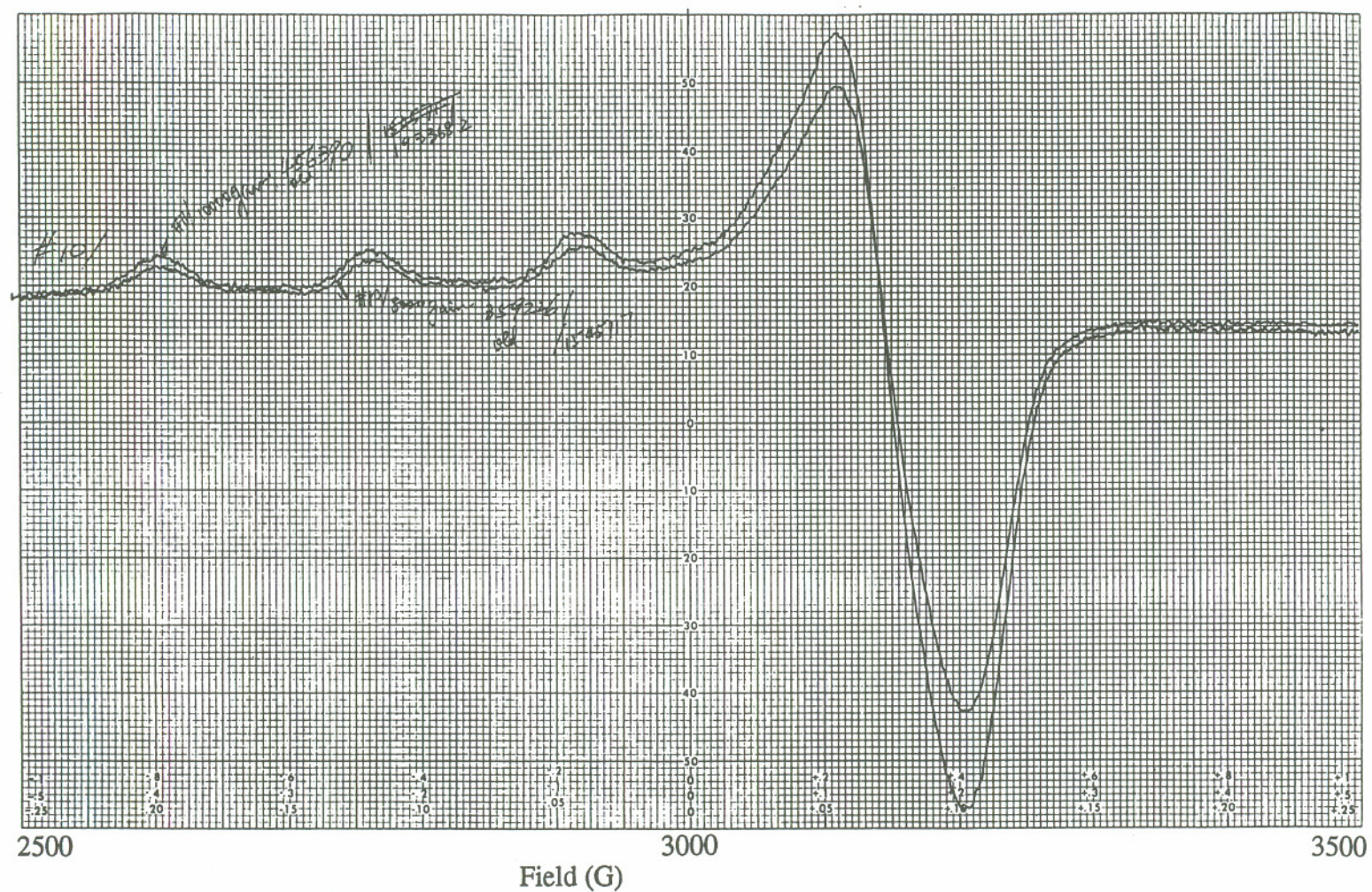


Fig. 4. 7. EPR spectra of fully reconstituted DBH at $-170\text{ }^{\circ}\text{C}$. Two spectra in this figure are from same sample but at different gain. Magnetic field: 3000 G; scan range: 1000 G; Microwave frequency 9.13 GHz; Modulation amplitude 20 G; Microwave power 10 mW; Time constant 0.064 sec; Scan time 2 min.

intense negative band around 2048 cm^{-1} . This negative band also appeared in the IR spectrum of the azido-apo-DBH complex at high azide concentration (10 mM) (see Fig. 4.8.a), in the fully reconstituted DBH-azido complex at 2 mM azide (Fig.4.8.c), as well as in the fully reconstituted DBH-azido complex at high azide concentration (Fig.4.8.d). The intensity of this band is proportional to the amount of azide added to DBH solution. This negative band also appears in SOD-azido IR spectra when the azide concentration is very high ($> 50\text{ mM}$) (Fig.4.8.b). This is the reason that the method for preparing DBH-azido samples involves washing out as much free N_3^- without leading to dissociation of the DBH-azido complexes (see Chapter III experimental method section). The appearance of this negative band may be caused by the non-equilibrium filtration of DBH-azide solution during the centrifugation in the Centricon 30. A large amount of charge within a protein push more free azide into filtrate in order to balance the activities in the retentate and filtrate. On the other hand, the higher concentration of azide anion at the end of centrifugation would force more azide to bind to DBH, causing the lower free azide concentration in the retentate. In the case of half-apo DBH, washing out free N_3^- from azide-half-apo DBH solution results in the disappearance of the 2040 cm^{-1} band. Because the frequency of this band is close to that of the free N_3^- IR band and the negative peak exists in all DBH-azido samples at high N_3^- concentration, it is believed to be free N_3^- which is derived from non-equilibrium separation during the sample preparation process (slightly higher $[\text{N}_3^-]$ in filtrate than in retentate). In order to obtain better spectra of the half-apo DBH-azide complex, the IR spectrum of retentate has been multiplied by a small factor (eg. 1.05) before subtracting the IR spectrum of filtrate. In this way, the negative free N_3^- band is removed so that the vibrational frequency of half-apo bound N_3^- can be determined accurately.

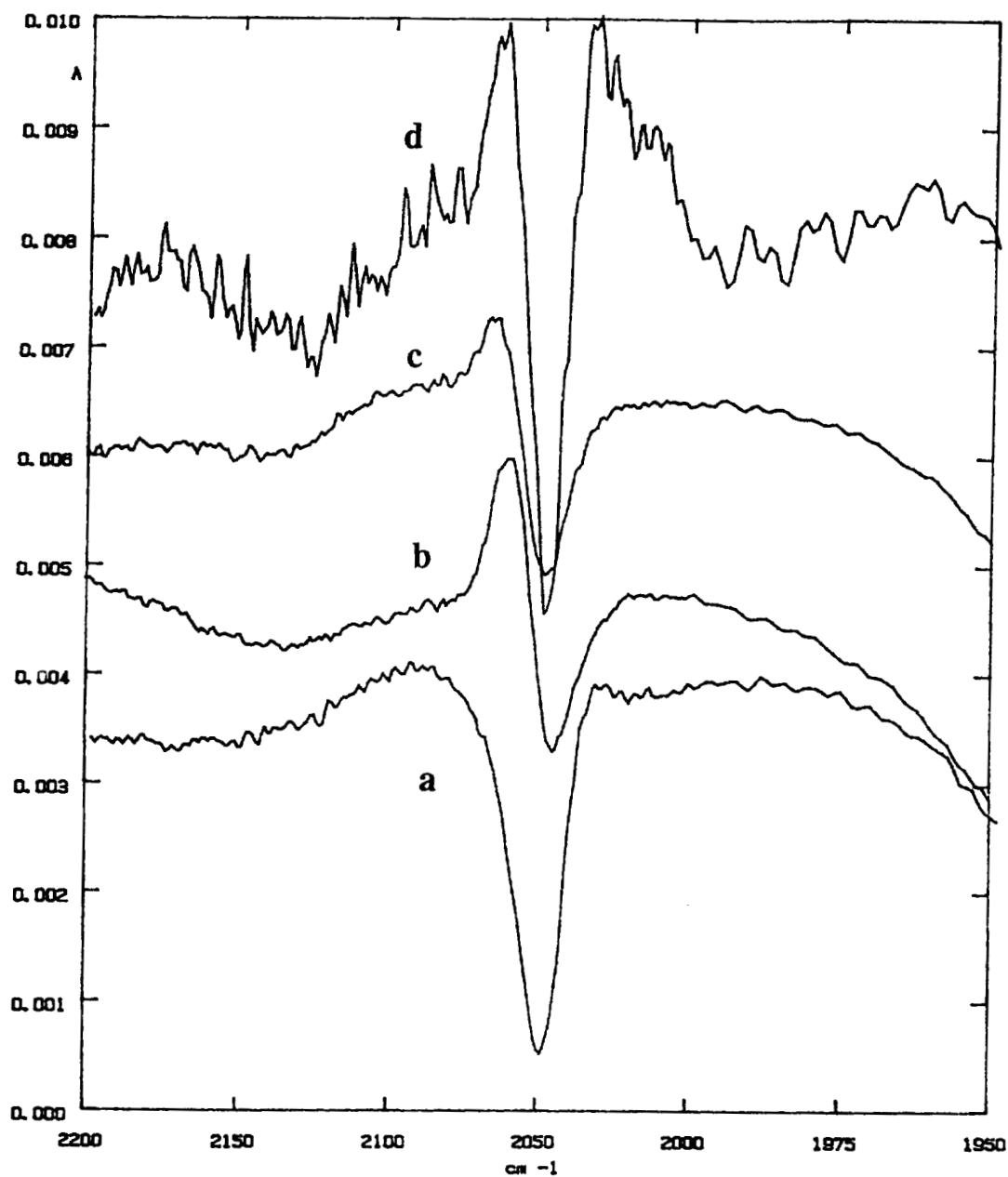


Fig. 4. 8. IR spectra of DBH-azide and SOD-azide complexes. (a) apo-DBH-azide in 10 mM azide solution; (b) azido-SOD in 10 mM azide solution; (c) azido-DBH in 2 mM azide solution; (d) azido-DBH in 10 mM azide solution.

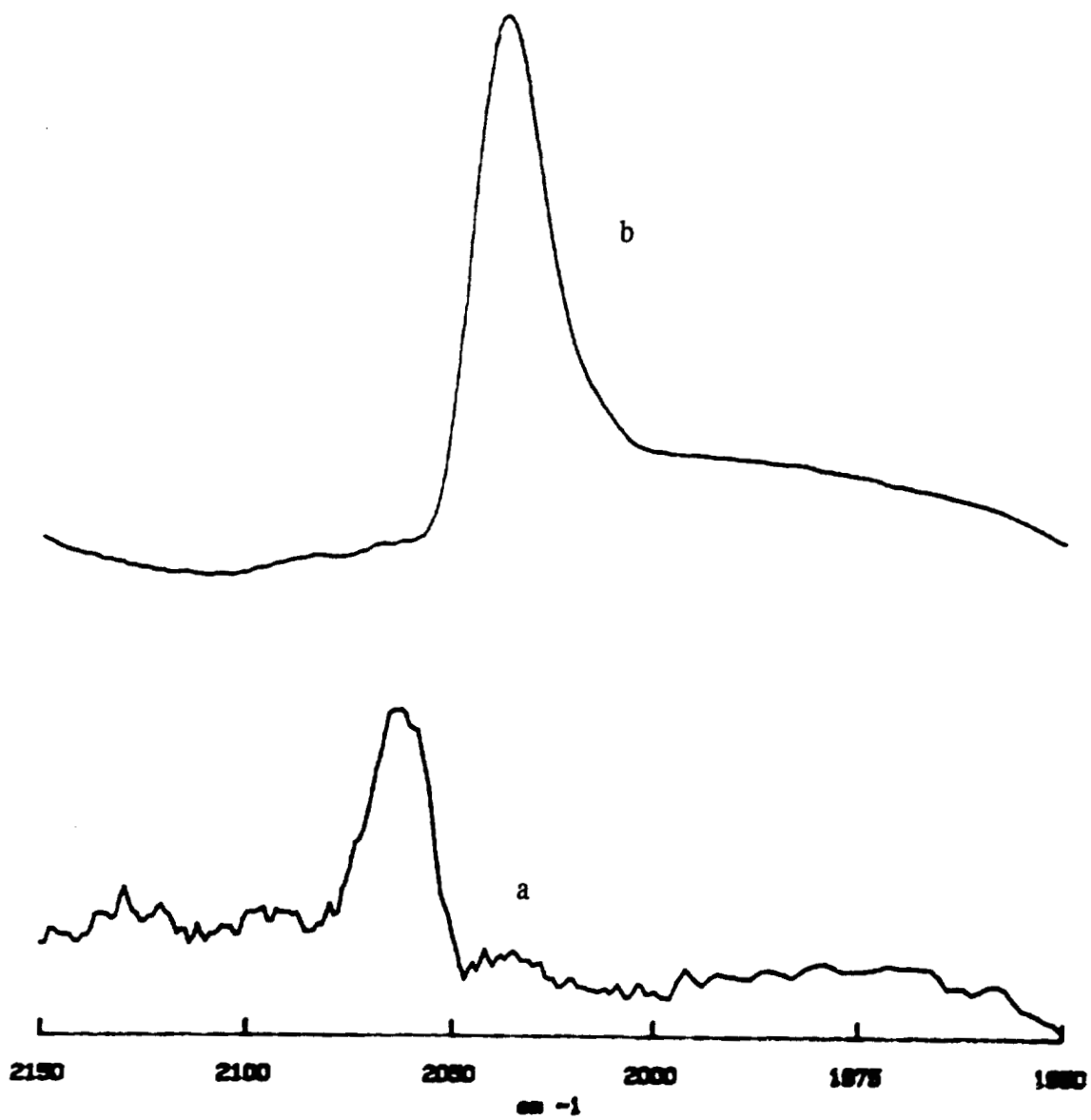


Fig. 4. 9. IR spectra of the DBH-azide complex at low azide concentration (a) and the half-apo DBH-azide complex (b).

The IR spectra of the half-apo DBH- N_3^- complex is compared with fully metallated azido-DBH in Fig. 4.9. $\nu_{\text{N}_3^-}$ shifts from 2048 cm^{-1} for free azide band to 2038 cm^{-1} for half-apo DBH bound azide. The IR band is much narrower than that in the fully metallated DBH- N_3^- complex at high $[\text{N}_3^-]$, but is comparable to the peak at the lower N_3^- concentration (Fig. 4.9.a). For the half-apo enzyme, no bands have been observed at low azide concentration, whereas addition of a relatively high concentration of azide caused the appearance of IR band b. Based on the N_3^- binding affinity to copper centers, the obvious conclusion is that band a is derived from $\text{Cu}_a^{2+} - \text{N}_3^-$ and band b from $\text{Cu}_b^{2+} - \text{N}_3^-$. Their vibrational frequencies show a relatively large difference; band b is at 2038 cm^{-1} and band a is at 2061 cm^{-1} — a 23 cm^{-1} difference.

4. 4. Discussion

4. 4. 1. Absorption spectra of azido-half-apo DBH

The fact that half-apo azido-DBH exhibits the same λ_{max} as the azide to copper charge transfer band in fully metallated enzyme indicates that N_3^- does coordinate to the Cu^{2+} center terminally in fully reconstituted DBH. This is the only mode that could happen in half-apo DBH, since, if N_3^- formed a bridged complex with copper centers, absorption spectra of half-apo and fully reconstituted DBH would be quite different due to the different electronic structures. The symmetry and configuration of two copper centers in each subunit after binding to N_3^- may be quite similar. As showed in Table 1. 2., if the copper-azido complexes are in different configurations (such as trigonal bipyramidal vs. tetragonal configuration), they will have different λ_{max} . As a consequence, the number of ligands in Cu_a^{2+} and Cu_b^{2+} should also be identical.

The smaller extinction coefficient may be an indication that Cu_a^{2+} and Cu_b^{2+} have different electron density. Because the intensity of an absorption spectrum is proportional to $|\int \psi M \psi^{ex} d\tau|^2$, the transition moment integral (Drago, 1977), these two chromophores — $\text{Cu}_a^{2+} - \text{N}_3^-$ and $\text{Cu}_b^{2+} - \text{N}_3^-$ must have different electric dipole moments. The electric dipole moment operator, M , is defined as the distance between the centers of gravity of the positive and negative charges times the magnitude of these charges. The center of gravity of the positive charges in a molecule is fixed by the nuclei, but the center of gravity of the electrons is an average over the probability function (Drago, 1977). The intensity of the absorption spectra will be affected by the distance between the N_1 atom in $\text{N}_1\text{-N}_2\text{-N}_3$ and the Cu^{2+} center as well as the electron densities of N_1 and Cu^{2+} atoms. Lower electron density at Cu_a^{2+} than at Cu_b^{2+} would be a reasonable explanation for the different ϵ value for the $\text{Cu}_a^{2+} - \text{N}_3^-$ and $\text{Cu}_b^{2+} - \text{N}_3^-$ complexes. The environment, or ligands for Cu_a^{2+} , should be made up of less negatively charged donor-atoms that provide less negative charge to the Cu_a^{2+} center in order to produce a more positive electron density. Just as described in Chapter 3, Cu_b may contain an O type ligand (other than tyrasinate) to supply more negative charge. This speculation is consistent with the conclusion from the IR spectra of the DBH-N_3^- complex (see Chapter 3, section 3.3.3.). The second possibility for the lower extinction coefficient for the $\text{Cu}_b^{2+}\text{-N}_3^-$ center is that the bond length between Cu_b and N_1 may be longer, forming a more axial type azide interaction and causing a weaker chemical bond that makes the charge transfer from the N_3^- ligand to the copper center relatively more difficult.

Since the binding constant of half-apo DBH is lower than that of fully reconstituted DBH, Cu_a and Cu_b have different azide binding affinity, and Cu_b (in half-apo DBH) should be the copper whose N_3^- binding affinity is smaller, in other words, the association constant,

K_a , for $\text{Cu}_a^{2+} - \text{N}_3^-$ is much larger than that for $\text{Cu}_b^{2+} - \text{N}_3^-$.

The Hill constant of half-apo DBH binding to azide (0.69) indicates that this binding process is noncooperative, meaning that the azide binding is an independent process and that there is no interaction among N_3^- molecules binding to copper centers in different subunits. The different Hill constants between fully reconstituted (0.69) and half-apo DBH-azido complexes (0.96) prove that a single copper center in a DBH monomer can not provide interaction between the two N_3^- ions, as in the case of fully reconstituted DBH where azide molecules bound at Cu_a and Cu_b are located far enough apart to exclude a magnetic interaction (Blackburn et al, 1988) but close enough to cause the interaction between bound azide ligands. The distances between the copper centers in different subunits thus may be longer than that between two coppers in the same subunit.

Comparing absorption spectra, cooperativity, extinction coefficients, and binding constants between half-apo DBH- N_3^- and fully reconstituted DBH- N_3^- complexes, we are able to conclude that Cu_a^{2+} and Cu_b^{2+} have similar symmetry and configuration but different types of ligands and that the cooperativity of N_3^- binding is induced by binding at the two copper centers in the same subunit.

4. 4. 2. EPR spectra of half-apo DBH and fully reconstituted DBH

That EPR spectra of half-apo DBH and fully reconstituted DBH are identical also indicate Cu_a^{2+} and Cu_b^{2+} have very similar symmetry, since EPR spectra are very sensitive to the configuration of a paramagnetic center. From the previous results, half-apo DBH and fully reconstituted DBH-azido complexes displayed different IR spectra, indicating the

differences between two copper centers in each subunit at room temperature. Thus, the copper centers do not scramble at room temperature; then it is even harder for coppers scrambling in DBH at liquid nitrogen temperature. From the thermodynamic point of view, at room temperature, $\Delta G = \Delta H - T\Delta S > 0$, since the process does not occur spontaneously. During the scrambling process, ΔS should be close to zero because of no changes of the number of molecules; thus $\Delta G = \Delta H > 0$ and does not vary with temperature. The coppers scrambling then becomes a kinetics driven process and is determined by the rate of molecular collision, by thermo-movement of molecules, therefore, by temperature. Generally, the reaction rate doubles as temperature increases 10 K (Atkins, 1986). When temperature decreases from room temperature to $-170\text{ }^\circ\text{C}$ (the temperature used for EPR measurements), the molecular movement will decrease at least 7×10^5 times. Therefore, it is almost impossible for the coppers in half-apo DBH to scramble between two sites at $-170\text{ }^\circ\text{C}$, since they are relatively stable at room temperature.

4. 4. 3. CD spectra of azido-half-apo DBH

The absorption spectra of molecules depend on their constituent chemical groups, but circular dichroism depends entirely on spatial relationships among groups, and hence, on the molecular geometry. Thus, optical activity derives from stereochemistry and springs directly from the orientation of groups relative to one another, not from groups themselves (Vallee and Holmquist, 1980). The CD spectrum is supposed to be much more sensitive to the symmetry of a chromophore and the conformation of a vicinal group than the absorption spectra. For example, the model compounds, $([\text{Co}^{2+}\text{L-R}])$, $\text{R} = \text{Ala}_3, \text{Leu}_3$ and Pro_3 , in which Co^{2+} coordinates the same atoms, have absorption spectra that are

basically the same except that the wavelength of $[\text{Co}^{2+}\text{-L-Pro}_3]$ is shifted a little towards lower energy. But their CD spectra are quite different in the number of peaks, sign, and intensity (Denning and Piper, 1966). In the case of the DBH-N_3^- and half-apo DBH-N_3^- complexes, the CD spectra are similar in intensity, shape, band position, and sign, strongly suggesting geometric similarities between the two copper centers.

4. 4. 4. IR spectra of azido-half-apo DBH

The theory of vibrational spectra in N_3^- - Cu complexes indicates that the frequency of the azide asymmetric stretch is determined by the inequivalence of the $\text{N}_1\text{-N}_2$ bond and the $\text{N}_2\text{-N}_3$ bond (see discussion in Chapter 3, and Fig. 3.13.); the more significant the bond's inequivalence is, the higher the N_3^- IR frequency. We have speculated that the Cu_a^{2+} should be more positively charged than Cu_b^{2+} . Thus, Cu_b^{2+} fits more to situation A in Fig. 3.13., and which indicates the presence of one or more oxygen like ligands at the Cu_b center other than the N atom from the His ligands, because the O (other than tyrosinate) atom possesses more negative electron density than N (from His) to donate to the Cu_b^{2+} center. The two azide bonds are less inequivalent for azide bound at Cu_b^{2+} than for azide bound at the Cu_a^{2+} center, which provides the explanation of lower frequency for N_3^- - Cu_b^{2+} . That Cu_b^{2+} contains the oxygen atom as a ligand is a reasonable conclusion for the IR spectra.

The structure of the active center after binding azide then should be $\text{Cu}_a^{2+}(\text{His})_3\text{N}_3^-$ - $\text{Cu}_b^{2+}\text{N}_3^-(\text{His})_2\text{O}$ (other than tyrosinate), and there may be some H_2O molecules occupying axial positions in both centers. As discussed in Chapter 3, N_3^- removes the equatorial H_2O molecule. Thus the possible configuration of Cu_a^{2+} is 3 His and one H_2O

with axial H_2O ligands forming a tetragonal configuration, and at the Cu_b^{2+} , two His, one O type ligand, and one water also forming a tetragonal configuration in which a little distortion may exist (see Fig. 4.11.). It is Cu_b^{2+} that is responsible for oxygen binding (because CO coordinates at the Cu_b , and CO is a competitive inhibitor with respect to O_2).

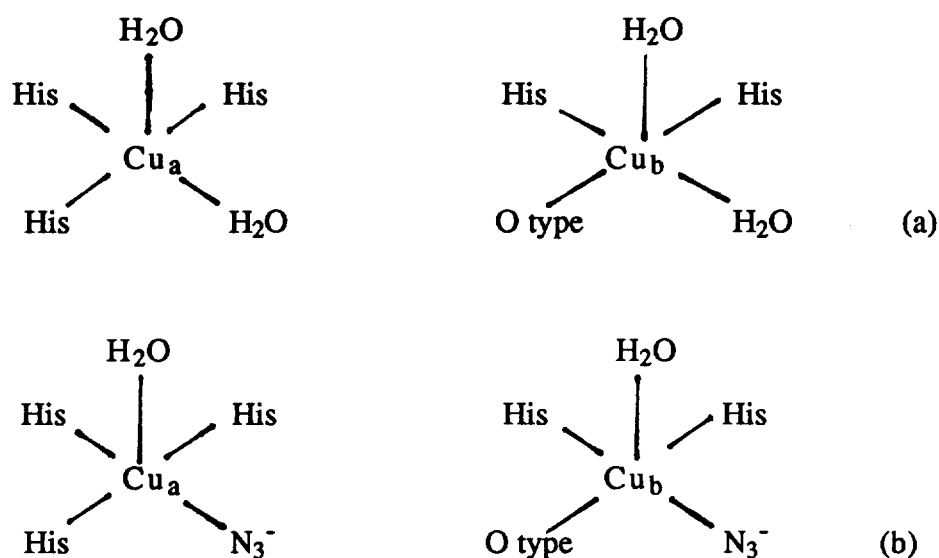


Fig. 4. 10. The possible environment of the Cu (II) centers in native DBH each subunit (a) and in the DBH-azide complex (b).

4. 4. Conclusion

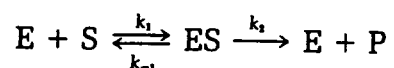
Strong evidence from the comparison of spectroscopic studies between the half-apo and fully reconstituted DBH-azide complexes indicates similarity in coordination number and symmetry but different type of ligands for Cu_a and Cu_b centers in DBH. Cu_a probably contains three His ligands and one or two water molecules; Cu_b contains two His ligands, one O type (O from an amino acid other than tyrosinate) ligand, and one or two water ligands.

CHAPTER V

DBH INHIBITION BY N_3^- AND SCN^- -ENZYME KINETIC STUDIES

5. 1. Introduction

Enzyme kinetics is the branch of enzymology that deals with the rates of enzyme-catalyzed reactions. For an enzyme catalyzed reaction:



Scheme 5.1.

The rate equation (Michaelis-Menten rate law) can be expressed as $v = \frac{V[S]}{K_m + [S]}$, in which K_m is the substrate concentration which gives half-maximal reaction velocity; V is defined as the maximum rate of reaction; $[S]$ is the substrate concentration.

Such enzyme kinetic studies are able to deduce the kinetic mechanism of the catalytic reaction, the order in which substrates add, products leave the enzyme, and classes of

enzyme-substrate and enzyme-product complexes formed and thereby the architecture of the active site. It can provide insight into enzyme specificity and parameters that characterize the physical properties of enzymes. In some cases, kinetics of a reaction provide evidence for stable, covalently - bound intermediates that are undetectable by ordinary chemical analyses. Certain kinetic constants can be determined, and from these we can obtain useful information concerning the usual intracellular concentrations of substrates and products as well as the physiological direction of the reaction. Kinetics of a reaction may indicate the way in which the activity of the enzyme is regulated *in vivo*. A kinetic analysis can lead to a model for an enzyme-catalyzed reaction and, conversely, the principles of enzyme kinetics can be used to write the kinetic equation for an attractive model. The kinetic equation tells us exactly how all ligands of a system interact to affect the velocity of the reaction.

Enzyme inhibition is enormously important in enzymology. The studies of enzyme inhibition can help us to understand how the enzyme works. By systematic modification of the structure of a substrate, an active site of the enzyme or an allosteric binding site can be "mapped". The inhibition of enzyme activity is one of major regulatory devices of living cells and one of the most important diagnostic procedures. Inhibition studies often tell us something about the specificity of enzymes. Once the detailed chemistry of the active site has been deciphered, it becomes possible to carry out the rational design of inhibitors with therapeutic value.

The simple type of inhibition, in which only one type of inhibitor is present at anytime, can be classified into three classes: competitive, noncompetitive, and uncompetitive inhibition. A competitive inhibitor is a substance that combines with free enzyme in a

manner that prevents substrate binding. That is, the inhibitor and the substrate are mutually exclusive, often because of true competition for the same site. A classical noncompetitive inhibitor has no effect on substrate binding, or vice versa. The inhibitor and the substrate bind reversibly, randomly, and independently at different sites. In this case, the inhibitor, I, binds to both E (enzyme) and ES (the enzyme•substrate complex); S binds to E and to EI (the enzyme•inhibitor complex). The binding of an inhibitor has no effect on the dissociation constant of the substrate. However, the resulting ESI (enzyme•substrate•inhibitor) complex is inactive. An uncompetitive inhibitor is a compound that binds reversibly to the enzyme•substrate complex yielding an inactive ESI complex. The inhibitor does not bind to the free enzyme. Uncompetitive inhibition requires that the inhibitor affects the catalytic function of the enzyme but not its substrate binding.

Both N_3^- and SCN^- ions manifest inhibition of DBH, which will be discussed in this chapter. Some earlier results have shown that N_3^- functions as an uncompetitive inhibitor with respect of the substrate, tyramine, but as a mixed type inhibitor with regard to the substrate, ascorbate (Blackburn, 1984). SCN^- belongs to the same type of ligands as N_3^- but is a softer base than N_3^- ; softness of SCN^- ligand may affect the electron density at copper centers if SCN^- is able to coordinate to copper. From infrared spectra, it is very clear that a ligand like O from amino acids other than tyrosinate (or S from Met) would moderate the positive charge at copper centers, thus, SCN^- would be a good probe to test the effect of a S atom coordinating to the copper centers in DBH. Because SCN^- does not show any ligand to copper (in DBH) charge transfer transition in absorption spectra, it is very difficult to study the binding of SCN^- at the copper centers. Kinetics would provide an effective method to fulfill this task.

5. 2. Experimental Methods

5. 2. 1. DBH inhibition by SCN^- with tyramine or ascorbate as the variable substrate.

The experiment was set up as in the activity assay system to measure the oxygen consumption with a Clark oxygen electrode (see chapter 2). When tyramine was the varied substrate, its concentration was varied from 0.1 mM to 1.0 mM, and SCN^- concentration maintained at 0 mM for the first series of reaction rate measurements. For the second series of velocity measurements, SCN^- concentration was kept at 0.1 mM. For the third series, SCN^- concentration was 0.2 mM; and for the fourth, $[\text{SCN}^-]$ was 0.3 mM. The enzyme concentration was kept constant for each series of measurements, and oxygen concentration was kept at 236 μM which was the oxygen saturation concentration in 200 mM acetate buffer—the reaction buffer—at 25 °C. Then 50 μl , 1 M ascorbate (dissolved in water) was injected into the reaction mixture to start the reaction. The initial reaction rates were recorded with a Cole Parmer chart recorder.

For the series of experiments with ascorbate as the variable substrate, the concentration of tyramine in assay solution was maintained at 10 mM, [oxygen] was constant at 236 μM and ascorbate was varied from 0.075 mM to 1.0 mM. SCN^- concentrations for each series of velocity measurement were increased from 0, 0.1, 0.2, to 0.3 mM as above.

5. 2. 2. DBH inhibition by N_3^- and SCN^- with oxygen as the variable substrate.

DBH inhibition by N_3^- and SCN^- was also measured using an assay system that varies

the substrate (O_2) concentration while keeping other substrates (tyramine and ascorbate) fixed at 10 mM. The oxygen concentration was varied by mixing appropriate volumes of anaerobic acetate buffer and air-saturated buffer. The oxygen concentration in the assay solution was measured directly from the reading of the O_2 electrode calibrated with air-saturated buffer and pure Ar. After equilibration at 25° C for a few minutes, 50 μ l 1M ascorbate was injected to start the reaction. For both N_3^- and SCN^- inhibition measurements, the oxygen concentration was varied from 30 μ M to 250 μ M. SCN^- concentration was set at 0, 5, 10 to 20 μ M for each series of measurement. N_3^- concentration was fixed at 0, 1, 5, 10 mM.

5. 2. 3. EPR spectra of DBH in the presence of varying concentrations of SCN^-

Fully reconstituted, oxidized DBH EPR spectra in the presence of SCN^- were recorded with Varian E109 Electric Paramagnetic Resonance Spectrometer whose parameters were set as described in chapter 2, section 2. 6. 0.3 ml fully reconstituted DBH (the total copper concentration was about 300 μ M obtained from AA, and Cu^{2+} was about 250 μ M from EPR) was frozen at -170 ° C in liquid N_2 . SCN^- stock solution had a concentration 1 M, dissolved in 50 mM phosphate buffer, pH 7. 5. The titration was started by adding 1 μ l, 1 M SCN^- solution into DBH, mixing completely, and recording the EPR spectrum. Larger amounts of SCN^- solution were added late on; finally 40 μ l 20 M SCN^- was added, at which concentration, the DBH EPR spectrum did not change any more. The Cu^{2+} concentration was determined through double integration of the EPR spectra, calibrated with a series of copper standard solutions. DBH for this experiment had a concentration of about 13 mg / ml, 7.6 copper / DBH, activity about 17 μ mol / mg min.

5. 3. Results and Discussion

5. 3. 1. DBH inhibition by SCN^- with tyramine or ascorbate as the variable substrate

The double reciprocal plots (also called Lineweaver-Burk plots) of SCN^- inhibition while tyramine concentration is varied are shown in Fig. 5.1. A series of parallel straight lines is found whose slopes do not change. This type of inhibition belongs to the uncompetitive type, in which the intercept at the $1/V$ axis is related to V_{\max} by the relation

$$1/V_{\text{app}} = (1 + [I]/K_i) / V_{\max}$$

and the intercept at the $1/[S]$ axis is given by the equation,

$$1/K_{\text{mapp}} = (1 + [I]/K_i) / K_m$$

here K_i is the dissociation constant of an inhibitor, $K_i = [\text{ES}][\text{I}] / [\text{ESI}]$. The replot of $1/V_{\text{app}}$ against $[I]$ is shown in Fig. 5.2, from which the K_i is calculated from the slope of the replot to be 0.156 mM. K_i calculated from replot of $1/K_{\text{mapp}}$ versus $[I]$ was 0.228 mM (see Fig. 5. 2.). Since the replots are not perfect straight lines, the K_i values from the two different replots are in reasonable agreement. The replots are not linear but parabolic at higher SCN^- concentration. A non-linear replot is an indication that more than one inhibitor molecule binds to the enzyme.

When ascorbate is the variable substrate, the double reciprocal plots are also parallel with each other (see Fig. 5. 3.), indicating that SCN^- is an uncompetitive inhibitor with ascorbate as the varied substrate. The fundamental kinetic behavior expected for uncompetitive inhibition is that the value of both K_{mapp} and V_{\max} are altered by a factor, $1 + [I]/K_i$; the apparent maximum rate of the reaction V_{app} is decreased,

$$V_{\text{app}} = V_{\max} / (1 + [I]/K_i)$$

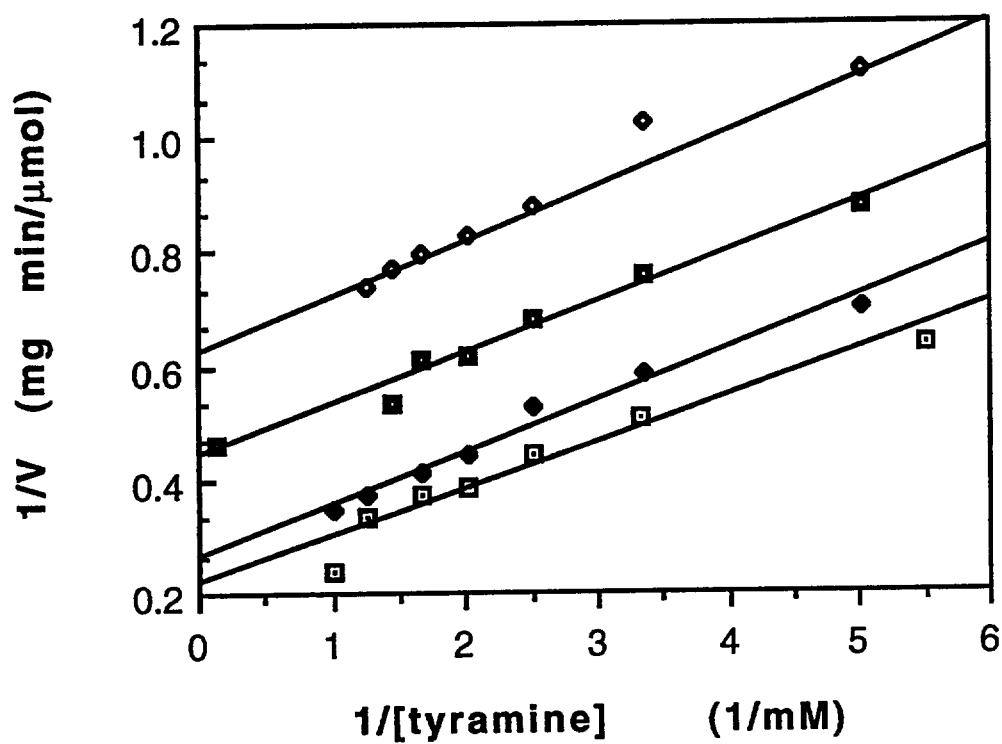


Fig. 5. 1. Double reciprocal plots of DBH inhibition by SCN⁻ with oxygen and ascorbate saturating and tyramine as variable substrate at 298 K. [SCN⁻]: □, 0 mM; ●, 0.1 mM; ■, 0.2 mM; ◆, 0.3 mM.

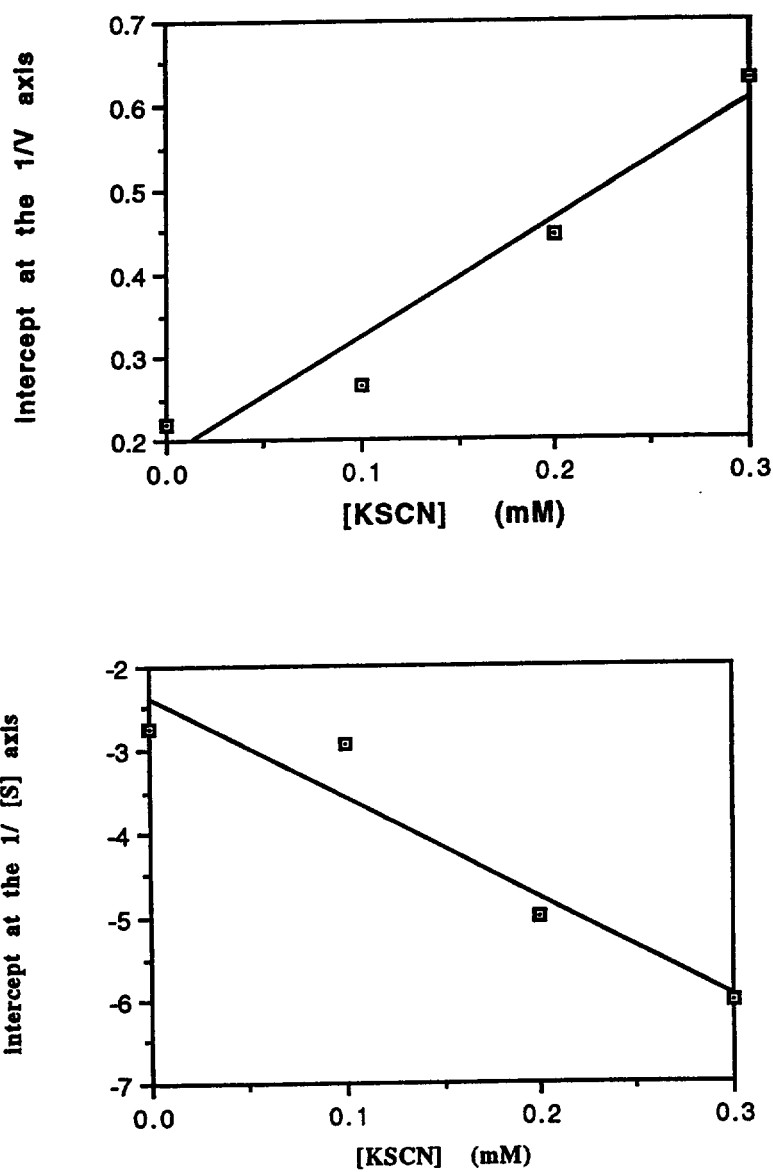


Fig. 5. 2. Replots of DBH inhibition by SCN^- with oxygen and ascorbate saturating and tyramine as variable substrate at 298 K. Top: replot of the intercept at the $1/V$ axis versus $[\text{SCN}^-]$. Bottom: replot of the intercept at the $1/[S]$ axis versus $[\text{SCN}^-]$.

and the apparent K_m is also decreased,

$$K_{mapp} = K_m / (1 + [I] / K_i)$$

The replot of $1 / V_{app}$ versus $[I]$ displays a parabolic line and gives $K_i = 0.064$ mM (see Fig. 5. 4.). K_i calculated from the slope of the replot of $1 / K_{mapp}$ versus $[I]$ is 0.104 mM (see Fig. 5.4.). The replot is very good straight lines in this case. K_i is smaller than that when tyramine is the variable substrate.

Uncompetitive inhibition is very common in steady-state multi reactant system. The inhibitor, SCN^- , will be uncompetitive with respect to a given substrate, tyramine; it binds to DBH only after tyramine binds (although the inhibitor rarely binds to a central complex when all the substrate binding sites are filled). At any $[SCN^-]$, an infinitely high tyramine concentration will not drive all of the enzyme to the ES form; some nonproductive ESI complex will always be present. Consequently, we can predict that V_{max} in the presence of an uncompetitive inhibitor will be lower than the V_{max} in the absence of an inhibitor. Unlike noncompetitive inhibition, the K_{mapp} value will decrease. The decrease occurs because the reaction $ES + I \rightleftharpoons ESI$ removes some ES, causing the reaction $E + S \rightleftharpoons ES$ to proceed to the right. The degree of inhibition depends on the substrate concentration, but unlike competitive inhibition, the degree of inhibition increases as [tyramine] increases. This is to be expected, because an uncompetitive inhibitor combines only with the DBH•tyramine complex, and the concentration of DBH•tyramine increases as [tyramine] increases, therefore, more inhibitor molecules are able to associate with the enzyme.

The mechanism for uncompetitive inhibition has to include a conformation change of enzyme after binding to the substrate to form or to unmask the inhibitor binding site in

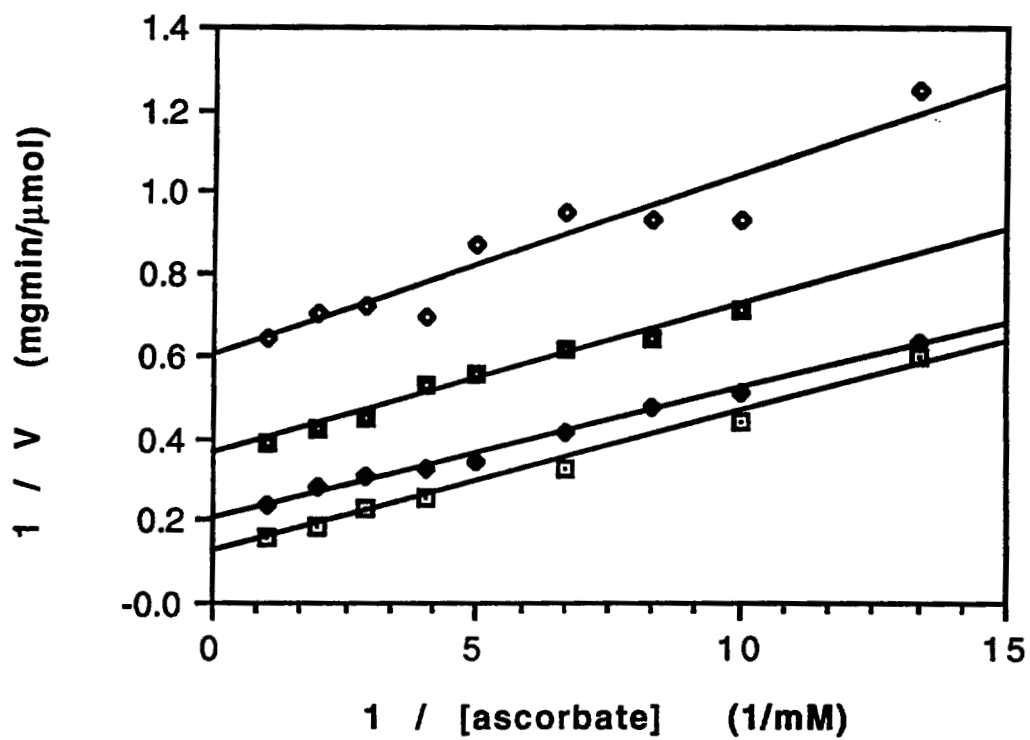


Fig. 5.3 Inhibition of DBH by SCN^- with oxygen and tyramine saturating and ascorbate as variable substrate at 298 K. $[\text{SCN}^-]$: \square , 0 mM; \bullet , 0.1 mM; \blacksquare , 0.2 mM; \blacklozenge , 0.3 mM.

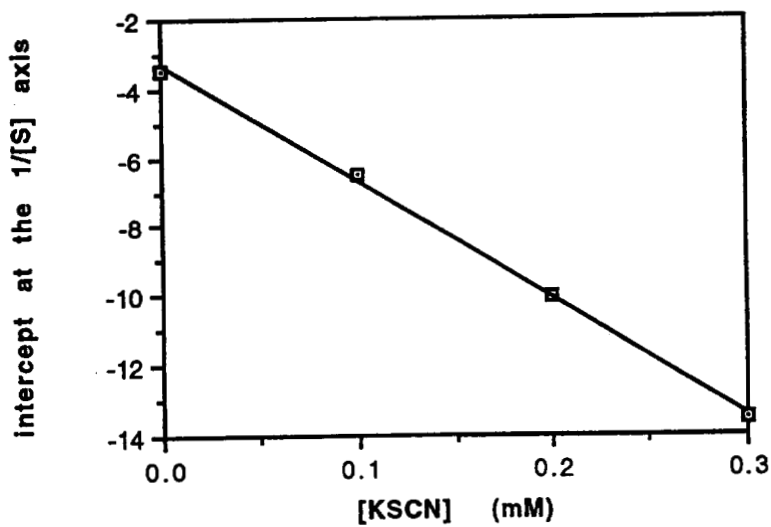
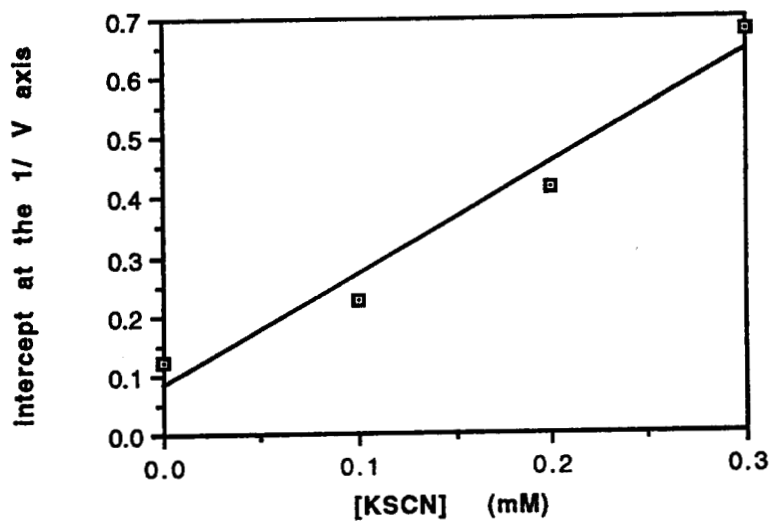


Fig. 5. 4. Replots of DBH inhibition by SCN^- with oxygen and tyramine saturating and ascorbate as variable substrate at 298 K. Top: replot of the intercept at the $1/V$ axis versus $[\text{SCN}^-]$. Bottom: replot of the intercept at the $1/[S]$ axis versus $[\text{SCN}^-]$.

order to be able to form the ESI complex (see Fig. 5.5., from Segel, 1975). The native DBH, without the substrate, tyramine, present, is not able to coordinate to its inhibitor, SCN^- . This probably is the reason that there is no obvious electronic spectra existing for the DBH• SCN^- complex. However, N_3^- also displays uncompetitive inhibition with tyramine as the variable substrate (see Fig. 5.6., from Blackburn, 1984). Addition of azide to the enzyme leads to immediate formation of a ligand to copper charge transfer transition at 385 nm in the absorption spectrum. This may be due to the high N_3^- concentration changing the DBH conformation to make the N_3^- binding sites become available. The observation that the N_3^- dissociation constant from kinetic data (tyramine is present) is only about 1/3 of that from spectrophotometric titration (without tyramine) (Blackburn et al, 1984) suggests that resting DBH can coordinate to N_3^- only at higher azide concentrations. Thus, an anion inhibitor, like azide, seems able to alter the conformational structure of DBH. For SCN^- , either the ligand to copper charge transfer transition can not occur, or SCN^- is unable to change DBH conformation to unmask the SCN^- binding site even at high SCN^- concentration.

SCN^- expresses uncompetitive inhibition when ascorbate is the variable substrate. As described above, it is assumed that SCN^- can bind only to the DBH•ascorbate complex, not free DBH. ESI is a dead end complex, not being able to convert to the product at all. SCN^- inhibition when ascorbate is a variable substrate suggests that ascorbate has to reduce DBH first in order for SCN^- to bind at the Cu centers, or SCN^- binds only to the Cu^+ form of enzyme. At any $[\text{SCN}^-]$, a portion of DBH will remain as the unproductive Enzyme•Ascorbate• SCN^- complex. For uncompetitive inhibition, an inhibitor is actually an activator with respect to K_m . If the substrate concentration is low enough so that the reaction is essentially first-order, the effect of an uncompetitive inhibitor on V_{max} will be

UNCOMPETITIVE INHIBITION

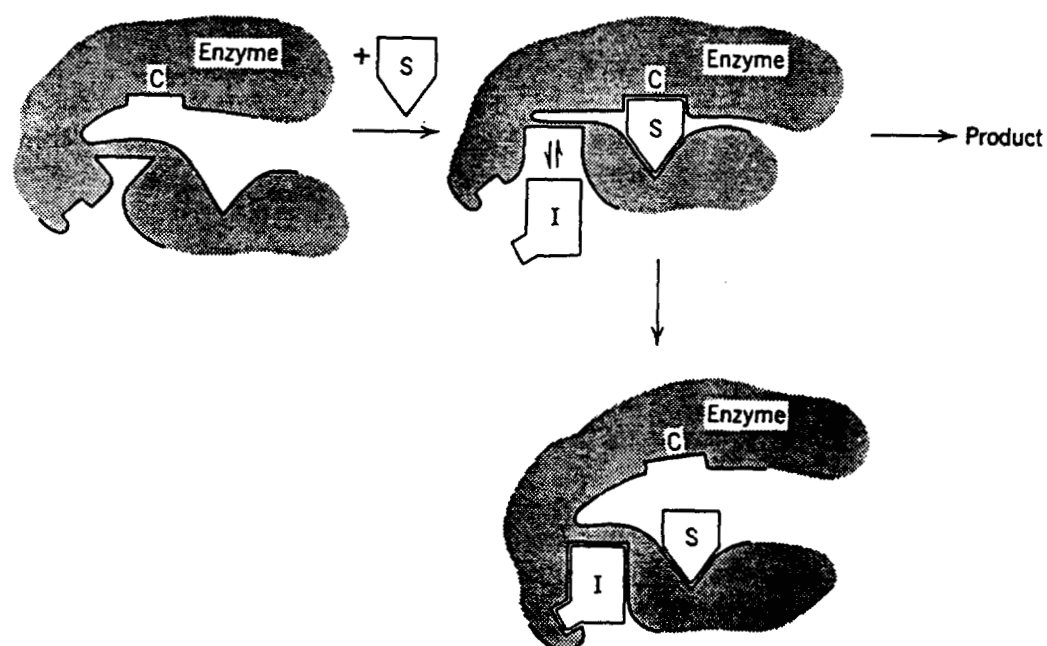


Fig. 5.5. Uncompetitive inhibition; I binds only to the ES complex. When S binds, a conformational change occurs in the enzyme which forms or unmasks the I site. The resulting ESI complex is catalytically inactive; C represents the catalytic center of the enzyme.

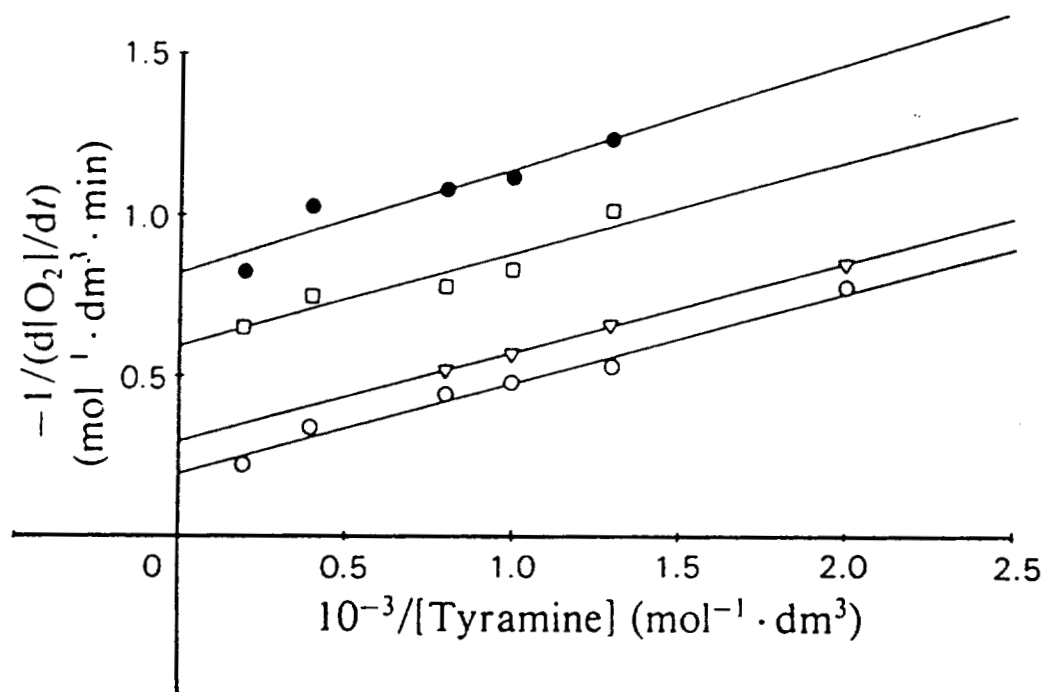


Fig. 5. 6. *Inhibition of dopamine β -mono-oxygenase by N_3^- with ascorbic acid saturating ($1.0 \times 10^{-2} \text{ mol} \cdot \text{dm}^{-3}$) and tyramine as variable substrate at $298 \pm 0.1 \text{ K}$*
 $10^3 \times [\text{N}_3^-]$ ($\text{mol} \cdot \text{dm}^{-3}$): \circ , 0; ∇ , 6.0; \square , 15.0, \bullet , 60.0. Rates were measured by using an oxygen-sensitive electrode as described in the text.

almost completely canceled by its opposite effect on K_m and little or no inhibition will be observed.

Uncompetitive inhibition definitely is an indication that the inhibitor, SCN^- , and the substrate, ascorbate, do not bind to DBH at the same site to exclude each other since they form the $\text{DBH}\cdot\text{ascorbate}\cdot\text{SCN}^-$ complex. Ascorbate is the substrate that reduces the Cu^{2+} form of DBH into Cu^+ during turnover and binds to DBH before other substrates, tyramine and O_2 , are able to bind to the enzyme. If ascorbate directly transfers electrons to the copper centers, and does not go through any intermediate, it should be able to bind at the copper centers. On the other hand, SCN^- as a copper ligand certainly binds at the copper centers. Thus, both ascorbate and SCN^- coordinate to copper centers in DBH, but probably at different sites, SCN^- is at one copper center, and ascorbate has to be at the other copper center in each subunit.

Unlike SCN^- , N_3^- displays linear mixed-type inhibition with respect to ascorbate (see Fig. 5. 7. from Blackburn, 1984), which affects both the K_m and V_{\max} values of an enzyme-catalyzed reaction. This type of inhibition can arise from several situations: a mixture of partial competitive and pure noncompetitive inhibition, a mixture of pure competitive and noncompetitive inhibition, or a mixture of pure competitive and pure uncompetitive inhibition. N_3^- has been proven to coordinate to both copper centers by spectroscopic studies; consequently, no matter which of the above situation is followed, as a mixed type inhibitor, one N_3^- molecule always competes with ascorbate for the binding site at the active center; at the same time, the other N_3^- molecule does not influence ascorbate binding to DBH.

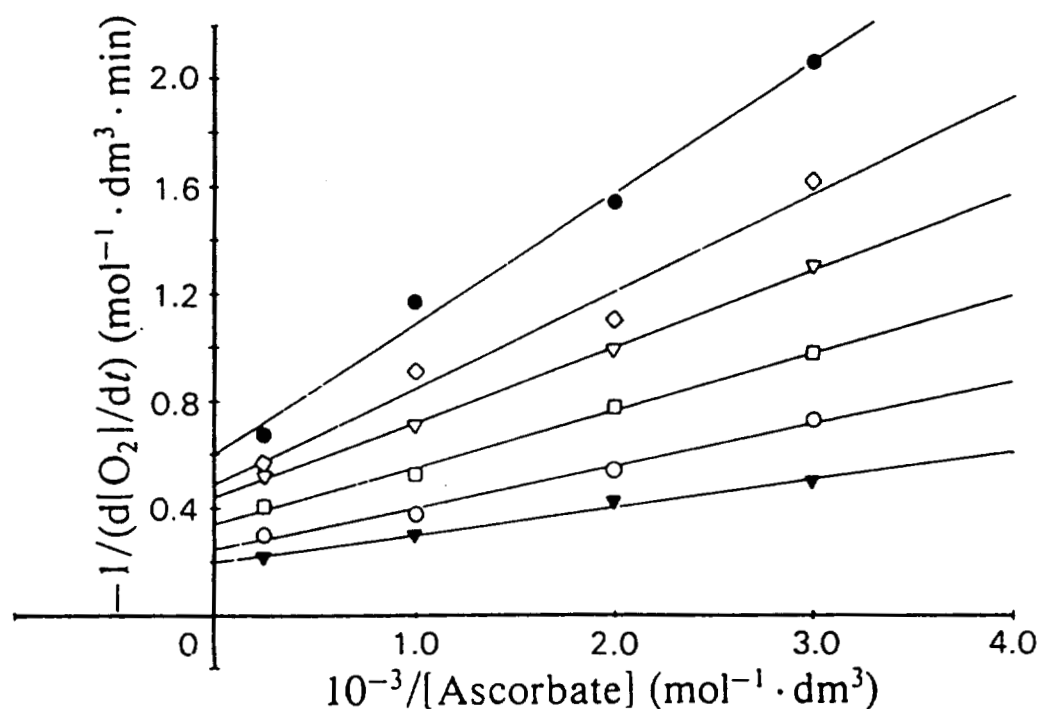


Fig. 5.7. Inhibition of dopamine β -mono-oxygenase by N_3^- with tyramine saturating ($2.0 \times 10^{-3} \text{ mol} \cdot \text{dm}^{-3}$) and ascorbate as variable substrate at $298 \pm 0.1 \text{ K}$
 $10^3 \times [N_3^-]$ (mol · dm⁻³): ▼, 0; ○, 0.6; □, 1.0; ▽, 2.0; ◇, 3.0; ●, 6.0. Rates were measured by using an oxygen-sensitive electrode as described in the text.

The kinetic data confirm that two analogous copper ligands, N_3^- and SCN^- , behave differently; N_3^- coordinates at both copper sites, and SCN^- at the only one copper center — the non ascorbate binding site.

5. 3. 2. DBH inhibition by SCN^- with oxygen as the variable substrate

When oxygen is the variable substrate, a series straight Lineweaver-Burk plots for SCN^- inhibition intersect at one point on the $1 / V$ axis (Fig. 5.8.), implicating competitive inhibition. For competitive inhibition, the substrate oxygen and the inhibitor SCN^- compete for the same binding site at DBH. The inhibitor must resemble the substrate O_2 structurally. The initial velocity of the reaction is proportional to the steady-state concentration of the DBH- O_2 complex. All the enzyme species are reversibly connected. Consequently, at any fixed unsaturating concentration of inhibitor, the velocity can be driven to equal V_{\max} at the higher substrate concentration. Therefore, the apparent K_m will increase in the presence of a competitive inhibitor, $K_{m\text{app}} = K_m (1 + [I] / K_i)$, because at any inhibitor concentration, a portion of the enzyme exists in the EI form which has no affinity for the substrate.

The replot of the slope of each reciprocal plot versus the corresponding inhibitor concentration, $[\text{SCN}^-]$, is shown in Fig. 5. 9. K_i is determined from the slope of the replot ($K_i = 0.0108 \text{ mM}$). This value is much lower than that with tyramine or ascorbate as the variable substrate. SCN^- is a more efficient inhibitor at the relatively lower oxygen concentration compared with the situation when the oxygen concentration is saturating. The replot is a straight line that distinguishes pure competitive inhibition from

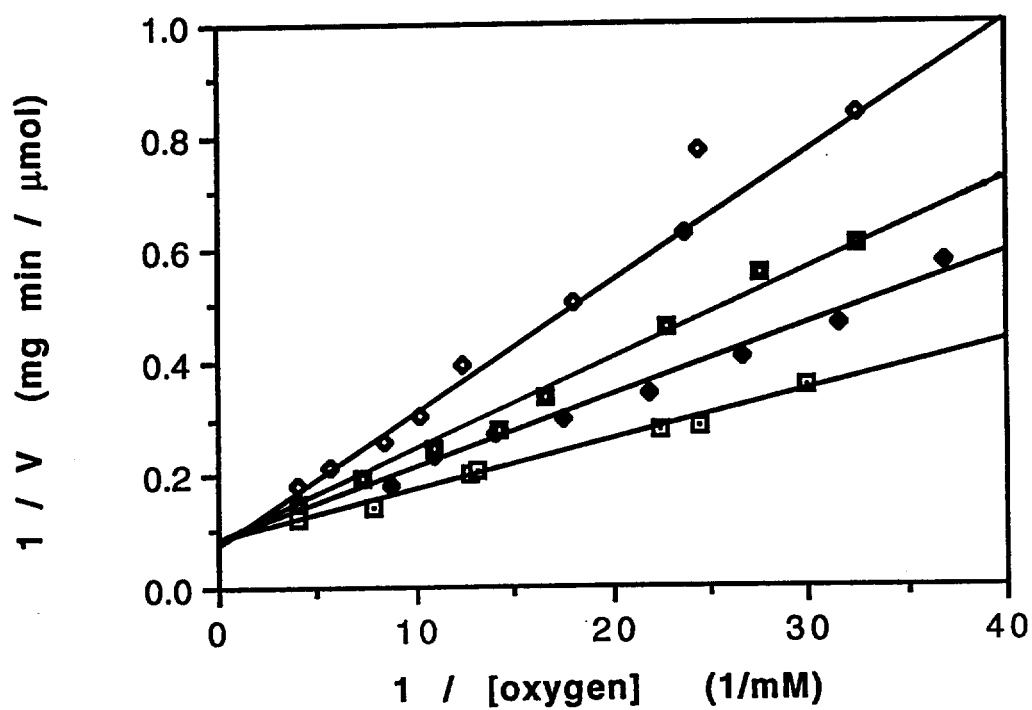


Fig. 5.8. Inhibition of DBH by SCN^- with tyramine and ascorbate saturating and oxygen as variable substrate at 298 K. $[\text{SCN}^-]$: \square , 0 μM ; \bullet , 5 μM ; \blacksquare , 10 μM ; \blacklozenge , 20 μM

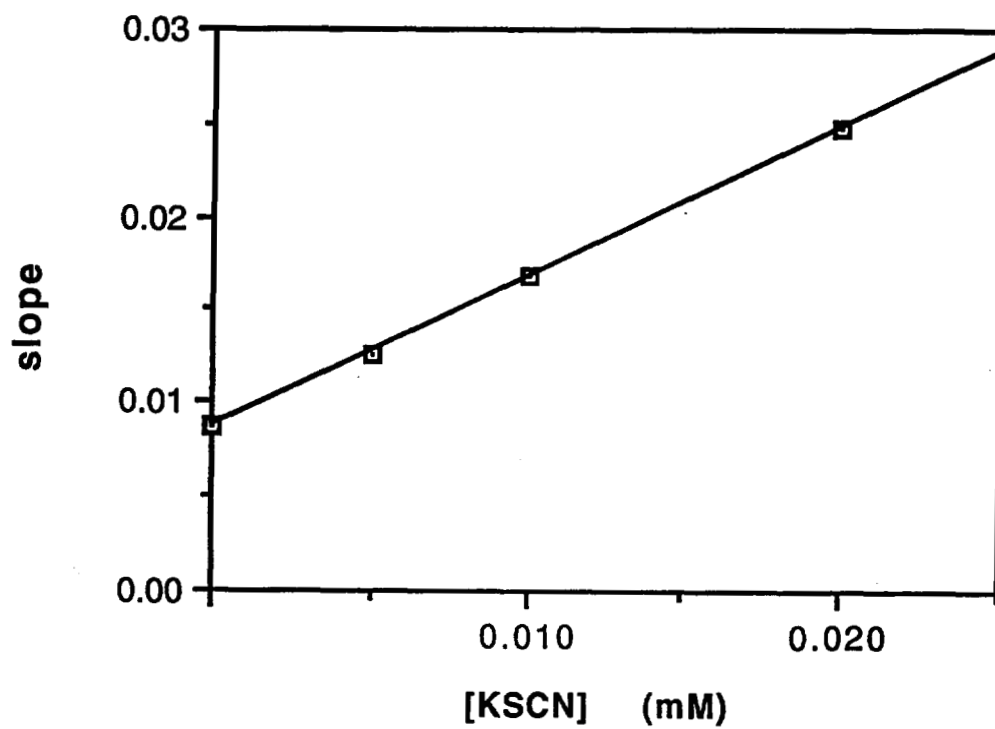


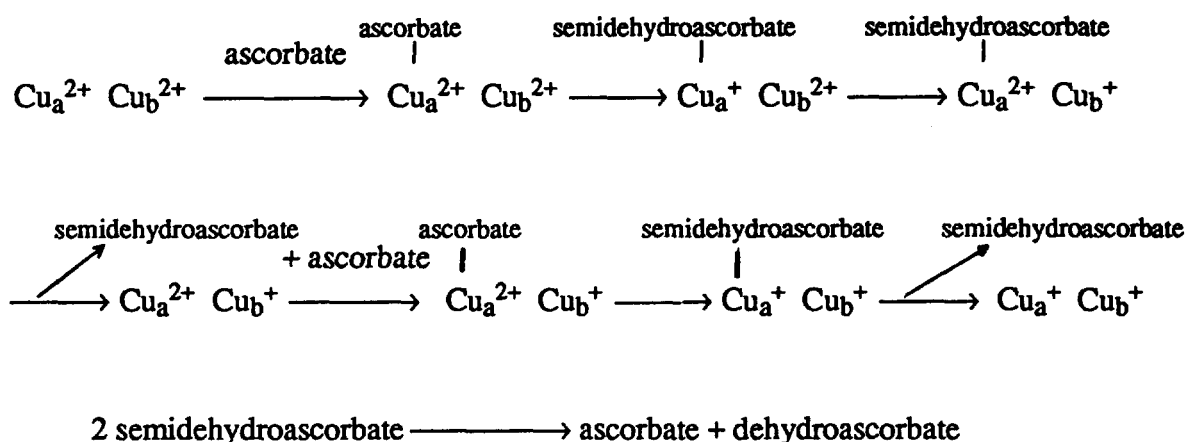
Fig. 5. 9. Replot of DBH inhibition by SCN^- with tyramine and ascorbate saturating and oxygen as variable substrate. Replot of the slope versus $[\text{SCN}^-]$.

partial competitive inhibition; the latter gives hyperbolic replots. The increase in the K_m value does not mean that the EI complex has a lower affinity for the substrate. The EI has no affinity at all for the substrate, while the affinity of enzyme (the only form that can bind substrate) is unchanged. The apparent increase in K_m results from a distribution of available enzyme between the "full affinity" and "no affinity" forms. The factor $1 + [I] / K_i$ may be considered as an $[I]$ dependent statistical factor describing the distribution of enzyme between the E and EI forms.

Based on the mechanism of competitive inhibition, SCN^- must occupy the same binding site at DBH as oxygen does, which has been assumed to be Cu_b . Considering that the copper center at which SCN^- binds to differs from that for ascorbate, ascorbate must bind only at Cu_a not Cu_b . This conclusion is very surprising because it is to the Cu_b that O_2 binds and at which the O-O bond is broken, and one oxygen atom transfers to the substrate, forming the water molecule. Without direct electron transfer from ascorbate, Cu_b has to receive two electrons from Cu_a for every turnover. We know that the distance between Cu_a and Cu_b has to be longer than 6 Å and electron transfer is not the rate-determining step (Stewart and Klinman, 1988); it will be very interesting to know how electron transport from Cu_a to Cu_b occurs at a much faster rate than the observed apparent rate (the rate constant, $k_{obs} = 250 \text{ s}^{-1}$ under conditions of saturating ascorbate) (Brenner et al, 1989). The rate of enzyme reduction is at least 5-fold faster than the apparent reaction rate (Klinman et al, 1990).

The former kinetic results suggest that ascorbate, oxygen, and tyramine obey a Ping-Pong mechanism (Goldstein et al, 1968), meaning that ascorbate binds to DBH first, followed by the release of the product, semidehydroascorbate, and then other substrates,

tyramine and O_2 , are able to bind to enzyme. The electron transfer pathway, therefore, should follow scheme 5. 2.



Scheme 5. 2.

Ascorbate coordinates at Cu_a first, reducing Cu_a^{2+} to Cu_a^+ ; and then Cu_a^+ delivers one electron to Cu_b^{2+} to form Cu_b^+ ; the next step is that semidehydroascorbate remits the second electron to Cu_a^{2+} ; finally the first substrate, dehydroascorbate is reduced and released. At this moment, other substrates, tyramine and O_2 , are able to enter their binding sites on DBH. Since Cu_a^+ is able to reduce Cu_b^{2+} , the redox potential of Cu_a should be lower than that of Cu_b .

SCN^- is not the only inhibitor functioning as a competitive inhibitor for DBH with respect to oxygen and an uncompetitive inhibitor with respect of ascorbate; other S containing inhibitors also display similar kinetic patterns. Kruse et al (Kruse et al, 1986) have prepared multisubstrate inhibitors that contain a S atom: 1-(4-Hydroxybenzylethyl) imidazole-2-thiol (1), (3, 5 - Difluoro-4-hydroxyphenethyl) imidazole-2-thiol (2), 1-

methylimidazole-2-thiol (3), *p*-Cresol (4) (structures see Fig. 5.10). These inhibitors incorporate a phenethylamine substrate mimic and an oxygen mimic into a single molecule. The steady-state kinetic patterns of these inhibitors at pH 6.6 are shown in Table 5.1. (from Kruse et al, 1986).

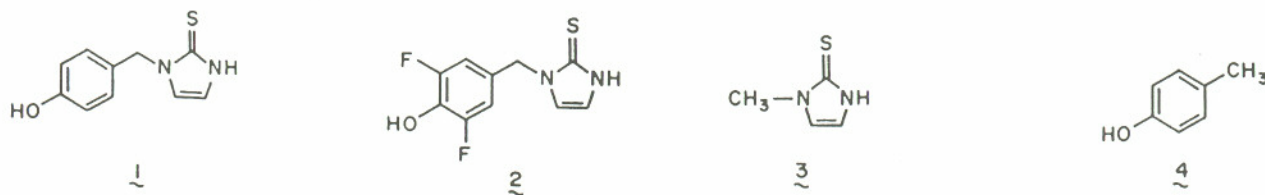
From the table, all inhibitors display uncompetitive inhibition towards ascorbate, indicating they bind exclusively to the ascorbate•DBH complex, or the reduced Cu^+ form of enzyme. Compounds 1 and 2, as multisubstrate inhibitors are competitive with both tyramine and oxygen at the active site. Compound 3 is an oxygen competitive inhibitor and unexpectedly a tyramine competitive inhibitor too. Therefore, these soft sulfur-containing ligands appear to bind to the reduced Cu^+ form of enzyme exclusively. This is significant for the simple ligand 3 because of its affinity for Cu^{2+} ions in solution (Hanlon and Shuman, 1975). Compound 3 binds to the Cu^+ form of enzyme 10 - to 100 - fold tighter than to the Cu^{2+} form. Unfortunately, the authors were unable to prove direct sulfur ligand-copper interaction between those ligands and DBH by EPR because of their selective binding to the Cu^+ diamagnetic form of enzyme. But it is very difficult to think the competitive binding of inhibitors versus oxygen arising from anything other than a direct binding to the copper atoms. Inhibitor 4, which is a simple analog of tyramine, is a competitive inhibitor with tyramine as the variable substrate but a noncompetitive inhibitor toward oxygen. Therefore, competitive inhibition of inhibitors 1, 2, and 3 when oxygen is the variable substrate is purely from thiol-imidazole.

There must be a special element that makes SCN^- and those sulfur-containing ligands all display competitive inhibition against oxygen but uncompetitive inhibition against ascorbate. This element may be structural dissimilarities or characteristic redox potential

Table 5.1. Predicted and Observed Kinetic Patterns and Apparent Kinetic Constants as a Function of pH and Fumarate Activation^a

compd	1	2	3	4
	pH 6.6			
ascorbate	U (U)		U (U)	U (U)
$K_m = 0.42 \pm 0.4$ mM	0.533 ± 0.035		639 ± 53	3470 ± 340
oxygen	C (C)		C (C)	N (N)
$K_m = 0.61 \pm 0.23$ mM	0.965 ± 0.148		266 ± 34	$K_{is} = 11\,300 \pm 1900$
tyramine	C (C)	C (C)	N (C)	C (C)
$K_m = 4.02 \pm 1.77$ mM	0.344 ± 0.016	0.039 ± 0.008	716 ± 126	4870 ± 390
oxygen (+10 mM fumarate)	N (N)		N (N)	
$K_m = 0.084 \pm 0.006$ mM	$K_{is} = 1.95 \pm 0.69$		$K_{is} = 284 \pm 29$	
	$K_{ii} = 1.26 \pm 0.13$		$K_{ii} = 711 \pm 31$	

^a Kinetic patterns: C, competitive; N, noncompetitive; U, uncompetitive; I, indeterminate. Experimentally observed patterns are given in parentheses. Binding constants are reported in μM units with standard errors. Inhibition constants are K_{is} values for C patterns and K_{ii} values for U patterns. Experimental conditions and data analysis are reported in Materials and Methods. ^b Apparent induced substrate inhibition precludes a simple analysis of data. However, fitting the data for each inhibitor concentration to the equation for substrate inhibition and replotting the theoretical lines yields a noncompetitive pattern.

**Fig. 5. 10.** Structures of DBH inhibitors 1-4.

between these two copper centers in order for oxygen to distinguish two copper centers at the active site.

5. 3. 3. DBH inhibition by azide with oxygen as the variable substrate

Previously Blackburn et al (Blackburn et al, 1984) reported the results of DBH inhibition by azide under saturating O_2 concentration. Azide appears to be an uncompetitive inhibitor while tyramine is the varied substrate, but a mixed type inhibitor while ascorbate is the varied substrate. We have now completed the kinetic data by inactivating DBH with azide under conditions of varying oxygen concentration and keeping tyramine and ascorbate concentrations constant. Under these conditions, linear mixed type inhibition (Dixon and Webb, 1979; Segel, 1975) is observed because of the plot of $1/V$ vs $1/[S]$ intersecting at a common point other than on an axis (Fig. 5.11.). Linear mixed-type inhibition can result from an inhibitor, I, binding at two different sites. Binding of I at one site completely excludes the substrate S (see Scheme 5.3.). Binding of I at the second site has no effect on the binding of S, but the resulting ESI complex is catalytically inactive. This form of inhibition is characterized by two inhibitor dissociation constants, K_{i1} and K_{i2} (see Scheme 5. 3. $K_i = 1 / K_a$, K_a is association constant). Mixed-type inhibition can be also as the result of EI having a lower affinity for substrate than E, and the ESI complex is nonproductive (see scheme 5.4.). This system may be considered a mixture of partial competitive inhibition and pure noncompetitive inhibition. In this case, as long as I is present, some of the enzyme will be always in the nonproductive ESI form, even at an infinitely high [S]. Also, at any [I], a portion of the enzyme is available for combination with substrate, O_2 , in the lower affinity EI form. Consequently, $V_{maxi} < V_{max}$ and $K_{mapp} > V_m$.

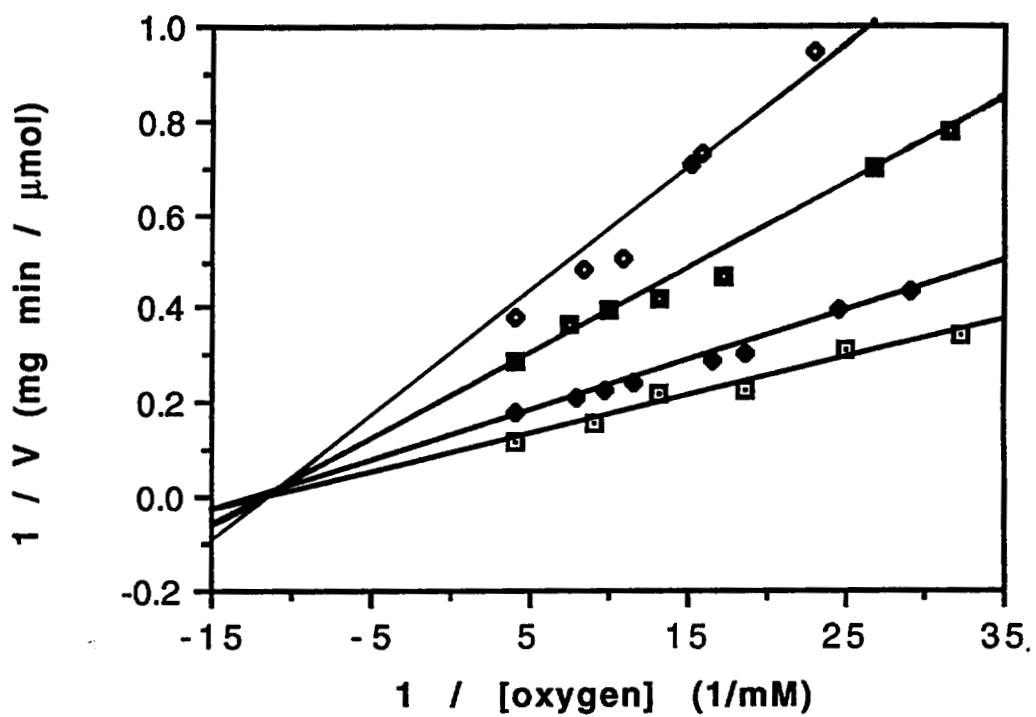
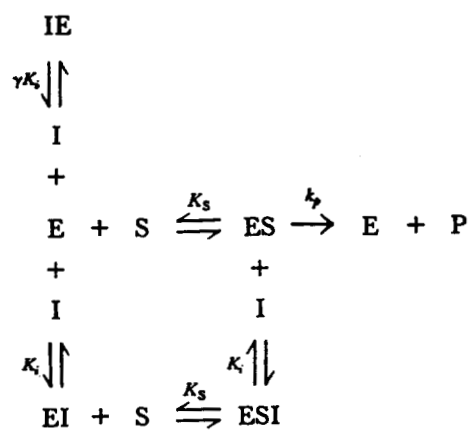
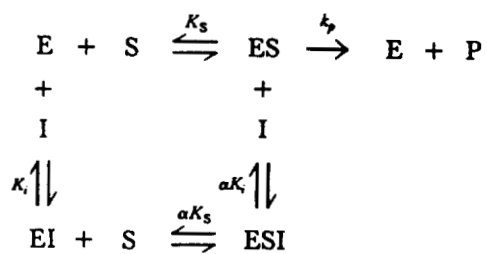


Fig. 5. 11. Inhibition of DBH by azide with tyramine and ascorbate saturating and oxygen as the variable substrate at 298 K. [azide]: \square , 0 mM; \bullet , 1 mM; \blacksquare , 5 mM; \diamond , 10 mM.



Scheme 5. 3. Linear Mixed Inhibition When I Binds at Two Sites



Scheme 5. 4. Linear Mixed-Type Inhibition

Because it is known from the IR spectra of the DBH-azide complexes that azide is able to coordinate to both copper centers, the Scheme 5. 3. including two different binding sites for inhibitor is the most plausible mechanism for azide inhibition with respect to substrate, O₂. For the scheme 5.3., the velocity equation is

$$\frac{v}{V_{\max}} = \frac{[S]}{K_s \left(1 + \frac{[I]}{\frac{\gamma}{1+\gamma} K_i} \right) + [S] \left(1 + \frac{[I]}{K_i} \right)}$$

Equation 5.1. Velocity equation of mixed inhibition

in which $K_{i1} = K_i$ (the inhibitor dissociation constant at the oxygen binding site), $K_{i2} = \gamma K_i$ (dissociation constant at the second site — the ascorbate binding site), the slope of plots = $K_s / V_{\max} [1 + [I] / (\gamma / 1 + \gamma) K_i]$ and the intercept at the $1 / V_{\text{app}}$ axis of plots = $(1 + [I] / K_i) / V_{\max}$. From the replot of the intercept at the $1 / V$ axis versus $[N_3^-]$, K_{i1} is acquired, and K_{i2} is calculated from the replot of the slope versus $[N_3^-]$ (see Fig. 5.12. and Fig. 5.13.). Based on this inhibition mechanism and kinetic data described previously, K_{i1} is the dissociation constant of azide binding at Cu_b, the oxygen binding site; K_{i2} is the azide dissociation constant at Cu_a, the ascorbate binding site. The value of K_{i1} and K_{i2} are 16.9 mM and 7.9 mM, respectively. By comparing inhibitor dissociation constants, K_{i2} is obviously smaller than K_{i1} , implying azide is easier to dissociate from Cu_b than from Cu_a. In other words, N_3^- has lower affinity at the oxygen

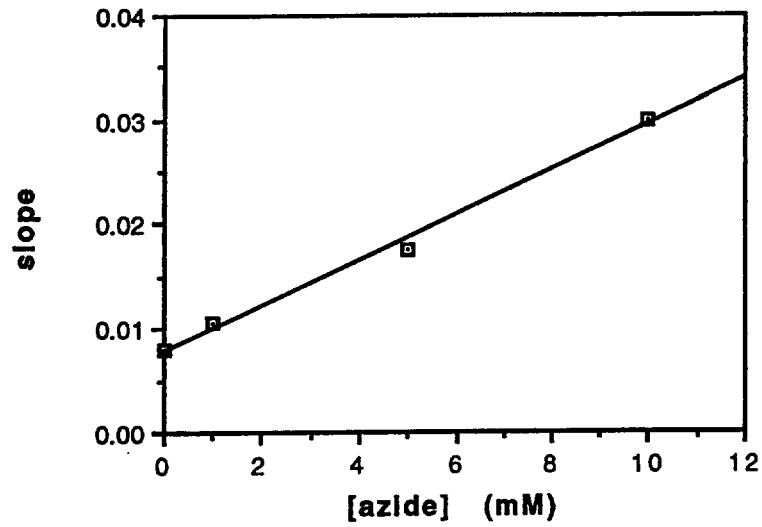


Fig. 5. 12. Replot of the slope versus azide concentration.

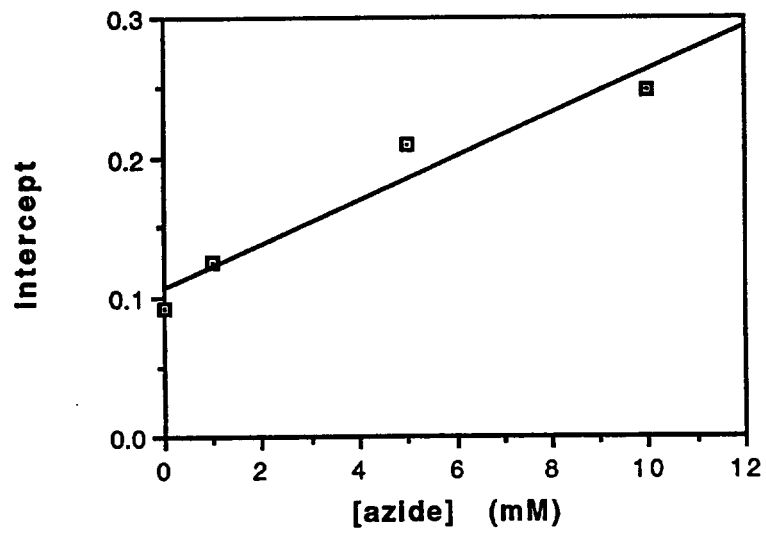


Fig. 5. 13. Replot of the intercept at the $1/V$ axis versus [azide].

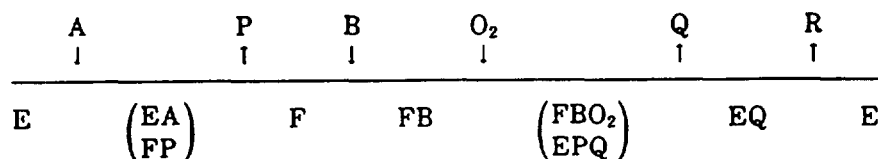
binding site than at the ascorbate site because of the greater dissociation constant. The kinetic data not only confirm the azide IR results that azide at one copper center has higher affinity than at the other copper center, but they have also identified which copper center has higher azide affinity. From the mechanism of mixed-type inhibition (Scheme 5. 3.), it is noticed that azide can bind free DBH without oxygen binding first. Because DBH inhibition by azide is also a mixed type inhibition when ascorbate is a variable substrate, the same conclusion can be made that azide is capable of binding to DBH no matter whether ascorbate also binds at DBH or not. Therefore, unlike SCN^- , N_3^- can coordinate at both Cu^{2+} and Cu^+ centers. The oxidation state of copper does not affect this binding, but the binding constant is different at these two centers.

Considering (1) the previous N_3^- inhibition results (Blackburn et al, 1984) in which the N_3^- also causes linear mixed type inhibition when the concentration of ascorbate is varied, (2) the size of an azide molecule is not big enough to cover both oxygen and ascorbate binding sites because the distance between two coppers is longer than 6 Å, (3) azide can only coordinate to copper terminally according to the optical spectrum of the N_3^- - DBH complex, (4) the binding site of azide to DBH has to be on the copper center since it produces an azide to Cu (II) charge transfer transition; N_3^- appears to bind to both copper centers of each subunit, but with a different affinity. One N_3^- binds to the oxygen site, and the other N_3^- to the ascorbate site. N_3^- binding at oxygen site excludes the binding of oxygen completely, but N_3^- binding to the ascorbate site decreases the reactivity of the enzyme without affecting the binding of oxygen. The same situation can be applied to ascorbate. The N_3^- binding to ascorbate's site restricts ascorbate from binding to DBH, preventing normal enzyme reduction.

Azide and thiocyanate together with CN^- are often classified as the same type of ligands for copper proteins (Spira-Solomon and Solomon, 1987), which is true in other copper proteins like SOD or amine oxidases. For DBH, by contrast, N_3^- and SCN^- not only have been shown to have different patterns of kinetic inhibition, but also different electronic spectra. DBH exhibits an intense N_3^- to copper charge transfer band at 385 nm but not any apparent SCN^- to copper charge transfer features. The question thus is why the same class of ligands behave differently. The discrepancy between these two molecules is the presence of S atom in SCN^- that makes SCN^- become a softer base than N_3^- and prefers to bind to a softer acid. Since the molecular size of these two anions are similar, structural consideration seems not to be an important cause for these binding differences.

The whole discussion and conclusion from kinetic data is based on the ping - pong mechanism for the binding of substrates, tyramine, oxygen, and ascorbate, on DBH. However, third mechanism is controversial; some workers have noted that the parallel lines in double reciprocal plots are not sufficient to define such a mechanism, since the occurrence of any irreversible step between the binding of the two substrates will result in such a pattern. However, steady-state kinetics with ferrocyanide as reductant indicates that steady-state kinetic parameters for tyramine and oxygen as substrates are basically the same with either ascorbate or potassium ferrocyanide as the reductant. The apparent V / K_m value is unaffected by substituting ferrocyanide for ascorbate as the reductant. This is consistent with both oxygen and tyramine reacting with the form of enzyme which does not have reductant bound (Fitzpatrick et al, 1986). The isotope effect of deuterated tyramine as the substrate (Cook and Cleland, 1981; Nothrop, 1975) suggests that the reaction is ordered, with tyramine binding before oxygen (Klinman et al, 1980; Ahn and

Klinman, 1983). So the whole reaction obeys Uni-Uni-Bi-Bi mechanism (see scheme 5. 5.), in which ascorbate binds to the enzyme first, followed by the release of semidehydroascorbate, then the second substrate tyramine (use B to present tyramine), and finally O_2 binds to the enzyme. The binding site of tyramine, in the Cu (II) form, is believed to be 4 - 6 Å from the coppers (Fitzpatrick and Villafranca, 1987). The copper-substrate distance is greater than what has been expected for a reaction between copper species and the benzylic position of the substrate.



Scheme 5. 5. Uni-Uni-Bi-Bi Reaction

The environment of the copper sites is still controversial. Many issues need to be clarified. Although the results of DBH inhibition by azide and thiocyanate can not give conclusions, they suggest strongly that ligands of two copper centers are not same.

5. 3. 4. DBH EPR spectra in the presence of different concentration of SCN^-

Unlike azide, binding of SCN^- does not change the shape, the g-value, or A-value of the DBH EPR spectra; but SCN^- decreases the intensity of DBH signal (see Fig. 5. 14.). The fully reconstituted DBH has been oxidized with $K_3Fe(CN)_6$ to give the EPR spectrum

which is shown in Fig. 5. 14. a. The intensity of the EPR spectra decreases with increasing SCN^- concentration. Fig. 5. 14. b represents the SCN^- concentration at 3.32 mM; c at 26.3 mM; d at 316 mM; e at 2310 mM; f at 3280 mM; and g at 4930 mM. The relationship between enzyme-bound $[\text{Cu}^{2+}]$ and $[\text{SCN}^-]$ is shown in Fig. 5. 15. It is clear that $[\text{Cu}^{2+}]$ does not decrease to zero but approaches a limiting value ($[\text{Cu}^{2+}] = 134.8 \mu\text{M}$) regardless of how much SCN^- is added. The final $[\text{Cu}^{2+}]$ ($134.8 \mu\text{M}$) is about half of the initial $[\text{Cu}^{2+}]$ ($251.5 \mu\text{M}$). Therefore, about half of the total Cu^{2+} in DBH is reduced to Cu^+ by SCN^- .

From the kinetic data, we know that SCN^- is a competitive inhibitor with respect to oxygen so that 50 % of the copper which is reduced must be the Cu_b^+ ; the other half of total Cu^{2+} that can not be reduced by SCN^- , then, must be Cu_a , which is an indication that an electron is able to transfer only from Cu_a to Cu_b (like the reduction by ascorbate) but not from Cu_b to Cu_a . Because bound SCN^- reduces Cu_b^{2+} to Cu_b^+ , it doubtless will not generate the ligand to copper charge transfer transition for the d^{10} state of Cu_b^+ , which explains the lack of a LMCT transition for the DBH- SCN^- complex.

The EPR spectrum of DBH in the presence of SCN^- implies that SCN^- indeed can coordinate to Cu_b^{2+} unlike O_2 that has to bind at Cu_b^+ center. In their studies of SCN^- binding to SOD, Dooley and McGuirl (Dooley and McGuirl, 1986a) have discovered that SCN^- displays a ligand to copper charge transfer transition at 355 nm; thus, the copper center must remain in the oxidized state. Although the intensity of this LMCT band is much lower than that in the SOD - azide complex, the temperature dependence of the

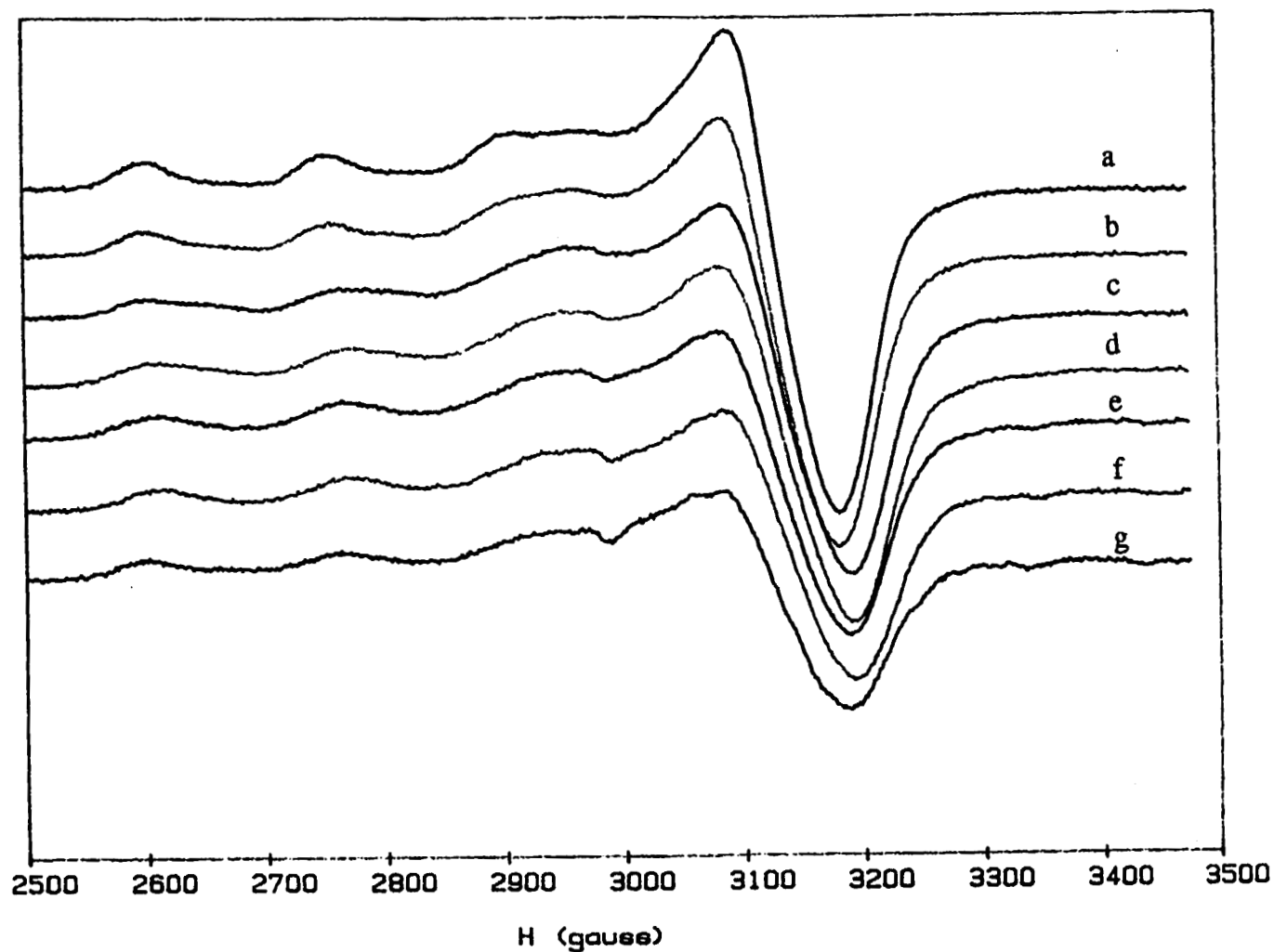


Fig. 5.14. DBH EPR spectra in the presence of SCN^- at -170°C . $[\text{SCN}^-]$: a, 0 mM; b, 3.32 mM; c, 26.3 mM; d, 0.316 M; e, 2.31 M; f, 3.28 M; g, 4.93 M. The magnetic field was at 3000 G and the scan range 1000 G. The microwave power was 10 mw, modulation amplitude 20 G, microwave frequency 9.125 GHz, time constant 0.064 second, and scan time 2 minutes.

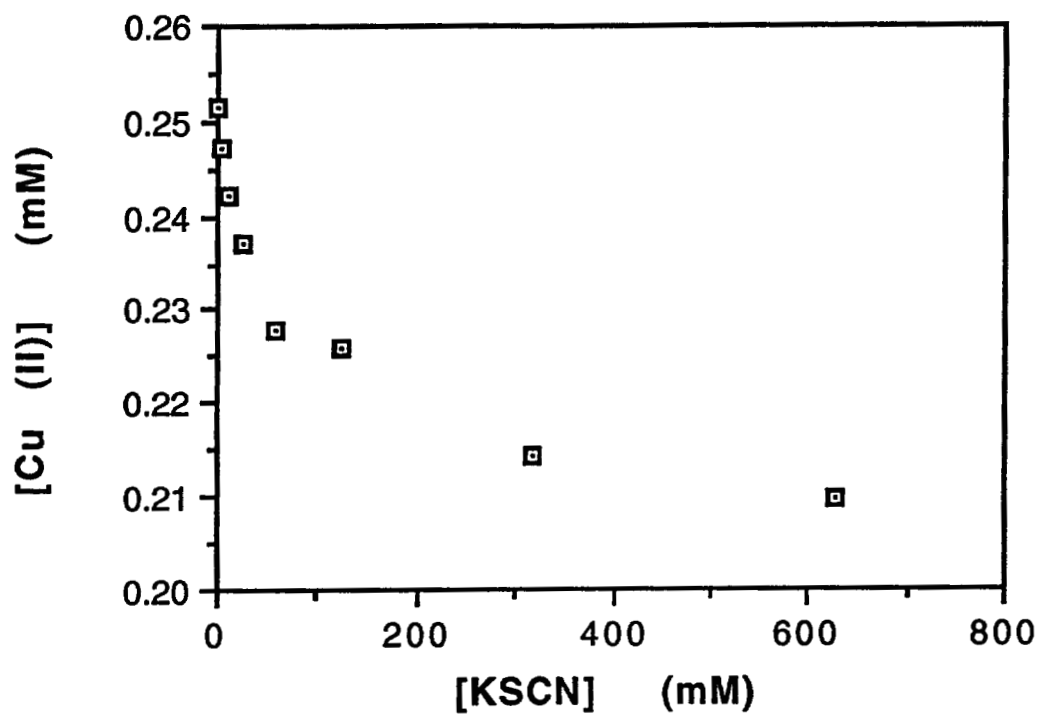


Fig. 5. 15. Cu^{2+} concentration of fully reconstituted DBH in the presence of SCN^- .
Initial Cu^{2+} concentration of DBH is $250 \mu\text{M}$.

LMCT has been determined. The properties of SCN^- titration suggest that it is the S atom, not N atom, coordinating at the copper center. SCN^- is an ambidentate ligand towards heavier metals, where it tends to be S-bonded rather than N-bonded (Greenwood and Earnshaw, 1984).

That SCN^- reduces Cu^{2+} in copper proteins has never been noted before. SOD EPR spectra in the presence of 200-fold molar excess of SCN^- show no sign of any decrease in the magnitude of the signal (Fee and Gaber, 1972). The EPR parameters for the adduct are $g_{\parallel} = 2.27$, $g_{\perp} = 2.06$, $A_{\parallel} = 0.0153 \text{ cm}^{-1}$, which vary a little comparing with $g_{\parallel} = 2.27$, $g_{\perp} = 2.08$, $A_{\parallel} = 0.01543 \text{ cm}^{-1}$ for the native SOD (Bertini et al, 1980). EPR spectra thus indeed reflect changes in the electronic parameters of the copper chromophore upon addition of SCN^- . The SOD NMR relaxation data of the SCN^- adduct indicate the existence of large contact interaction between copper centers in the enzyme and SCN^- (Bertini et al, 1980).

Similar results have been observed in pig kidney diamine oxidase. The parameters of the EPR spectra of the SCN^- adduct ($g_{\parallel} = 2.286$, $g_{\perp} = 2.045$, $A_{\parallel} = 0.0190 \text{ cm}^{-1}$) vary slightly from that of the native enzyme ($g_{\parallel} = 2.27$, $g_{\perp} = 2.061$, $A_{\parallel} = 0.0171 \text{ cm}^{-1}$) (Dooley and McGuirl, 1986b; Peisach and Blumberg, 1974). The changes in g-values between the native enzyme and the SCN^- complex suggest that the covalence of the copper sites is perturbed by anion binding. In bovine plasma amine oxidase, the SCN^- adduct displays the same trends so that the binding of SCN^- causes the copper centers to become more symmetric due to the increase of g-values and decrease of A_{\parallel} -values (Bertini and Scozzafava, 1981). In the case of galactose oxidase, although the difference of EPR parameters between the SCN^- adduct and the resting enzyme is much smaller than that in

amine oxidase, SCN^- does produce a unique spectrum when added to galactose oxidase (Giordano et al, 1974).

Existing EPR spectra of SCN^- - type III copper proteins, such as half-met tyrosinase- SCN^- (Himmelwright et al, 1980), half-met hemocyanin- SCN^- , as well as met-apo hemocyanin- SCN^- (Himmelwright et al, 1979) all show slight changes in the spectra shape, in g-values, and in A_{\parallel} -values, but high concentrations (about 0.1 M) of KSCN yields reduction (5 % - 10 %) of some half-met hemocyanin sites, which upon removal of excess SCN^- become oxygenated.

Thus, reduction of DBH by SCN^- raises a question why the copper centers in DBH differ from those of other type II copper proteins and also type III copper proteins. DBH may belong to a unique type of copper monooxygenases, also peptidylglycine α -amidating monooxygenase and tyrosine 3-monooxygenase.

5. 4. Conclusion

The same class of anion ligands, N_3^- and SCN^- , behave differently in their kinetic properties. SCN^- displays uncompetitive inhibition towards tyramine and ascorbate but competitive inhibition towards oxygen. By contrast, N_3^- is an uncompetitive inhibitor for tyramine but a mixed-type inhibitor for ascorbate and oxygen. As a consequence, SCN^- coordinates only to Cu_b , and N_3^- coordinates to both Cu_a and Cu_b . The DBH EPR spectrum in the presence of SCN^- decreases its intensity to about half of the initial intensity, implicating half of Cu^{2+} is reduced to Cu^+ . From kinetic data and EPR spectra,

we can conclude that Cu_b can be reduced through Cu_a by ascorbate, but Cu_a can not be reduced through Cu_b by SCN^- . The special characters of Cu_b is due to an oxygen type (other than tyrosinate) ligand which is absent at Cu_a ; this ligand cause Cu_b to possess more electron density and prefer to coordinate to SCN^- .

CHAPTER VI MECHANISMS OF THE DBH CATALYZED REACTION

6. 1. The Existing Mechanisms

Through intense research in kinetics, mechanism, and the structure of the active center in DBH, several different mechanisms for the DBH catalyzed reaction have been proposed. In early 80s, Villafranca proposed two mechanisms — one electron and two electron mechanisms (see Fig. 6.1., from Villafranca, 1981) that had been observed for cytochrome p-450 (Sligar et al, 1980). Obviously, the one copper active site is not suitable anymore since DBH has been proven to contain two coppers per active center and both coppers are involved in the redox chemistry (Klinman et al, 1984; Ash et al, 1984). In the two copper active site mechanism (Villafranca, 1981), O₂ binds to both coppers, followed by electron transfer to O₂ and the binding of tyramine. The form of oxygen involved in the hydroxylation could be an acyl peroxide or O₂²⁻ that is stabilized between two Cu²⁺ ions as suggested for the tyrosinase reaction. But no one is able to detect O₂⁻ escaping from the enzyme.

Later, Miller and Klinman (Miller and Klinman, 1985), based on microscopic rate constants and other available data on DBH, put forward a unified mechanism (see Fig. 6.2.), in which partial homolysis of O—O with substrate properly juxtaposed can

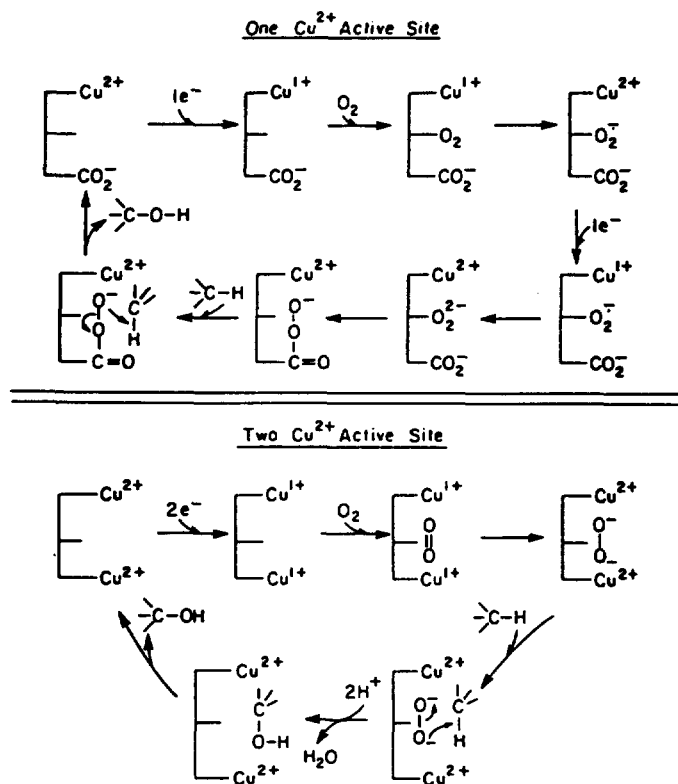


Fig. 6.1. Two proposed mechanisms for the DBH reaction -- one involving 1 Cu²⁺ per active site and the other for 2 Cu²⁺ per active site. In the top scheme an acyl peroxide is presumed to be formed in the catalytic sequence and serve as the hydroxylating species as has been observed for P-450. In the scheme with two Cu²⁺ per active site a model is proposed in which the two electrons add to a weakly coupled (for uncoupled) copper pair followed by addition of O₂, and substrate binding. The form of O₂²⁻ involved in the hydroxylation is not specified in this scheme and could be an acyl peroxide as depicted in the top scheme or a [Cu-O]²⁺ species (from Villafranca, 1981).

initiate C—H homolysis, leading to a transition state where both O—O and C—H bonds are significantly broken and an O—H bond is significantly formed. A major role for active-site copper in C—H bond cleavage is catalysis of the homolysis of the O—O bond. The most significant feature of the mechanism is a coupling of the energy released on transfer of hydrogen from carbon to oxygen (estimated as -34 kcal / mol) with the energy absorbed on transfer of oxygen from copper hydroperoxide (estimated as +30 kcal / mol).

In 1987, Fitzpatrick and Villafranca proposed a mechanism for substrate hydroxylation by DBH which involved hydrogen atom abstraction by a high potential copper - oxygen species (see Fig. 6. 3., from Fitzpatrick and Villafranca, 1987). They thought that since hemocyanin and tyrosinase were able to form the 1, 2 - μ -peroxo-copper species upon binding oxygen and since the binuclear Cu (I)-oxygen model complexes could form μ -peroxo-Cu (II) species, DBH should be able to form the same species.

It was disputed by Klinman whose newest mechanism indicated the distinct copper sites in DBH performing separate functions (see Fig. 6.4., from Brenner and Klinman, 1989). A reductant and a substrate binding sites are magnetically isolated, functioning as electron transfer and substrate hydroxylation, respectively. Electron transfer between the copper centers allows a two electron reduction of oxygen to form a copper - hydroperoxide complex that may react with bound substrate without further activation. A series of single-turnover studies have been initiated in which pre-reduced DBH has been mixed with substrate in the absence of excess reductant. These experiments permit a direct detection of product formation and of the reduced state of enzyme - bound copper, suggesting that the pre-reduced enzyme is a viable catalytic complex and that the enzyme-

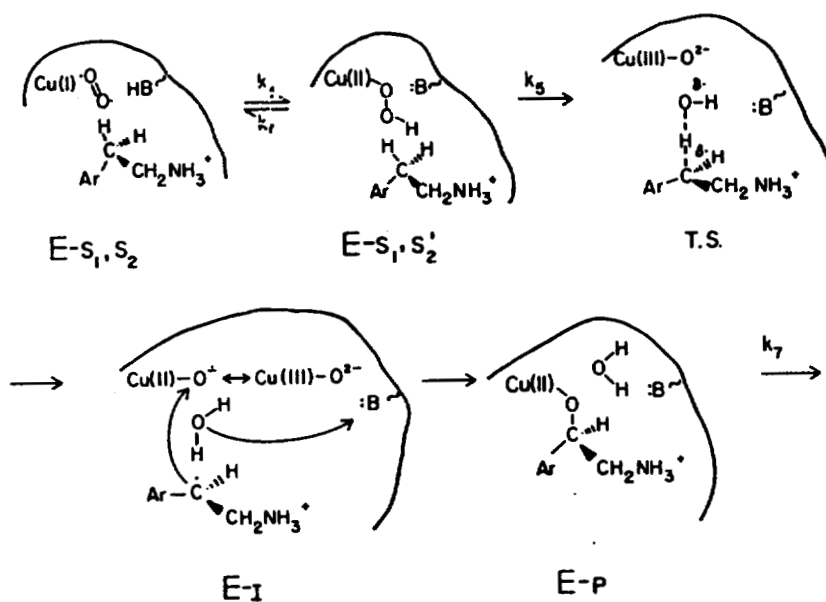


Fig. 6.2. A proposed chemical mechanism for the dopamine hydroxylase reaction. Only a single active site copper atom is depicted. $\text{E-S}_1\text{S}_2$ and $\text{E-S}_1\text{S}_2'$ refer to the initial ternary complex and Cu(II)-OOH intermediate, respectively E-I and E-P present the substrate-derived radical intermediate and enzyme-product complex, respectively. (from Miller and Klinman, 1985)

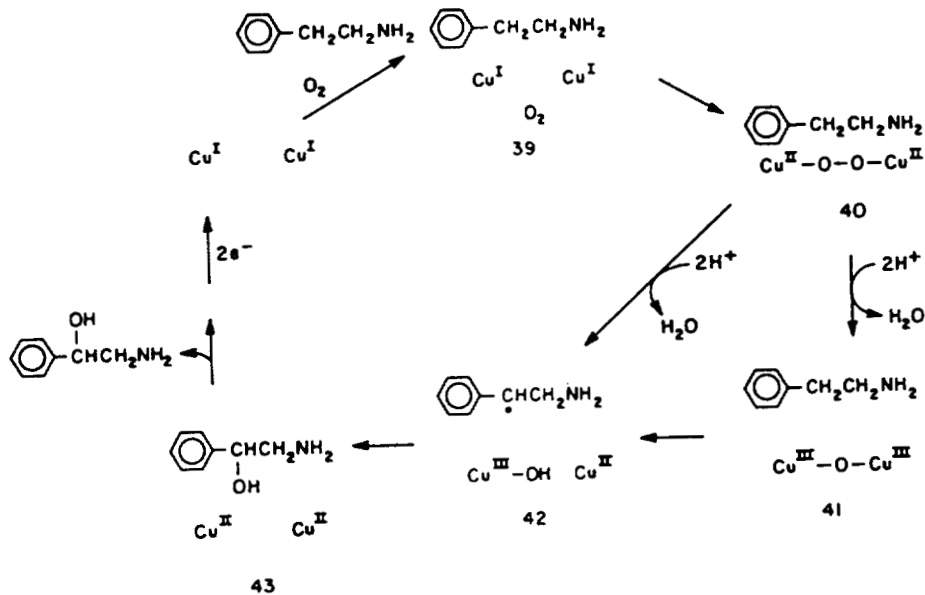


Fig. 6.3. A proposed mechanism for the DBH reaction involving a tyramine radical and μ -peroxo species (from Fitzpatrick and Villafranca, 1987).

product complex contains a fully detectable EPR Cu^{2+} signal; therefore, in the final stage of the mechanism, two electrons are added *via* the reductant copper site to generate the E-Cu (II)-P complex. This inter-copper electron transfer is expected to be at least as fast as the C—H bond cleavage, since it is a substep of the C—H bond cleavage.

From the discussion in this dissertation, Klinman's mechanism seems to better fit our results. The bridged O_2 -copper intermediate is not likely to be formed. The reasons are as follow: first of all, the Cu — Cu distance in DBH has to be larger than 6 Å (since EPR spectrum does not show any sign of two antiferromagnetically coupled Cu centers). Secondly, the kinetic data and the results of N_3^- , SCN^- and CO ligand binding experiments clearly show that CO and N_3^- coordinate to copper terminally, CO coordinates a single copper per active center, and CO is a competitive inhibitor with respect to oxygen; oxygen, therefore, is expected to bind at only one copper center terminally. So the single copper site for the O_2 binding should be the proper mechanism for the DBH reaction.

6. 2. Whether radical is formed during the reaction

There is much speculation about whether there are radicals including a substrate radical and an amino acid radical in DBH (Villafranca and Desai, 1990) formed during turnover. Existence of ascorbate and tyramine radicals has been mentioned. The Klinman group has used freeze-quench EPR techniques to detect the semidehydroascorbate radical at $g = 2.00518$ (see Fig. 6.5. from Brenner et al, 1989), 25 millisecond after addition of ascorbate to DBH. The freeze - quenched DBH remarkably remains $100 \pm 20 \%$ its

original enzymatic activity after the thawing process. The detection of semidehydroascorbate radicals indicates that DBH reduction by ascorbate is through two concerted steps though in a very short time. The reduction involving a radical will be beneficial for electron transfer from one copper center to the other or for H abstraction from C — H in tyramine to form a tyramine radical as reported by several workers (Fitzpatrick et al, 1985; Wimalasena and May, 1981; Padgette et al, 1985).

Fitzpatrick et al (Fitzpatrick et al, 1985; Fitzpatrick and Villafranca, 1985) first proposed the benzylic radical intermediate as the key chemical intermediate for the DBH reaction through the calculation of partition ratios for enzyme turnover versus inactivation using mechanism-based inhibitors — *p*-HO⁻, *p*-CH₃O⁻, *m*-HO⁻, *m*-CHO⁻, *p*-Br⁻, and *p*-CN⁻ substituted phenylpropenes. May (Wimalasena and May, 1981; Padgette et al, 1985) also demonstrated that DBH readily catalyzed oxidative N-dealkylation of N-phenylethylene diamine (PEDA) and N-methyl-N-phenylethylenediamine (N-MePEDA). Their data strongly support a mechanism in which the amine substrate undergoes initial single-electron oxidation to generate a transient nitrogen cation radical intermediate, which partitions between enzyme inactivation and turnover. Further evidence that a radical intermediate is involved comes from the results with 3-phenylpropynes, 1-benzylcyclopropanes, and 3-phenylpropenes as mechanism based inhibitors of DBH (Fitzpatrick and Villafranca, 1985). The partition ratios supports the radical mechanism. For the benzylcyclopropanes, generation of a radical species, a cyclopropane group, can result in ring opening to produce a highly reactive primary carbon centered radical at the enzyme active site. This radical will react rapidly with a group on the protein, inactivating the enzyme.

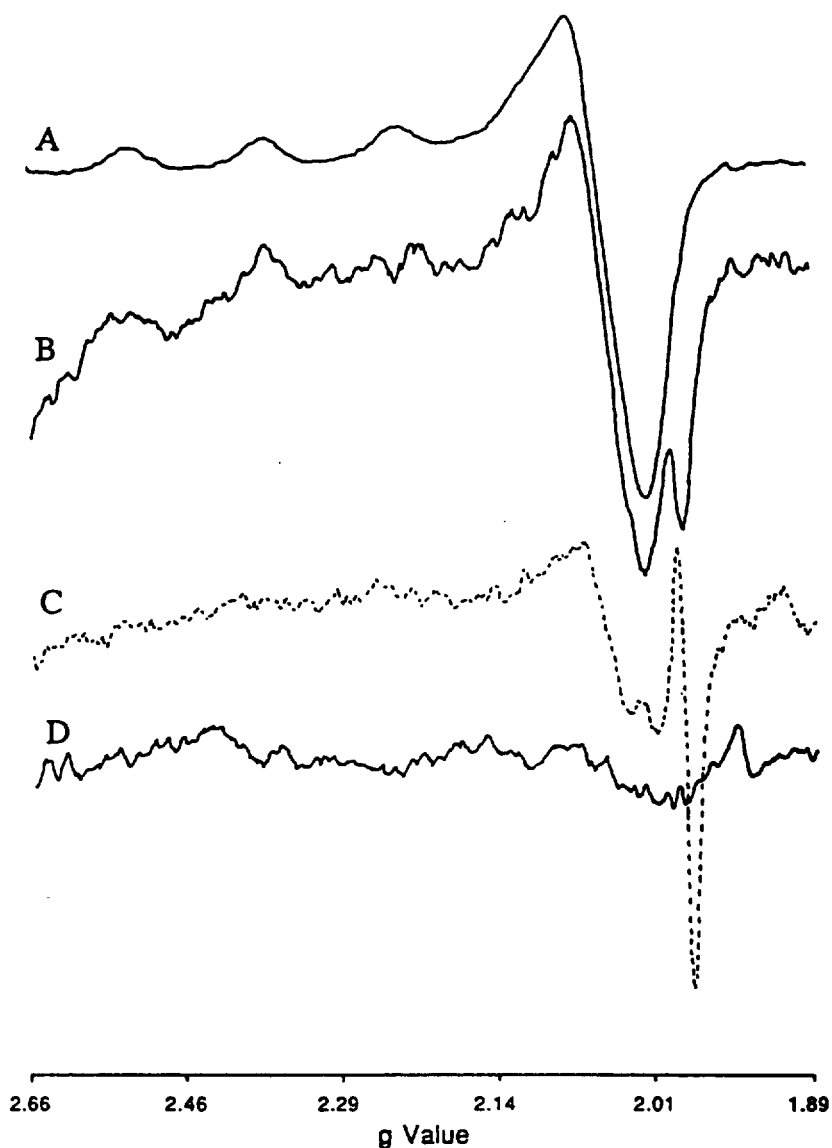
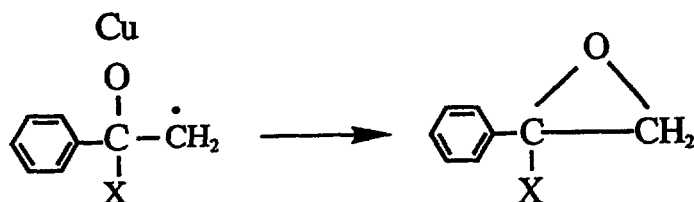


Fig. 6. 4. EPR spectra of freeze-quenched D β M. Unless stated otherwise, EPR settings were as follows: 5-mW microwave power, 20-G modulation width, 2970 ± 500 G field sweep, 57 s/scan \times four scans, 0.3-s time constant, and $T \approx 16$ K. EPR gain was identical throughout. (A) Non-freeze-quenched $57.9 \mu\text{M}$ D β M subunits in 5 mM KPi , pH 6.5, with 2 Cu^{2+} /subunit: microwave power = 0.2 mW, modulation width = 10 G, and $T = 14.7$ K. (B) Freeze-quenched $15 \mu\text{M}$ D β M subunits with two coppers per subunit in 25 mM potassium phosphate with 10 mM disodium fumarate and 5 mM chloride, pH 6.0. (C) Freeze-quenched D β M as in (B), after reaction with 2.0 mM ascorbic acid for 23 ms. (D) The cavity signal was obtained with an EPR tube containing distilled water.

Certain styrenes also rapidly inactivate DBH under turnover conditions (Farrington et al, 1987). For *p*-methoxy styrene as inhibitor, the product has been identified as the epoxide, but the latter has been ruled out as the inactivating species. Therefore, the mechanism has to involve the benzylic radical intermediate. Electrophilic attack of the active Cu-oxygen species upon the double bond generates the radical:



Inhibition by all the suicide substrates is consistent with a radical mechanism involving an electrophilic copper-oxygen species, although substrate radical has not been observed by EPR to date.

The cytochrome p-450 reaction undergoes a one-electron oxidation to a free radical with substrates phenylenediamines and aminophenols (O'Brien, 1984). This is very similar to the DBH catalyzed reaction and increases the possibility for DBH going through a similar radical mechanism. Cytochrome p-450 possesses peroxidase activity that catalyzes epoxidation, aromatic ring hydroxylation, side chain oxidation, N-hydroxylation, and O-dealkylation by a two-electron oxidation (O'Brien, 1983). Horseradish peroxidase and cytochrome p-450 also readily carry out a N-demethylation for some N-alkly aromatic compounds that could be substrates for DBH as well. Some cation-radicals are formed in the N-demethylation reaction via a one-electron oxidation mechanism (Griffin et al, 1980). The amount of cation-radical formed is very small and is not formed in the presence of reducing agents that do not affect the N-demethylation.

Since both ascorbate and dopamine are expected to form radicals during turnover, then we may ask whether DBH also forms a radical during the reaction and what kind of radical it is. In order to answer these questions, a method used by Whittakers (Whittaker and Whittaker, 1988) to detect the galactose oxidase radical (Whittaker, 1985) was applied to detect the DBH radical signal with the EPR spectrometer. Because copper in DBH displayed an intense g_{\perp} signal around $g = 2.00$, it was impossible to isolate the radical signal even if the radical indeed exist. In order to solve this problem, apo-DBH (copper content about 0.1 copper / enzyme measured with an atomic absorption spectrophotometer) EPR spectra were measured, followed by oxidizing DBH with large excess amount of $K_3Fe(CN)_6$ and freezing it immediately in liquid N_2 for running EPR spectra. The EPR instrumental settings were as described in chapter II, except that the modulation amplitude was decreased to 2 G in order to minimize saturation of the radical signal, and the gain was set at the maximum to increase the signal sensitivity, and the time constant was decreased to 0.032 s. The oxidized apo-DBH EPR spectrum is shown in Fig. 6. 6. There was small amount of Cu^{2+} existing in the enzyme, but there was clearly also a small radical peak at $H = 3225$ G, g value was 2.005, which was calculated from the equation $g = hv / \beta H$. From the g value and the shape of the signal, it no doubt was a radical signal. It was not possible to come from contamination because EPR spectrum of apo DBH did not show any signal. The experiment was repeated three times and the same results were observed.

Considering that DBH has to be reduced to correspond to the conditions of the enzymatic reaction, the apo-DBH sample from the third experiment was washed with 50 mM phosphate buffer, pH 7.5, using ultrafiltration in a centricon 30. The EPR spectrum of the washed apo-DBH sample was monitored, and no signal was detected. Then 10 μ l

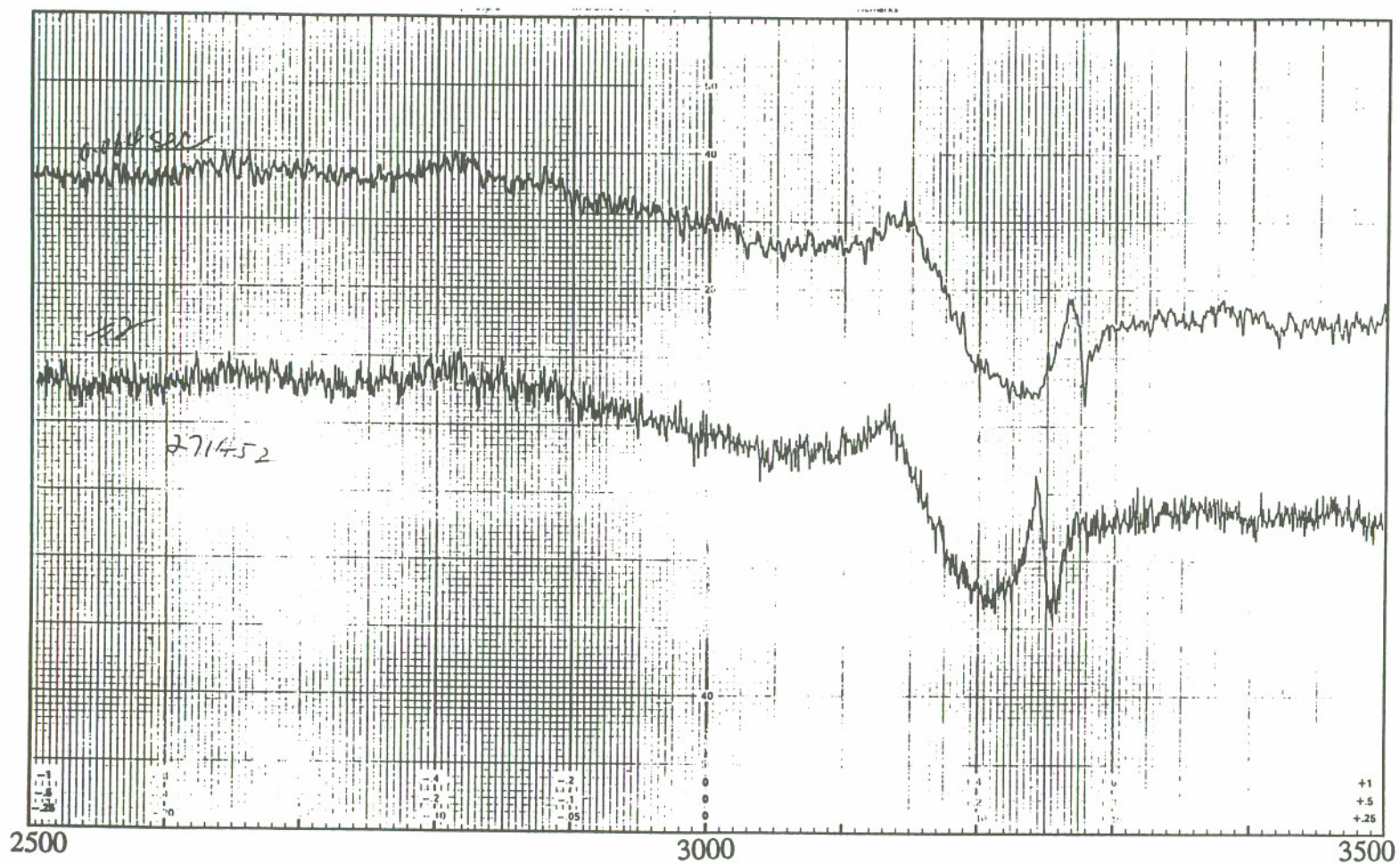


Fig. 6. 5. EPR spectra of apo-DBH in the presence of $K_3Fe(CN)_6$ at $-167\text{ }^\circ\text{C}$. EPR settings were as follow: $3000 \pm 1000\text{ G}$ field sweep, 2 G modulation amplitude, 16 min scan (bottom spectrum the top one with 0.064 sec. time constant and 4 min scan), 0.032 sec. time constant, 5 mW microwave power.

1.5 M ascorbate was added into the enzyme sample and mixed thoroughly, and the sample was frozen quickly in liquid N₂. The EPR spectrum was measured again (see Fig. 6. 6). EPR spectrum contained 3 peaks with intensity ratio 1: 2 : 1. The g value for the most intense peak was at 2.02, and the A value is about 10 G. This radical signal was definitely not from dehydroascorbate whose EPR spectrum had been identified (see Fig. 6.5., from Brenner et al, 1989). The assignment is uncertain: it does not look like a tyrosyl radical or other known amino acid radical EPR signal, but its g value was in the range for peroxy radicals (2.01 - 2.02) or sulfur-containing radicals (2.02 - 2.06) (Borg, 1976). A very important phenomena was that radicals in the reduced and oxidized forms were different in intensities and in number of peaks.

Unfortunately, the EPR spectrum of apo-DBH in the presence of ascorbate was not able to be repeated. The reason was that the EPR spectrometer had to be very stable and sensitive since the signal was very small, which was not the case much of the time, especially when the instrument was used very frequently. Whenever the apo-DBH radical signal in the presence of ascorbate could not be observed, the radical EPR signal of the oxidized form of apo-DBH was not able to be detected either, although it had been detected three times.

6.3. The mechanism of DBH catalyzed reaction

In this section, a mechanism for the DBH reaction is proposed, based on results of experiments described here and the existing mechanisms. First, the radical shown in EPR spectra of apo-DBH would favor the radical mechanism presented by Villafranca et al (Fitzpatrick and Villafranca, 1987). Second, DBH inhibition by SCN⁻ and EPR spectra in

the presence of SCN^- indicate that an electron transfers from Cu_a to Cu_b , but not the reverse. Also ascorbate binding only at Cu_a suggests that the single activation center mechanism proposed by Klinman fits our results perfectly (Klinman et al, 1984). The question is that for half-apo DBH, how ascorbate can transfer electrons to Cu_b without Cu_a — the sole ascorbate binding site. If an amino acid radical in DBH does exist, an electron can be transferred to Cu_b from ascorbate through this radical. Since we can see the free radical EPR signal in apo-DBH, DBH reduction by ascorbate is able to create this radical without the existence of coppers. As the consequence, in half-apo DBH, Cu_b can be reduced by ascorbate through this radical without ascorbate binding at the Cu_a center. From this point of view, the amino acid radical in DBH becomes very important for the DBH reduction by ascorbate. This radical probably plays other important roles in the activation process too, such as helping to form the benzilic radical of tyramine by abstracting the H atom from C-H, which would provide the possible mechanism for producing the substrate radical.

Fig. 6.7. is the mechanism of DBH catalyzed reaction based on the results in this dissertation, in which it is still unclear what kind of Cu-oxygen species is at the active center although the dinuclear bridged oxygen species can almost certainly be ruled out. The reduction of DBH by ascorbate produces a radical from an amino acid residue that helps electron transfer from Cu_a to Cu_b . Tyramine forms a cation radical after the abstraction of the H atom. The single turnover experiment described by Brenner and Klinman (Brenner and Klinman, 1989) implies that the enzyme-product tertiary complex is reduced by ascorbate before releasing the products; therefore, in this step, ascorbate binds to Cu_a when norepinephrine is still coordinated at Cu_b of DBH. Then the last and the rate-determining step is the release of the product, norepinephrine.

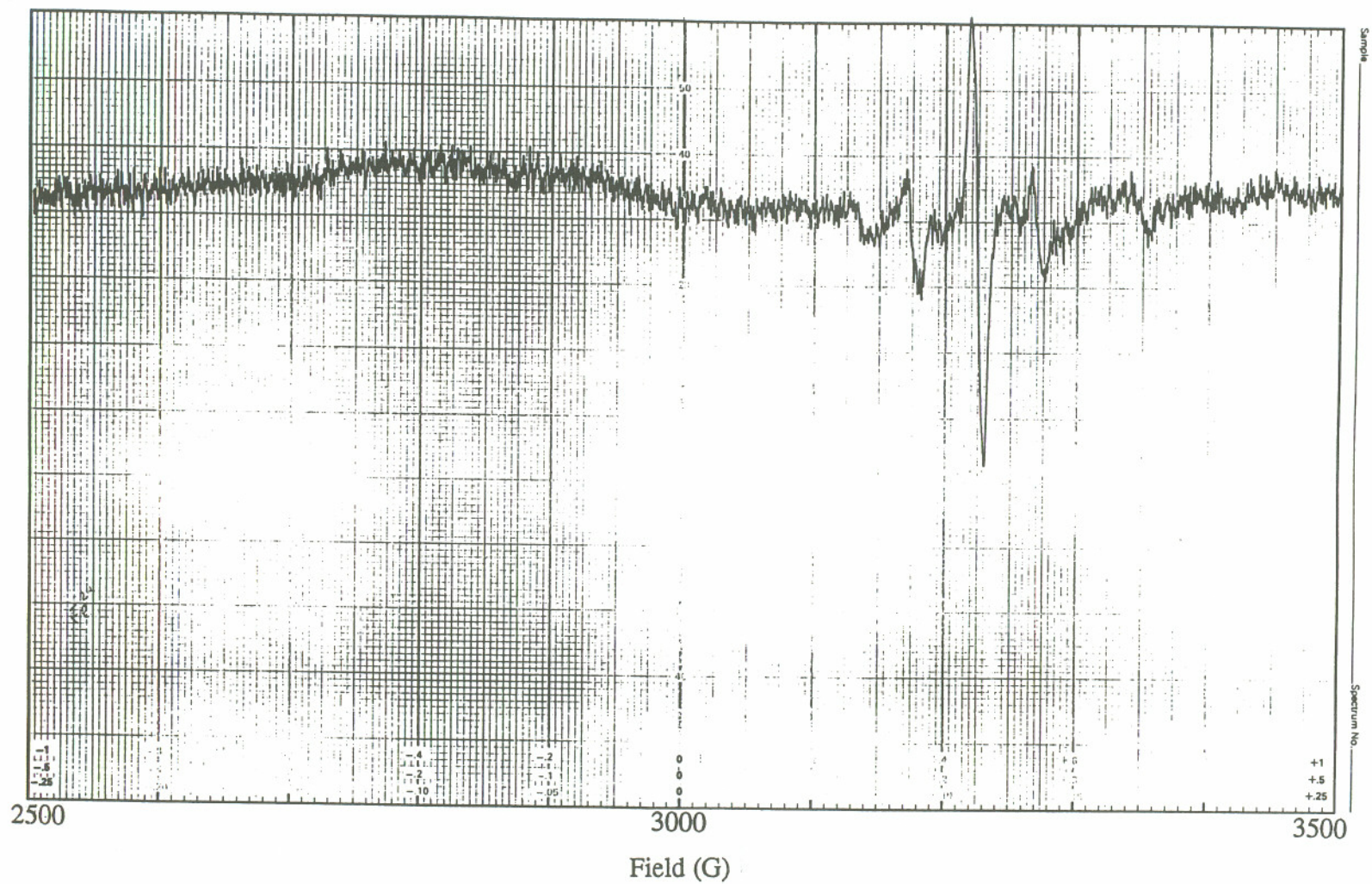
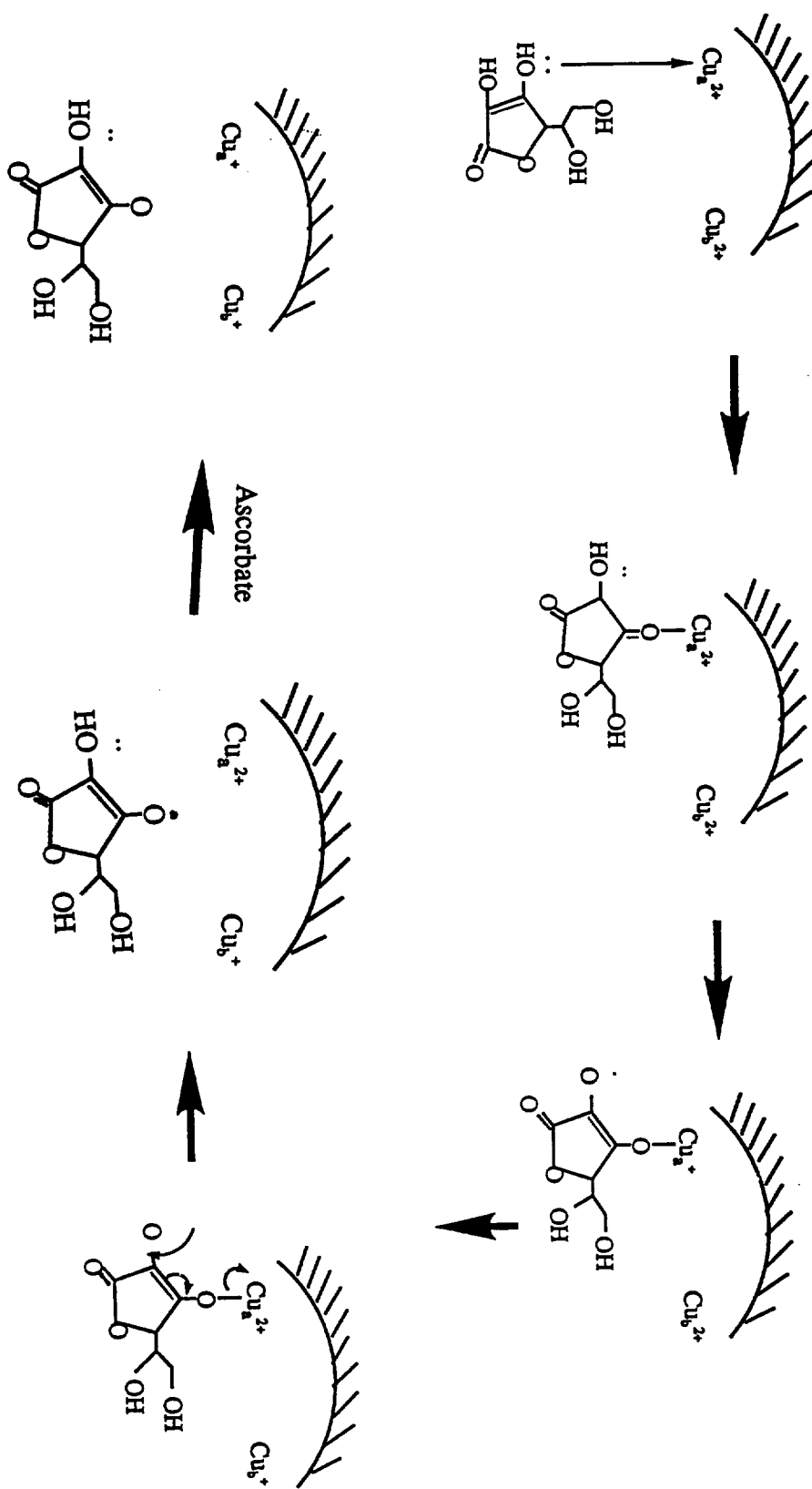
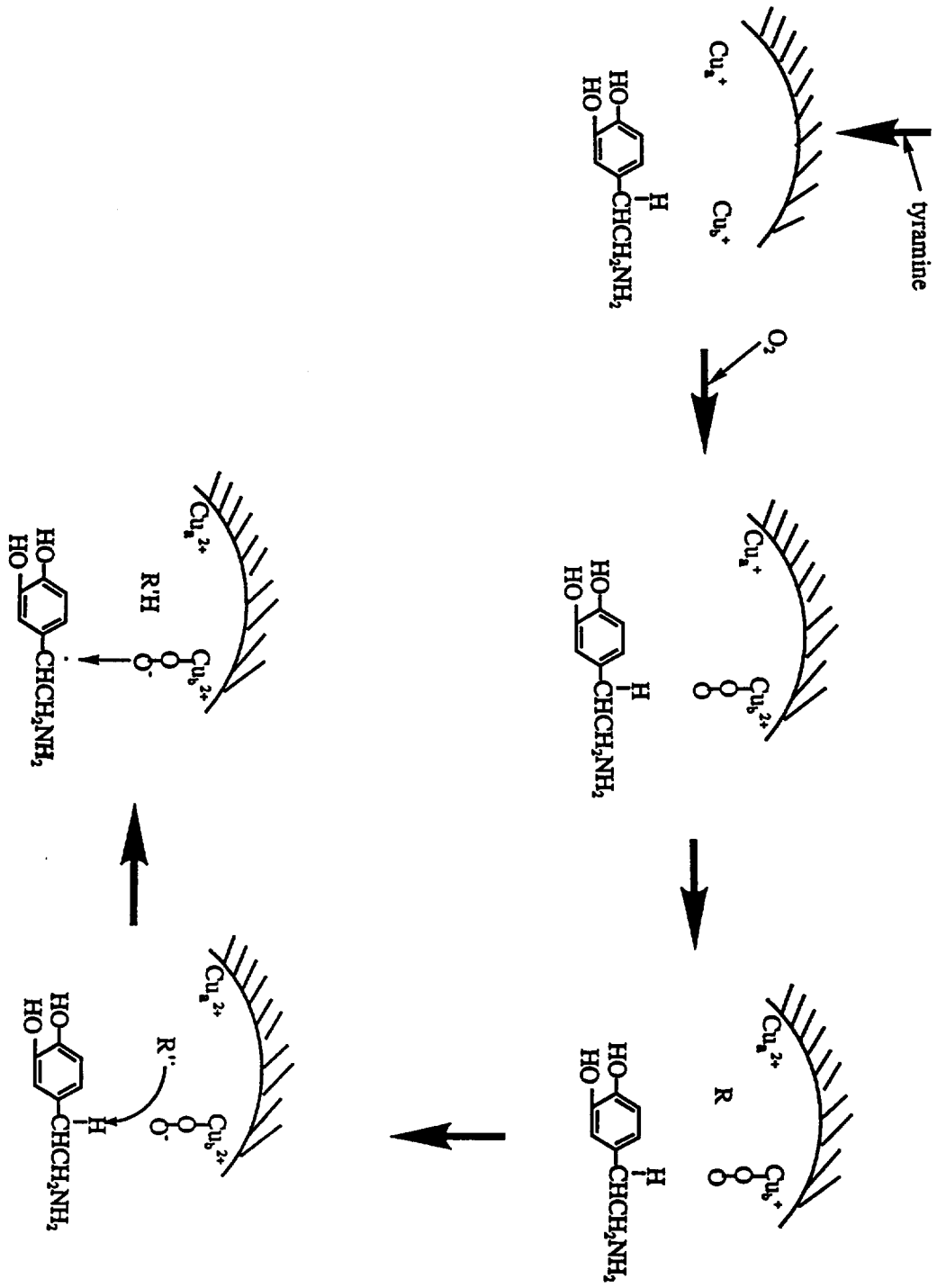


Fig. 6. 6. EPR spectra of apo-DBH in the presence of ascorbate at -170° . Conditions are same as in Fig. 6.5.





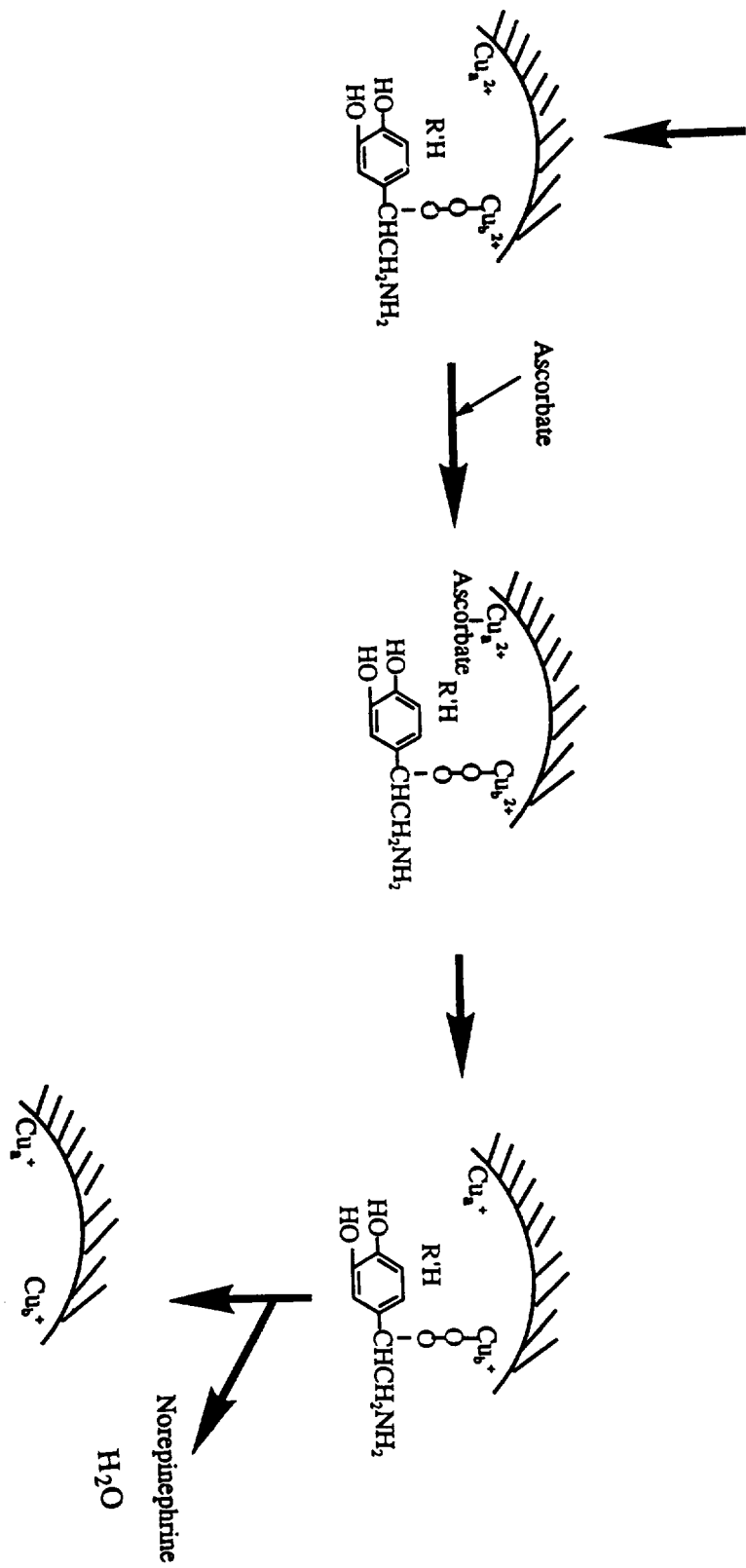


Fig. 6. 7. The mechanism of the DBH catalyzed reaction

6. 4. Future Work

The successes in preparing half-apo DBH that contains only Cu_b and in measurement of optical properties make it worth while to prepare the other kind of half-apo DBH containing only Cu_a. If this is possible, it will open up a new area for the study of structural and functional differences between the two copper centers of each subunit. From the mechanism discussed above, DBH containing only Cu_a should have no activity at all and not be able to bind to oxygen. But it will be very difficult to fulfill this task because of the lower binding constant of Cu_a than that of Cu_b (Blackburn et al, 1987). The alternative is to choose a bulky sulfur-containing ligand that only binds to Cu_b in half-apo DBH prepared as described in chapter IV. And then the ligand coordinated enzyme will be reconstituted with copper to form 8 coppers / tetramer. If the sulfur-containing ligand is still binding at Cu_b and left Cu_a exposed, the properties of Cu_a can be determined solely.

Of course, the crystal structure of DBH should be the main target for the future studies because it is most powerful method to characterize the structure of the enzyme. Site-directed mutagenesis is another very important method to characterize the properties of the enzyme. Since the expressed DBH is inactive, peptidylglycine α -amidating monooxygenase that contains large number of conserved amino acid residues with DBH would be a good candidate to prepare some mutants in which the possible copper ligands — His or Met residues could be changed to non-ligand residues like Leu or Ile or to a Cys residue to make a blue copper protein that is easier for studying because of the intense absorption band around 600 nm.

REFERENCES

- Abernethy, J. L., Steinman, H. M., and Hill, R. L. (1974) *J. Biol. Chem.* 249, 7339 - 47.
- Agrell, I. (1971) *Acta Chem. Scand.* 25, 2965-74.
- Ahn, N. and Klinman, J. P. (1983) *Biochemistry* 22, 3096 - 3106.
- Allendorf, M. D., Spira, D. J., and Solomon, E. I. (1984) *Proc. Natl. Acad. Sci. USA* 82, 3063 -7.
- Ash, D. E., Papadopoulos, N. J., Colombo, G., and Villafranca, J. J. (1984) *J. Biol. Chem.* 259, 3395 - 8.
- Atkins, P.W. (1986) in *Physical Chemistry* 3rd. ed., W. H. Freeman, New York.
- Avigliano, L., Davis, J. L., Graziani, M. T., Marchesini, A., Mims, W. B., Mondovi, B., and Peisach, J. (1981) *FEBS Lett.* 136, 80 - 4.
- Baker, E. N. (1988) *J. Mol. Biol.* 203, 1071 - 95.
- Barker, R., Boden, N., Cayley, G., Charlton, S. C., Henson, C., Holmes, M. C., Kelly, I. D., and Knowles, P. F. (1979) *Biochem. J.*, 177, 289 - 302.
- Bergman, C., Gandvik, E. -K., Nyman, P. O., and Strid, L. (1977) *Biochem. Biophys. Res. Comm.* 77, 1052.
- Bertini, I., Luchinat, C., and Scozzafava, A. (1980) *J. Am. Chem. Soc.* 102, 7349 - 53.
- Bertini, I. and Scozzafava, A. (1981) in *Metal Ions in Biological Systems* vol. 12 (Sigel, H., ed.) pp31 - 74, Marcel Dekker, Inc., New York.
- Bertini, I., Lanini, G., Luchinat, C., Messori, L., Monnanni, R., and Scozzafava, A (1985), *J. Am. Chem. Soc.*, 107, 4391- 6.
- Blackburn, N. J., Collison, D., Sutton, J., and Mabbs, F. E. (1984) *Biochem. J.* 220, 447 - 54.
- Blackburn, N. J., Concannon, M., Shahiyan, S. K., Mabbs, F. E., and Collison, D. (1988) *Biochemistry* 27, 6001 - 8. 27, 6001 - 8.

- Blackburn, N. J., Pettingill, T. M., Seagraves, K. S., and Shigeta, R. T. (1990) *J. Biol. Chem.* 265, 15383 - 6.
- Blackburn, N. J., Hasnain, S. S., Pettingill, T. M., and Strange, R. W. (1991) *J. Biol. Chem.* 266, 23120 - 7.
- Blumberg, W. E., Desai, P. R., Powers, L., Freedman, J. H., and Villafranca, J. J. (1989) *J. Biol. Chem.* 264, 6029 - 32.
- Borg, D. C. (1976) in *Free Radicals in Biology* (Pryor, W. A. ed.) vol. 1, pp 69 - 147, Academic Press, New York.
- Brenner, M. C., Murray, C. J., and Klinman, J. P. (1989) *Biochem.* 28, 4656 - 64.
- Brenner, M. C. and Klinman, J. P. (1989) *Biochem.* 28, 4664 - 70.
- Coates, J. H., Collins, P. R., and Lincoln, S. F. (1979) *J. Chem. Soc. Faraday Trans.* 75, 1236.
- Collyer, C. A., Guss, J. M., Sugimura, Y., Yoshizaki, F., and Freeman, H. C. (1990) *J. Mol. Biol.* 211, 617 - 32.
- Colman, P. M., Freeman, H. C., Guss, J. M., Murata, M., Norris, V. A., Ramshaw, J. A. M., and Venkatappa, M. P. (1978) *Nature* (London) 272, 319.
- Colombo, G., Rajashekhar, B., Giedroc, D. P., and Villafranca, J. J. (1984) *Biochemistry* 23, 3590 - 8.
- Colombo, G. and Villafranca, J. J. (1984) *J. Biol. Chem.* 259, 15017 - 20.
- Colombo, G., Papadopoulos, N. J., Ash, D. E., and Villafranca, J. J. (1987) *Arch. Biochem. Biophys.* 252, 71 - 80.
- Cook, P. F. and Cleland, W. W. (1981) *Biochemistry* 20, 1790 - 6.
- Dawson, J. H., Dooley, D. M., Clark, R., Stephens, P. J., and Gray, H. B. (1979) *J. Am. Chem. Soc.* 101, 5046.
- Denning, R. G. and Piper, T. S. (1966) *Inorganic Chemistry* 5, 1056 - 65.
- Desideri, A., Morpurgo, L., Rotilio, G., and Mondovi, B. (1979) *FEBS Lett.* 98, 339.
- DeWolf, W. E. Jr., Carr, S. A., Varrichio, A., Goodhart, P. J., Mentzer, M. A., Roberts, G. D., Southan, C., Dolle, R. E., and Kruse, L. I. (1988) *Biochemistry* 27, 9093 - 101.
- DeWolf, W. E. Jr., Chambers, P. A., Southan, C., Saunders, D., and Kruse, L. I. (1989) *Biochemistry* 28, 3833 - 42.
- DiVaira, M. and Orioli, P. L. (1968) *Acta Crystallogr. Sect. B.* B 24, 595.

- Dixon, M. and Webb, E. C. (1979 3rd. ed.) *Enzyme*, 3rd ed. pp 340-341, New York, Academic Press Inc.
- Dooley, D. M., Rawlings, J., Dawson, J. H., Stephens, P. J., Andreasson, L. E., Malmstrom, B. G., and Gray, H. B. (1979) *J. Am. Chem. Soc.* 101, 5038.
- Dooley, D. M. and Golnik, K. C. (1983) *J. Biol. Chem.*, 258, 4245 - 8.
- Dooley, D. M. and Cote, C. E. (1985) *Inorg. Chem.* 24, 3996-4000.
- Dooley, D. M. and McGuirl, M. A. (1986 a) *Inorg. Chem.* 25, 1261-64.
- Dooley, D. M. and McGuirl, M. A. (1986 b) *Inorg. Chemica Acta* 123, 231- 236.
- Dori, Z. and Ziolo, R. F. (1973) *Chemical Reviews*, 73, 247-54.
- Douglas, B. E. and Yamada, S. (1965) *Inorganic Chemistry* 4, 1561 - 5.
- Drago, R. S. (1977) in *Physical Methods in Chemistry* pp108 - 110, W.B. Saunders Co., Philadelphia, PA.
- Dubois, K., Gilles, K. A., Hamilton, J. K., Rebers, P. A., and Smith, F. (1956) *Anal. Chem.* 28, 350 - 6.
- Eipper, B. A., Mains, R. E., Glembofski, C. G. (1983) *Proc. Natl. Acad. Sci. USA* 80, 5144 - 8.
- Eipper, B. H. and Mains, R. E. (1988) *Annu. Rev. Physiol.* 50, 333 - 44.
- Ettinger, M. J. (1974) *Biochemistry* 13, 1242.
- Ettinger, M. J. and Kosman, D. J. (1981) in *Copper Proteins* (Spiro, T. G., ed) pp219 - 61, Wiley, New York.
- Fager, L. Y. and Alben, J. O. (1972) *Biochemistry* 11, 4786 - 92.
- Farrington, G. K., Kumar, A., Fitzpatrick, P. F., and Villafranca, J. J. (1987) *Fed. Proc.* 46, 2123.
- Farrington, G.K., Kumar, A., and Villafranca, J. J. (1990) *J. Biol. Chem.* 265, 1036-40.
- Fee, J. A. and Gaber, B. P. (1972) *J. Biol. Chem.* 60 - 65
- Fee, J. A. (1975) *Struct. Bond* 23, 1.
- Fee, J. A., Peisach, J., and Mims, W. B. (1981) *J. Biol. Chem.* 256, 1910-14.
- Fee, J. A. and Valentine, J. S. (1977) in *Superoxide and Superoxide Dismutases* (Michelson, A. M., McCord, J. M., and Fridovich, I. eds.) pp 19 - 61 Academic Press, London.
- Felthouse, T. R. and Hendrickson, D. N. (1978) *Inorg. Chem.* 17, 444.

- Fitzpatrick, P. F., Flory, Jr., D. R., and Villafranca, J. J. (1985) *Biochem.* 24, 2108-14.
- Fitzpatrick, P. F. and Villafranca, J. J. (1985) *J. Am. Chem. Soc.* 107, 5022 - 3.
- Fitzpatrick, P. F., Harpel, M. R., and Villafranca, J. J. (1986) *Arch. Biochem. Biophys.* 249, 70 - 75.
- Fitzpatrick, P. F. and Villafranca, J. J. (1987) *Arch. Biochem. Biophys.* 257, 231-50.
- Friedman, D. and Kaufman, S. (1966) *J. Biol. Chem.* 241, 2256.
- Gaber, B. P., Brown, R. D., Koenig, S. H., and Fee, J. A. (1972) *Biochim. Biophys. Acta* 271, 1-5.
- Giordano, R. S., Bereman, R. D., Kosman, D. J., and Ettinger, M. J. (1974) *J. Am. Chem. Soc.* 96, 1023 - 6.
- Godden, J. W., Turley, S., Teller, D. C., Adman, E. T., Liu, M. Y., Payne, W. J., and LeGall, J. (1991) *Science* 253, 438 - 42.
- Goldstein, M., Lauber, E., and McKereghan, M. R. (1965) *J. Biol. Chem.* 240, 2066.
- Goldstein, M., Joh, T. H., and Garvey, T. Q. III (1968) *Biochemistry* 7, 2724 - 30.
- Gray, H. B. (1980) *Adv. Inorg. Biochem.* 2, 1.
- Gray, H. B. and Solomon, E. I. (1981) in *Copper Proteins* (Spiro, T. G. eds) pp1-39, Wiley - Interscience, New York.
- Greenwood, N. N. and Earnshaw, A. (1984) in *Chemistry of the Elements* pp795, Pergamon Press, Oxford.
- Griffin, B. W., Marth, C., Yasukochi, Y., and Masters, B. S. S. (1980) *Arch. Biochem. Biophys.* 175, 543.
- Hanlon, D. P. and Shuman, S. (1975) *Experienta*, 31, 1005.
- Hamilton, G. A. (1981) in *Copper Proteins* (Spiro, T. G. eds) pp193 - 218 Wiley-Interscience, New York.
- Hasnain, S. S., Diakun, G. P., Knowles, P. F., Binsted, N., Garner, C. D., and Blackburn, N. J. (1984) *Biochem. J.* 221, 545 - 8.
- Helle, K. B., Serck-Hanssen, G., and Bock, E. (1978) *Biochim. Biophys. Acta* 533, 396 - 407.
- Himmelwright, R. S., Eickman, N. C., and Solomon, E. I. (1979) *J. Am. Chem. Soc.* 101, 1576 - 86.
- Himmelwright, R. S., Eickman, N. C., LuBien, C. D., and Solomon, E. I. (1980) *J. Am. Chem. Soc.*, 102, 5378-88.

- Himmelwright, R. S., Eickman, N. C., Lubien, C. D., Lerch, K., and Solomon, E. I. (1980) *J. Am. Chem. Soc.* 102, 7339 - 44.
- Hodgman, C. D., Weast, R. C., Shankland, R. S., and Selby, S. M. (1963) in *Handbook of Chemistry and Physics* 44th Ed., CRC Press, Cleveland.
- Holwerda, R. A., Stevens, G., Anderson, C., and Wynn, M. (1982) *Biochemistry* 21, 4403-07.
- Hortnagl, H., Winkler, H., and Locks, H. (1972) *Biochem. J.* 129, 187 - 95.
- Hortnagl, H., Locks, H., and Winkler, H. (1974) *J. Neurochem.* 22, 197 - 9.
- Jabusch, J. R., Farb, D. L., Kerschensteiner, D. A., and Deutsch, H. F. (1980) *Biochemistry* 19, 2310 - 6.
- Ito, N., Phillips, S. E. V., Stevens, C., Ogel, Z. B., McPherson, M. J., Keen, J. N., Yadav, K. D. S., and Knowles, P. F. (1991) *Nature* 350, 87 - 90.
- Joh, T. H. and Hwang, O. (1987) *Ann. NY Acad. Sci.* 493, 342-50.
- Johansen, J. T., Overballe-Petersen, C., Martin, B., Hasemann, V., and Svendsen, I. (1979) *Carlsberg Res. Comm.* 44, 201 -17.
- Kevan, L. (1979) in *Time Domain Electron Spin Resonance* (Kevan, L. and Schwartz, R. N. eds.) pp 279-342, Wiley - Interscience, New York.
- Kahn, O., Sikorav, S., Gouteron, J., Jeannin, S., and Jeannin, Y. (1983) *Inorg. Chem.* 22, 2877-83.
- Karlin, K. D., Cohen, B. I., Hayes, J. C., Farooq, A., and Zubieta, J. (1987) *Inorg. Chem.* 26, 147-53.
- Karlin, K. D., Farooq, A., Hayes, J. C., Cohen, B. I., Rowe, T. M., Sinn, E., and Zubieta, J. (1987) *Inorg. Chem.* 26, 1271-80.
- Klinman, J. P., Krueger, M., Brenner, M., and Edmondson, D. E. (1984) *J. Biol. Chem.* 259, 3399 - 402.
- Klinman, J. P., Humphries, H., and Voet, J. G. (1980) *J. Biol. Chem.* 255, 11648 - 51.
- Klinman, J. P. and Brenner, M. C. (1987) *4th Int. Symp. on Oxidases and Related Redox Systems*. (King, T. E., Mason, H. S., and Morrison, M., eds.) pp227 - 48, Alan R. Liss, New York.
- Klinman, J. P., Huyghe, B., Stewart, L. C., and Taljanidisz, J. (1990) *Biol. Oxidation Systems* vol. 1, pp 329-46, Academic Press, New York.
- Kluetz, M. D. and Schmidt, P. G. (1980) *Biophys. J.* 29, 283.
- Kosman, D. J., Peisach, J., and Mims, W. B. (1980) *Biochemistry* 19, 1304 - 8.

- Kosman, D. J. (1984) in *Copper Proteins and Copper Enzymes* (Lontie, R., ed.) vol. 2, pp 1 - 26, CRC Press, Boca Raton, Fl.
- Kruse, L. I., DeWolf, Jr., W. E., Chambers, P. A., and Goodhart, P. J. (1986) *Biochemistry* 25, 7271 - 8.
- Lamouroux, A., Vigny, A., Biguet, N, F., Darmon, M. C., Frank, R., Henry, J.-P., Mallet, J. (1987) *EMBO J.* 6, 3931 - 7.
- Malmstrom, B. G. and Vanngard, T. (1960) *J. Mol. Biol.* 2, 118.
- Malmstrom, B. G., Reinhammar, B., and Vanngard, T. (1970) *Biochim. Biophys. Acta* 205, 48.
- Margolis, R. K., Finne, J., Krusius, T., and Margolis, R. U. (1984) *Arch. Biochem. Biophys.* 228, 443 - 9.
- May, S. W. and Phillips, R. S. (1980) *J. Am. Chem. Soc.* 102, 5981 - 3.
- May, S. W., Phillips, R. S., Mueller, P. W., and Herman, H. H. (1981) *J. Biol. Chem.* 256, 2258 - 61.
- May, S. W., Herman, H. H., Roberts, S. F., and Ciccarello, M. C. (1987) *Biochemistry* 26, 1626 - 33.
- McCracken, J., Peisach, J., and Dooley, D. M. (1987) *J. Am. Chem. Soc.* 109, 4064 - 72.
- McKee, V., Dagdigian, J. V., Bau, R., and Reed, C. A. (1981) *J. Am. Chem. Soc* 103, 7000-1.
- Messerschmidt, A., Rossi, A., Ladenstein, R., Huber, R., Bolognesi, M., Gatti, G., Marchesini, A., Petruzzelli R., and Finazzi-Agro, A. (1989) *J. Mol. Biol.* 206, 513 -29.
- Messerschmidt, A., Ladenstein, R., Huber, R., Bolognesi, M., Avigliano, L., Petruzzelli, R., Rossi, A., and Finazzi-Agro, A. (1992) *J. Mol. Biol.* 224, 179-205.
- Miller, S. M. and Klinman, J. P. (1983) *Biochemistry* 22, 3091 - 6.
- Miller, S. M. and Klinman, J. P., (1985) *Biochemistry* 24, 2114 - 27.
- Mims, W. B. and Peisach, J. (1978) *J. Chem. Phys.* 69, 4921 - 30.
- Mims, W. B. and Peisach, J. (1979) *J. Biol. Chem.* 254, 4321 - 3.
- Mims, W. B. and Peisach, J. (1981) in *Biological Magnetic Resonance* (Berliner, L. J. and Reuben, J. eds.) Vol. 3, pp212 - 264, Plenum, New York.
- Moffitt, W. and Moscowitz, A. (1959) *J. Chem. Physics* 30, 648.
- Morpurgo, L., Giovagnoli, C., and Rotilio, G. (1973) *Biochim. Biophys. Acta* 322, 204.

- Morpurgo, L., Rotilio, G., Finazzi-Agro, A., and Mondovi, B. (1974) *Biochem. Biophys. Acta* 336, 324.
- Nakomota, K. (1986) in *Infrared and Raman Spectra of Inorganic Compounds*, 4th ed., John Wiley & Sons, New York.
- Northrop, D. P. (1975) *Biochemistry* 22, 3096 - 106.
- Obata, A., Tanaka, H., and Kawazura, H. (1987) *Biochemistry* 26, 4962 - 8.
- O'Brien, P. J. (1983) in *Lipid Peroxides* (Yagi, K., ed.) pp137, Academic Press, New York.
- O'Brien, P. J. (1984) in *Free Radicals in Biology* (Pryor, W. A. ed.) Vol. VI, pp289 - 322, Academic Press, Inc., New York.
- Padgette, S. R., Wimalasena, K., Herman, H. H., Sirimanne, S. R., and May, S. W. (1985) *Biochemistry* 24, 5826 - 39.
- Park, D. H., Kashimoto, T., Ebstein, R. P., and Goldstein, M. (1976) *Mol. Pharmacol.* 12, 73-81.
- Pasquali, M. and Floriani, C. (1984) in *Copper Coordination Chemistry : Biochemical and Inorganic Perspectives* (Karlin, K. D. and Zubieta, J., eds.) pp 311 - 330, Adenine Press, New York.
- Pate, J. E., Ross, P. K., Thamann, T. J., Reed, C. A., Karlin, K. D., Sorrell, T. N., and Soleman, E. I. (1989) *J. Am. Chem. Soc.* 111, 5198 - 209.
- Peisach, J. and Blumberg, W. E. (1974) *Arch. Biochem. Biophys.* 165, 691-708.
- Pettingill, T. M., Strange, R. W., and Blackburn, N. J. (1991) *J. Biol. Chem.* 266, 16996 - 17003.
- Reinhammar, B. (1983) in *The Coordination Chemistry of Metalloenzymes* (Bertini, I., Drago, R. S., and Luchinat, C., eds) pp177 - 200, D. Reidel Publishing.
- Robertson, J. G., Desai, P. R., Kumar, A., Farrington, G. K., Fitzpatrick, P. F., Villafranca, J. J. (1990) *J. Biol. Chem.* 265, 1029 - 35.
- Rosenberg, R. C. and Lovenberg, W. (1977) *Mol. Pharmacol.* 13, 652-61.
- Rosenberg, R. C. and Lovenberg, W. (1986) *Essays in Neurochemistry and Neuroparmacol.* 4, 163 - 209.
- Rotilio, G., Morpurgo, L., Giovagnoli, C., Calabrese, L., Mondovi, B. (1972) *Biochemistry* 11, 2187 - 92.
- Saxena, A., Hensley, P., Osborne, J. C. Jr., and Fleming, P. J. (1985) *J. Biol. Chem.* 260, 3386-92.

- Scott, R. A., Sullivan, R. J., DeWolf, W. E. Jr., Dolle, R. E., and Kruse, L. I. (1988) *Biochemistry* 27, 5411-7.
- Segel, I. H. (1975) *Enzyme Kinetics*, P170 - 178, John & Sons, Inc., New York.
- Skotland, T., Ljones, T., Flatmark, T., and Sletten, K. (1977) *Biochem. Biophys. Res. Comm.* 74, 1483 - 9.
- Skotland, T. and Ljones, T. (1977) *Int. J. Pept. Protein Res.* 10, 311 - 4.
- Skotland, T., Ljones, T., Flatmark, T., and Sletten, K., (1977) *Biochem. Biophys. Res. Commun.* 74, 1483-89.
- Skotland, T. and Ljones, T. (1979) *Inorg. Perspect. Biol. Med.* 2, 151 - 80.
- Skotland, T., Peterson, L., Backstrom, D., Ljones, T., Flatmark, T., and Ehrenberg, A. (1980) *Eur. J. Biochem.* 103, 5 - 11.
- Skotland, T. and Ljones, T. (1983) *J. Inorg. Biochem.* 18, 11 - 8.
- Shepherd, G. M. (1988) in *Neurobiology* pp 145 - 76, Oxford Univ. Press Inc. New York.
- Sligar, S. G., Kennedy, K. A., and Pearson, D. C. (1980) *Proc. Natl. Acad. Sci. USA* 77, 1240.
- Solomon, E. I., Clendening, P. J., Gray, H. B., and Grunthaner, F. J. (1975) *J. Am. Chem. Soc.* 97, 3878.
- Solomon, E. I., Hare, J. W., and Gray, H. B. (1976) *Proc. Natl. Acad. Sci. USA* 73, 1389.
- Solomon, E. I. (1981) In *Copper Proteins* (Spiro, T. G. ed.) pp 41- 108, John Wiley & Sons Inc., New York.
- Sorrell, T. N., O'Connor, C. J., Anderson, O. P., and Reibenspies, J. H. (1985) *J. Am. Chem. Soc.* 107, 4199-206.
- Sorrell, T. N. (1986) In *Biological & Inorganic Copper Chemistry*, (Karlin, K. D., Zubieta, J., ed.) Vol. II. pp41-55 Adenine Press, Guilderland, NY.
- Sorell, T. N. and Borovick, A. S. (1987) *J. Am. Chem. Soc.* 109, 4255 - 60.
- Speedie, M. K., Wong, D. L., and Ciaranello, R. D. (1985) *J. Chromatogr.* 327, 351-357.
- Spira - Solomon, D. J. and Solomon, E. I (1987) *J. Am. Chem. Soc.*, 109, 6421- 32.
- Stewart, L. C. and Klinman, J. P. (1987) *Biochemistry* 26, 5302 - 09.
- Stewart, L. C. and Klinman, J. P. (1988) *Ann. Rev. Biochem.* 57, 551 - 92.
- Syvertsen, C., Gaustad, R., Schroder, K., and Ljones, T. (1986) *J. Inorg. Biochem.* 26, 63 - 76.

- Tainer, J. A., Getzoff, E. D., Beem, K. M., Richardson, J. S., and Richardson, D. C. (1982) *J. Mol. Biol.* 160, 181 - 217.
- Tainer, J. A., Getzoff, E. D., Richardson, J. S., and Richardson, D. C. (1983) *Nature* (London) 306, 284-7.
- Talor, C. S., Kent, U. M., and Patrick, S. F. (1989) *J. Biol. Chem.* 2264, 14 - 16.
- Tsien, R. W. (1987) in *Neuromodulation: The Biochemical Control of Neuronal Excitability* (Kaczmarek, L. K. and Levitan, I. B. eds.) pp 206 - 42, Oxford University Press, New York.
- Vallee, B. L. and Holmquist, B. (1980) in *Advances in Inorganic Biochemistry* (Darnall, D. W. and Wilkins, R., eds.) vol. 2, pp 27 -74, Elsevier North Holland, Inc. New York.
- Venneste, W. and Mason, H. S. (1966) in *Biochemistry of Copper* (Peisach, J., Aisen, P., and Blumberg, W. E., eds.) pp 465, Academic Press, New York.
- Villafranca, J. J. (1981) in *Copper Proteins* (Spiro, T. G., eds.) pp 263 - 289, Wiley-Interscience, New York.
- Villafranca, J. J., Colombo, G., Rajashekhar, B., Giedroc, D., and Baldoni, J. (1982) in *Oxygenases and Oxygen Metabolism* (Nozaki, M., Yamanioto, S., Ishimura, Y., Coon, M. J., Ernster, L., and Estabrook, R. W. eds.) pp125 - 35, Academic Press, New York.
- Villafranca, J. J. and Desai, P. R. (1990) in *Biological Oxidation Systems* vol. I, pp 297-327, Academic Press, New York.
- Weissbluth, M. (1974) in *Hemoglobin* p138, Springer-Verlag, New York.
- Whittaker, M. M. and Whittaker, J. W. (1988) *J. Biol. Chem.* 6074-80.
- Wimalasena, K. and May, S. W. (1987) *J. Am. Chem. Soc.* 109, 4036 - 46.
- Winkler, H. and Carmichael, S. W. (1982) in *The Secretory Granule* (Poisner, A. M. and Trifaro, J. M., eds.) pp 3 - 79. Elsevier Biomedical Press, Amsterdam.
- Ziolo, R. F., Allen, M., Titus, D. D., Gray, H. B., and Dori, Z. (1972) *Inorg. Chem.* 11, 3044-50.
- Zolla, L. and Brunori, M. (1983) *Anal. Biochem.* 133, 465 - 9.
- Zolla, L., Calabrese, L., and Brunori, M. (1984) *Biochim. Biophys. Acta* 788, 2206 - 13.

Vita

I am from Beijing, China for graduate studying in Biochemistry major. In the US, I have not only learnt science but also the meaning of democracy and freedom.

I received Bachelor of Science degree form Tsinghua University in Beijing, China, in 1984 and started graduate studies in 1986 in Dept. of biochemistry, Oklahoma State University. In 1988, I transferred to Oregon Graduate Institute to continue my graduate study under the guidance of Dr. Ninian Blackburn to study a very important enzyme, dopamine β -hydroxylase.